THE EFFECTS OF VARYING VIBRATION FREQUENCY AND POWER ON EFFICIENCY IN VIBRATION ASSISTED ROTARY DRILLING

YUSUF BABATUNDE OLAIYA

THE EFFECTS OF VARYING VIBRATION FREQUENCY AND POWER ON EFFICIENCY IN VIBRATION ASSISTED ROTARY DRILLING

© Yusuf Babatunde Olaiya, B.Eng (Hons)

A thesis submitted to School of Graduate Studies

in partial fulfillment of the requirements for the degree of

Master of Engineering

Faculty of Engineering and Applied Science

Memorial University of Newfoundland

St John's, Newfoundland, Canada

November, 2011

Abstract

Improving drilling efficiency and mitigating risk are major objectives of Vibration Assisted Rotary Drilling (VARD). Understanding the behavior of vibration energy applied to enhance drilling Rate of Penetration (ROP) and reducing bit wear is extensively looked at in this research.

A series of tests and analysis was carried out to provide data for the evaluation of the effects of varying vibration frequency and amplitude in rotary drilling. Two separate drill bits: impregnated diamond drag bit and the polycrystalline diamond compact (PDC) were used. Vibration frequencies were varied at different levels of amplitudes. With water used as the drilling fluid and drilling at atmospheric condition, rock samples with known Unconfined Compressive Strength (UCS) were drilled with a fully instrumented laboratory drill rig, and all operating parameters were closely monitored. The interpretation of results shows that vibration rotary drilling using impregnated diamond drag bit and PDC bit at controlled vibration frequencies has significant performance increase in ROP compared with conventional rotary drilling. The contribution of vibration to this performance increase was found to be very significant. Drilling runs were short, of necessity, in this study and bit wear was not significant.

Acknowledgement

I would like to express my sincere gratitude to Dr Stephen Butt and Dr John Molgaard for their invaluable guidance and patience during the different phases of my thesis development. I also would like to thank Farid Arvani for his contributions. I sincerely appreciate the works done by the work term students: Charles Gilles, Gordon Simeon, J Horton and Josh Roberts. Thanks also go to lab technicians Shawn Organ and Matt Curtis, as well as Engineering Technical Services employees, David Snook and Ron Monks for their assistance in tool development.

I acknowledge the Associate Dean of Graduate Studies, Dr L. Lye as well as Moya Crocker for her administrative assistance. Unlimited appreciation goes to John Green for his unforgettable fatherly support. I owe my deepest thanks to my family: my late dad for giving me a sound educational and personal foundation onto which this degree is built, my mum, my brother, my sisters, my lovely wife and our new baby girl, Maryam. I thank you all for your support, inspiration and encouragement.

Table of Contents

Chapter 3 Diamond Drag Bit Drilling

Chapter 4 PDC Bit Drilling

List of Tables

List of Figures

Abbreviations

VARD	Vibration Assisted Rotary Drilling
ROP	Rate of Penetration
N-ROP	Normalized Rate of Penetration
VSP	Vibration Shaker Power
LVSP	Low Vibration Shaker Power
MVSP	Medium Vibration Shaker Power
HVSP	High Vibration Shaker Power
EFF_D	Drilling Efficiency
HSI	Hydraulic Horsepower per Square Inch
DAQ	Data Acquisition
HMSE	Hydraulic Mechanical Specific Energy
WOB	Weight on Bit
RPM	Revolution per Minute
SE	Specific Energy
MSE	Mechanical Specific Energy
DSE	Drilling Specific Energy
CCS	Confined Compressive Strength
UCS	Unconfined Compressive Strength
GPM	Gallon per Minute

RMS	Root Mean Square
FFT	Fast Fourier Transform
MPa	Mega Pascal
PDC	Polycrystalline Diamond Compact
WR	Wear Rate
HP	Horse Power

Chapter 1

Introduction

About this chapter: The tasks addressed in the thesis are introduced in this chapter. The contributions of the thesis to drilling optimization in vibro-rotary drilling are provided. The general thesis organization is explained.

1.1 Introduction

Drilling penetration rate is one of the key elements affecting drilling costs. One of the main factors affecting cost is the bit wear or the rate at which the bit is worn while interacting with the formation drilled. The objective of improving drilling efficiency is a balance between increasing rate of penetration (ROP) and maintaining or reducing bit wear rate (WR). High ROP with high bit wear may actually be less efficient if more bit replacements are needed to reach the target. Figures 1 to 3 help explain the correlation between ROP and bit wear which are important in determining drilling efficiency. A scenario of high ROP is desired if not countered by high wear rate of the bit as seen in figure 1. In a similar fashion, low bit wear rate is good, but at low ROP, that advantage becomes neutralized as in figure 2. In order to optimize drilling efficiency, the condition

shown on figure 3 with high ROP alongside low wear rate should be the anticipated goal of every drilling program.

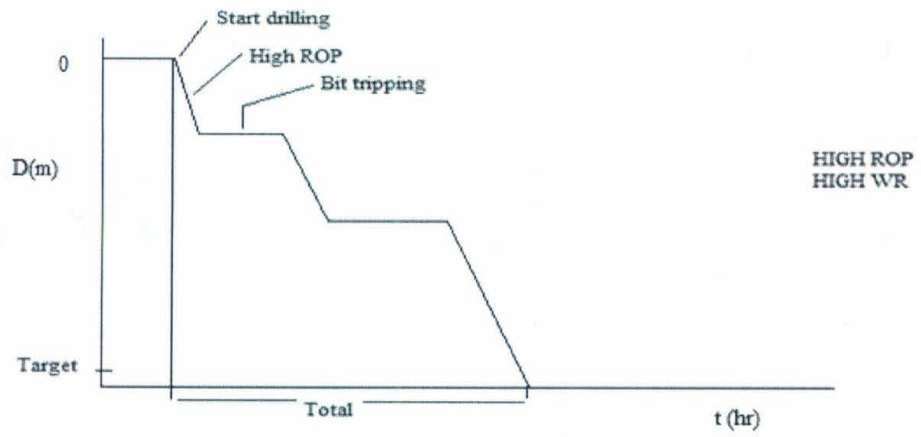

Figure 1. High ROP, High Wear Rate Scenario

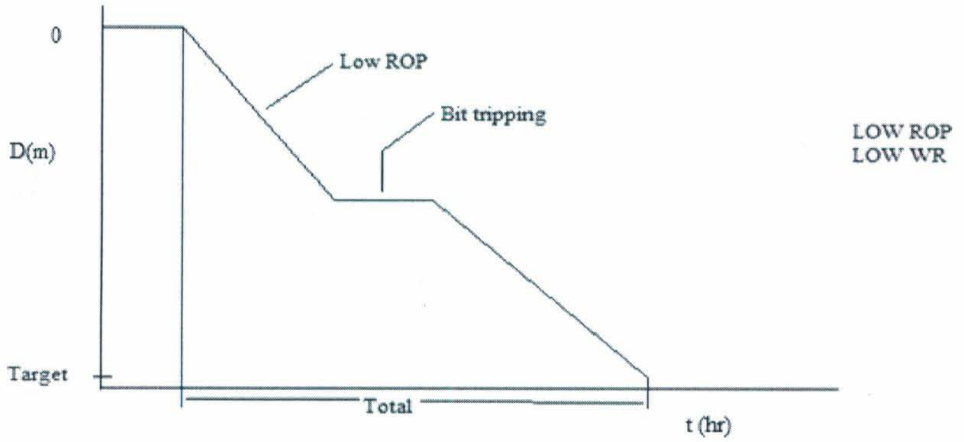

Figure 2. Low ROP, Low Wear Rate Scenario

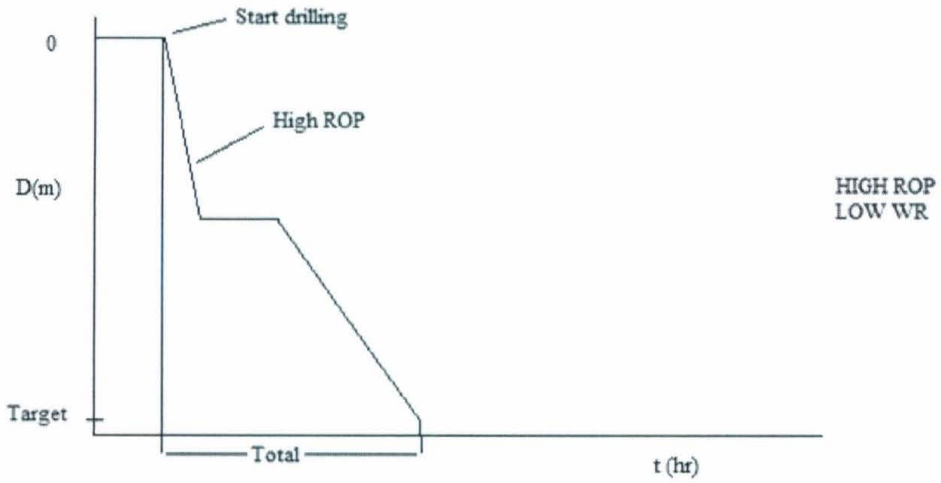

Figure 3. High ROP, Low Wear Rate Scenario

Vibration-Assisted Rotary Drilling (VARD) is a project that deals with the application of vibration to a rotary drilling setup with an overall aim of improving the drilling efficiency. The concept involves developing a downhole vibration tool which creates vibration near the bit. The experimental investigations carried out thus far confirmed the efficiency of this concept over conventional rotary drilling [1]. While the concept involves creating vibration of the bit, the pioneer VARD instrument which is currently in use consist of a vibration shaker table which will vibrate the drilled rock instead. This has been in use to study the fundamentals of VARD and understanding its role in improving drilling efficiency. The second stage VARD instrument which is at the stage of design and development will provide vibration at the bit and simulate

bottomhole conditions. Full description of the VARD tool developmental phases can be found in Li [1].

A drilling engineer always look forward to a point called the drilling founder; a point after which drilling becomes less efficient. At this point, an increase in WOB will not increase the ROP any longer but instead decrease it. As the WOB increases, the ROP is expected to increase until the founders point. The founder point is caused by a number of factors, the common of which is when the drilling fluid ceases to remove all of the cuttings from the bottom of the hole and the bit is drilling cuttings instead. Figure 4 below shows founder point as a quantifier of drilling inefficiency.

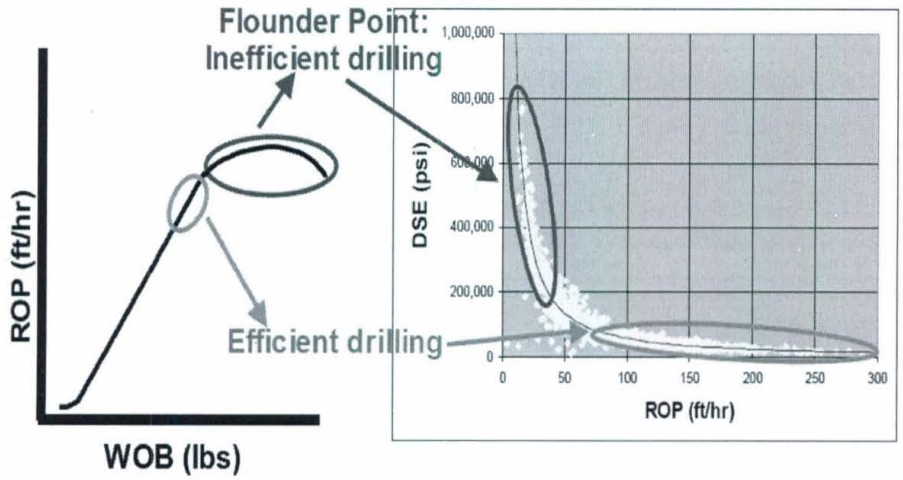

Figure 4. Relationship between the traditional ROP v. WOB plot and the DSE v. ROP plot [13]

A series of experiments have been conducted with the present VARD rig. Studies commenced by using a coring bit to drill prepared concrete samples. The experiment which actually confirmed the efficiency of this new technology was carried out using a coring bit. It was found that VARD technology can provide a significant increase in ROP at low levels of weight on bit (WOB). With increasing WOB, a curve which is similar to those in conventional drilling could be obtained. ROP increases proportionally with increasing rotary speed, as expected in a rotary drilling.

1.2 Research Objectives

The main focus of this research is to study drilling optimization in VARD by understanding the influence of varying the frequency and amplitude of vibration for vibration-assisted rotary drilling using a natural diamond impregnated drag bit and a Polycrystalline Diamond Compact (PDC) bit under different operational conditions. Furthermore, the research also involves series of experiments and analysis carried out on bit hydraulics to optimize ROP with the aim of generally improving the overall drilling efficiency. The main focus of this research is therefore to design vibration-assisted rotary drilling experiments such that:

- Effects of varying the frequency and amplitude of vibration on ROP and possibly bit wear will be understood.
- Drilling optimization is achieved by studying the impact of bit-hydraulics on improving ROP and drilling efficiency through proper understanding of Drilling Specific Energy (DSE) and Mechanical Specific Energy (MSE).

1.3 Contributions of the thesis

The resulting contributions from this thesis can be highlighted as follows:

- Adds to our understanding of the optimum vibration frequency and amplitude of vibration at different operational conditions suitable to obtain the highest ROP.
- Provides data on the impact of bit-hydraulics on drilling optimization and overall drilling efficiency.
- Highlights a quantitative correlation for estimating the percent energy contribution of induced vibration introduced to rock cuttings and chips removal.
- Provides a deeper understanding of the dynamic vibrations obtainable from the VARD concept through Real-Time data acquisition.

1.4 Thesis Organization

Chapter 2 provides the fundamental backgrounds and recent developments in application of vibration to oil and gas drilling. This chapter also reviews the basic concepts of DSE and MSE.

Chapter 3 presents the experimental drilling design, selection of operating factors and the results measured using the Impregnated Diamond Drag bit. The drilling data are adequately analyzed to reflect on their impact in optimization. MSE and DSE concepts are applied to the drilling results which provide a solid grip on the influence of bit hydraulics as well as vibration energy contribution to the overall drilling efficiency.

Chapter 4 presents a more systematic experimental drilling design which involves drilling with PDC bit to obtain real-time vibration and drilling data. Selection of operating factors and the results analysis were done in similar fashion as that done for the Impregnated diamond bit for clarity and to aid comparison.

Chapter 5 provides concluding remarks about the research and some recommendations for future work.

Chapter 2

Background

About this chapter: This chapter will first review some previous attempts on vibro-rotary drilling development. The preliminary results from VARD development are introduced and an introduction to drilling optimization by means of MSE and DSE is presented.

2.1 Vibro-Rotary Drilling techniques

Rotary drilling technique; a method introduced into the Petroleum industry in the middle of the 19th century, is today the most widely used method of drilling oil wells. This method has some limitations and many attempts had been made to supplement or supplant this method. This point enables the driller to know when drilling is no longer efficient. Several studies have been made to enhance rotary drilling by adding vibration. These include efforts made towards developing drilling methods that would optimize drilling rate of penetration (ROP) while decreasing bit wear with the sole aim of improving the overall drilling efficiency.

In a feature article by Simon in 1958 [2], he pointed out that only a fraction of the power capability of the rotary table can be realized as mechanical power output to the rock when drilling in the stronger formation at the maximum practical WOB and at the maximum practical rate of rotation. This he considered as one of the main limitations of rotary drilling. The author further described a magnetostrictive transducer vibratory drilling in which case the magnetostrictive transducer used changes slightly in dimensions when magnetized. Vibrations are produced by sending electric current through magnetizing coils to drive the column at a frequency of mechanical resonance. The drill string is rotated at the top of the hole at about same rate as for rotary drilling. He was fast to point out that the best general drilling method would be one allowing high ROP for the first few thousand feet, and, as the hole deepened, would allow increased footage by each bit even at the expense of some decrease in ROP. It was also emphasized that the new drilling methods represent technological advances of high order but do not represent "technological breakthroughs" in the strict sense because they still depend upon loading the rock mechanically in order to fracture it. He concluded that real technological breakthrough in rock drilling may come when some means other than mechanical loading is found for rapidly generating free surfaces of separation in the rock at the bottom of the hole.

The Institute of Technical Mechanics [3] in Ukraine conducted a research on developing a Hydro-Vibrator for vibro-rotary drilling as shown in Figure 5. This set-up consists of a high-frequency cavitation hydro-vibrator which is capable of producing up to 2 – 3 fold increase in penetration speed and the technology makes use of magnetostriction vibrator which enables the speed to be increased by about 3.2 to 4.3 times. Other advantages of the system as stated by the authors are that it has no moving or rotating parts, no pulsation at the inlet, drilling mud energy used for vibrations, simple design and service, higher reliability, smaller mass and dimensions, and vibratory drilling at high depth with bit diameter between 36 – 250 mm. Though this technology is yet to be put into field test at this time, the investigators planned to study the process of rock destruction, verify the serviceability of the hydro-vibrators in deep drilling, develop a scientific substantiation and development of a technique for application of the high-frequency cavitation as a part of core and noncore drilling assemblies for rocks of different strength.

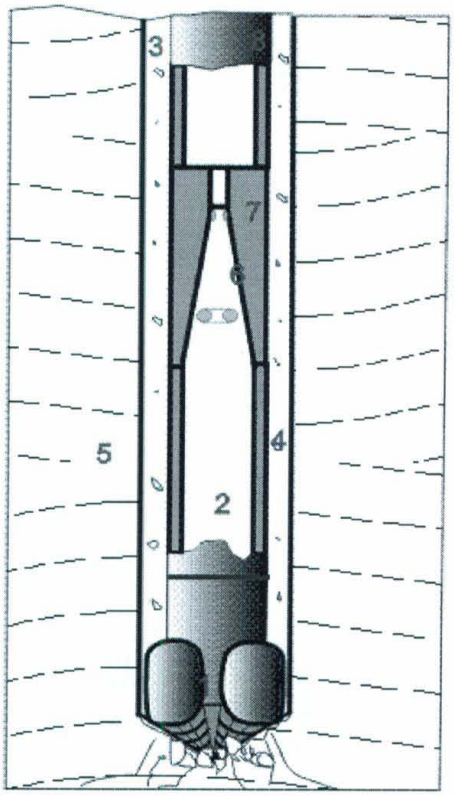

Figure 5. Scematic of vibratory rotary drilling using high frequency cavitation hydrovibrator. [1. Rock cutting tool. 2. Drilling mud. 3. Borehole. 4. Cuttings. 5. Rock. 6. Hydrovibrator shaped inner passage. 7. Hydrovibrator.8. drilling assembly. 9. Cavity. 10. Detached part of cavity. [3].

Wiercigroch M. [4] of the College of Physical Sciences, University of Aberdeen worked on resonance enhanced rotary drilling. The study involves improving drilling rate in medium to hard rock by applying reciprocal axial movement to the drill bit (percussive drilling) as it passes through the material to be drilled as shown in Figure 6. The impact of these axial movements promotes fractures in the drilled material making material removal easier. However, one disadvantage

of this is that these impacts compromise borehole stability, reduce borehole quality and cause accelerated and often catastrophic tool wear and or failure. Another drilling technique described is the application of ultrasonic axial vibration to a drill bit. In this particular case, ultrasonic vibration rather than isolated high load impact is used to promote fracture propagation. This method was said to offer significant advantages over percussive drilling in the sense that loads can be applied allowing for low WOB drilling. A major setback however is that the improvement exhibited by ultrasonic drilling is always consistent and are not as such directly applicable to downhole drilling. The vibration frequency of this apparatus is up to 1 kHz (far higher than what is being used presently in VARD) and the rotary speed is up to 200 rpm (close to the current VARD rotary speed). The weight of drill string for this apparatus is about 40 – 70% smaller than for conventional drilling. A magnetorestrictive stack can be used instead of piezoelectric transducer. It was explained that in soft formations, the oscillatory effect of drill bit could be turned off by the control means of the drill apparatus.

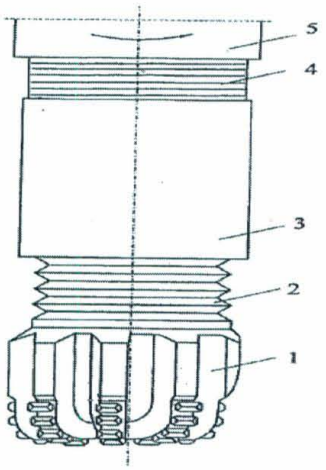

Figure 6. Resonance Enhanced Drilling [1. Polycrystalline diamond bit. 2. Vibro transmission section. 3. Piezoelectric transducer. 4. Coupling acting as vibration isolator. 5. Drill string]. [4]

A vibratory drilling patent by Eckel J.E [5] was an invention related to an improved apparatus (Figure 7) for vibratory rotary drilling. In this vibratory drill, a combination of torsional and percussive actions is applied to a drill bit which results in shearing and hammering of rock formation while drilling. According to this invention, the energy dissipation in vibratory drilling is decreased by utilizing a unique gaseous buffer zone positioned in the bit assembly. The vibration inducing apparatus may be hydro-driven or may be of the electrical type such as a magnetostrictive transducer or solenoid driven or piezoelectric transducer. This invention is used for frequencies between 10 to 500 Hz,

preferably 300 Hz with 0.0001 to 0.25 inch amplitude, preferably 0.01 inch amplitude.

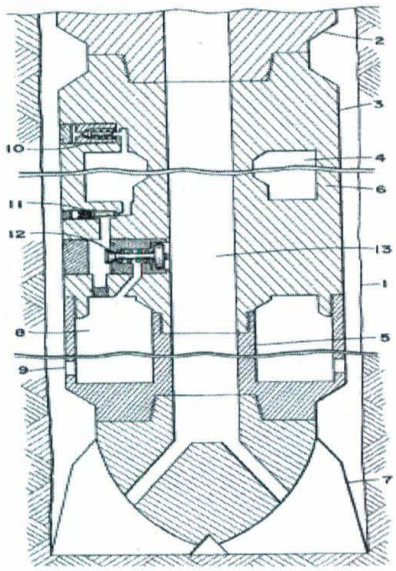

Figure 7. Vibratory drilling cross-sectional design which combines torsional and percussive actions on the bit. [2. Drill Collar. 3. Cylindrical Buffer Element. 4. Hollow Annulus. 6. Outer Wall. 7. Bit. 8. Surge Chamber. 9. Ports. 10. Filler Valve. 11. Metering Valve. 12. Bleeder Valve. 13. Mud Channel [5].

Xinghua Tao et. al. [6] of the Petroleum Drilling Research Institute, China developed an impact rotary drilling tool, shown in Figure 8, which also utilizes a vibration mechanism from fluid pulse transmitted to the collar and anvil using piston and anvil connections. The equipment was said to have been proven with series of Laboratory and field tests and found to improve ROP by about 60% depending on the kind of formation drilled producing good quality borehole. The study reveals that low impact power and high impact frequencies can help

break the rock while drilling soft and medium formations. Meanwhile, the complexity and practicality of the system in different field drilling conditions make it not to be commercially acceptable.

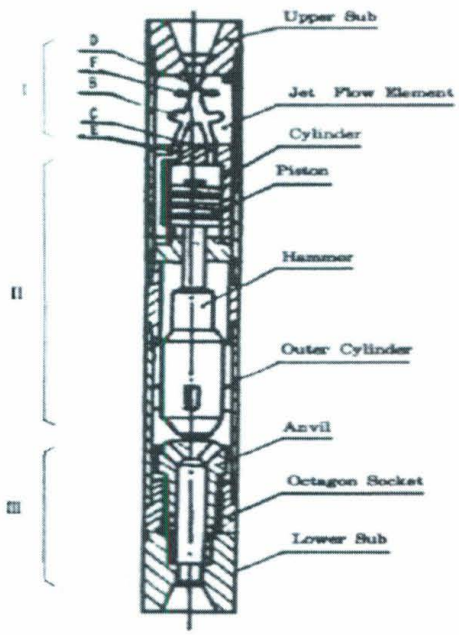

Figure 8. Resonance Enhanced Drilling [6]

2.2 Laboratory Scale VARD

A preliminary investigation aimed at verifying the basic concepts of vibration-assisted rotary drilling had been embarked upon since 2008 by the Advanced Exploration Drilling Group at Memorial University and had been extensively explained by Li et. al. [7]. This investigation was developed to evaluate the

influence of bit vibration on penetration rate. The laboratory scale VARD instrument is a drill which was modified and instrumented to perform drilling operations under different conditions of rotary speed, WOB, fluid flow rate and vibration amplitudes at a fixed frequency. The laboratory scale VARD facility was built from an electrical powered coring drill which could operate at two rotary speeds of 300rpm and 600rpm. A cylindrical rail guide was built which create room for travel for the drill and motor assembly. A wheel attached enable weights to be hanged to create axial force on the drilled sample. The source of vibration is an electromechanical axial shaker mounted at the bottom of the drill stand. A set of experiments were conducted on specially made concrete samples using coring bit, at the two rotary speeds obtainable. An accelerometer was used to monitor the vibration characteristics, which helped confirm the samples are being drilled at a frequency of 60 Hz. A knob on a box-controller was used to vary the vibration amplitude at five different positions signifying different vibration power and thus different force and displacement amplitudes (vibration power). Results of the investigation as seen in Figure 9 show that for most drilling runs, ROP increases proportionally with vibration power, and in certain instance, ROP increase seems greater around the peak of ROP-WOB curve. However, only few drilling runs where carried out at different drilling

combinations and vibration was only characterized by average displacement amplitude.

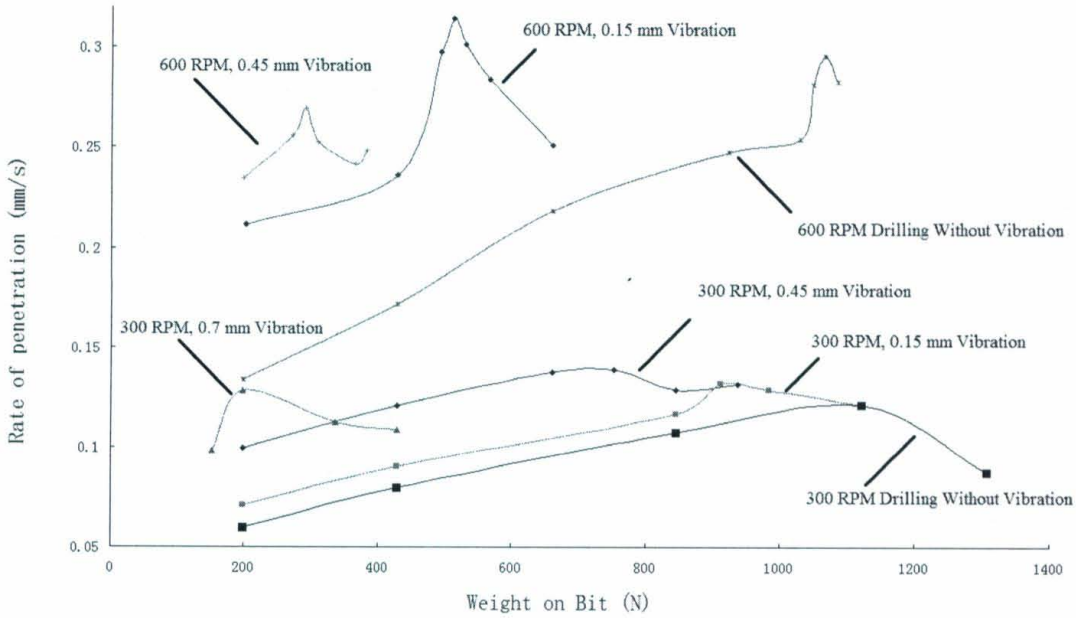

Figure 9. ROP v. WOB curves for vibration rotary drilling using coring bit at 300 rpm and 600 rpm [7].

In an attempt to utilize an industry-type drill bit, Li [1] proceeded to use a full faced bit to drill at similar conditions. The full faced bit was considered because it could take higher WOB before the peak, since it has large contact area which makes force per unit surface area exerted by the bit on the rock lower. This enables the full face bit take more drilling runs than the coring bit and as such gets closer to the founder point. The bit was used to drill concrete samples which

has unconfined compressive strength of 20 MPa. The bit was used to drill conventionally and with vibration using five different vibration energy levels. Generally, both for the conventional and vibration drilling, the typical ROP-WOB curve proposed by Maurer [9] was observed. The curve was still rising and would be said not to have gotten to the founder point. However, values of ROP, which is a major determinant in evaluating drilling efficiency, were relatively low compared to those obtained drilling with the coring bit. This therefore raises questions of the applicability of the VARD concept to industrial type drill bits, although, there were still possibilities of obtaining higher ROP if the WOB keep increasing. It should however be noted that drilling using coring bit were done at uncontrolled and unknown flow rate, and there is evidence of bit whirling which could have had effects on vibration distribution. The optimum flow rate was found by conducting some hydraulic flow experiments.

2.3 Specific Energy and Drilling Efficiency

2.3.1 Mechanical Specific Energy

The concept of specific energy (SE) was developed by Teale [14] who defined specific energy as the work done per unit volume of rock excavated by quantifying the relationship between input energy and output ROP, a ratio

which is constant for a given rock. He described rotary drilling as a combination of indentation and cutting of the rock. The equation was later modified in terms of rotary drilling parameters as the mechanical specific energy (MSE), which is calculated based on the component of thrust and rotation (axial and torsional work performed by the bit divided by the volume of rock drilled) and has a unit of Psi. The study revealed that when rock is drilled at atmospheric conditions, the MSE value approaches the value of the rock unconfined compressive strength (UCS). The rock UCS is seen as the minimum value of MSE required to break the rock and is divided by actual MSE in calculating the efficiency of drilling (EFF_D). This has however raised question of whether calculating drilling efficiency this way could also be used under reservoir pressurized conditions in which case we have the rock confined compressive strength (CCS).

$$SE = \frac{Input\ Energy}{Output\ ROP} \tag{1}$$

$$\text{MSE} = \frac{WOB}{A_b} + \frac{120\pi NT}{A_b ROP} \tag{2}$$

$$EFF_D = \frac{MSE_{min}}{MSE_{actual}} * 100 = \frac{UCS}{MSE} * 100 \tag{3}$$

WOB – weight on bit, A_b – Area of bit, N – rotary speed (RPM)

ROP – rate of penetration, and T = torque

Pessier and Fear [10] carried out a study on this. First of all, they modified Teale's MSE equation by introducing a bit specific coefficient of sliding friction from which torque is expressed as a function of WOB. The experiment was done under pressurized conditions simulating bottomhole conditions. Their results show that under same confining pressure, the CCS value is much lower than the measured MSE value while drilling.

$$T = \frac{1}{36}\mu * D_B * WOB \qquad (4)$$

$$MSE = \frac{WOB}{A_b} + \frac{13.33*\mu*RPM*WOB}{D_B*ROP} \qquad (5)$$

D_B is bit diameter and μ is the bit coefficient of sliding friction

Navid Rafatian et. al. [11] in their study of MSE of a single PDC cutter under simulated pressurized conditions, discovered a significant increase in the MSE was caused by an increase in the confining pressure as small as 150 psig, thereby cutting the efficiency by 50%. The Teale's MSE equation was simplified for a single cutter bit. They however were unable to attribute this to the strengthening of the rock under confining pressures.

$$MSE = \frac{Workdone\ \ in\ Cutting\ \ Action}{Volume\ \ of\ Rock\ Cut} = \frac{\int (Force).dx}{Volume\ \ of\ Cut} \qquad (6)$$

$$Efficiency = \frac{CCS\ (Confining\ \ Pressure\ )}{MSE\ (Confining\ \ Pressure\ )} \qquad (7)$$

Dupriest and Koederidtz [12] in an attempt to keep the values of MSE in reasonable terms with the value of rock compressive strength introduced an efficient factor of 35% regardless of bit type and WOB since Teale's MSE value would be around three times the rock CCS. They argued that bits are only about 30 - 40% efficient at peak performance. The MSE value is thus reduced to a value close to the compressive strength of the rock; this they said helps create MSE value meaningful to rig personnel on site, which enable them determine if the bit is operating efficiently and whether founder had occurred.

$$\text{MSE} = 0.35 * \{\frac{WOB}{A_b} + \frac{120*\pi*N*T}{A_b ROP}\} \qquad (8)$$

2.3.2 Drilling Specific Energy

Drilling specific energy (DSE) is a new concept which is very much related to the MSE. The major difference between DSE and MSE is that the former contains a hydraulic term. DSE is therefore defined as the amount of energy required to destroy and remove underneath the bit a unit volume of rock [Miguel Armenta, [13]]. Teale's MSE equation was modified also in this case to include a hydraulic term. Miguel Armenta made use of laboratory and field data to identify efficient, inefficient and transition drilling regions. The author utilizes both Teale's MSE equation, the modified versions by Pessier and Fear as well as Dupriest and Koederidtz's to calculate DSE values and compare with MSE. The calculated

specific energy has to be close to the rock CCS when the system is operating efficiently. The MSE calculated using equations 2 and 5 were found to be higher than the CCS which is an indication that the system is operating at inefficient conditions. Using equation 9, the CCS happens to cross the middle of the curves indicating the system could operate with MSE values of about 45% lower than the CCS, which looks unrealistic. The hydraulic horsepower per square inch (HSI), which is the ratio of the bit hydraulic power and the area of the bit was used to differentiate efficient and inefficient drilling regions and as a means of transitioning between these regions. From the study, the limit between efficient and inefficient drilling regions was set at 3.0 hp/in^2.

$$\text{DSE} = \frac{WOB}{A_B} + \frac{120*\pi*RPM*T}{A_B*ROP} - \frac{1{,}980{,}000*\lambda*HP_B}{ROP*A_B} \qquad (9)$$

The first two terms on the right side of the equation are the same terms included on Teale's original equation. The third term on the right side is the bit hydraulic-related term. The number 1,980,000 is a unit conversion factor. Lambda (λ) is a dimensionless bit-hydraulic factor depending on the bit diameter. The ratio of bit hydraulic power and bit area (HP_B/A_B) is the bit HSI (hp/in^2). ROP is the rate of penetration (ft/hr). [13].

In an attempt to identify inefficient drilling conditions for drilling optimization, Kshittij Mohan et. al. [15] developed a similar concept to DSE which they called

Hydro Mechanical Specific Energy (HMSE). By definition, HMSE is equivalent to DSE in the sense that it also has a hydraulic term added to the axial and torsional values of the MSE. This described the newly introduced hydraulic term as the key to correctly match the amount of energy required to drill and overcome the strength and stresses of formation drilled. This study is different from a single perspective; it aims at estimating the inefficiency in drilling brought about by pump off force against the weight on bit (WOB) due to fluid force. As the bit drill through the formation, there is a reaction force from fluid hitting the formation and pushing back the bit (similar to Newton's third law of motion) which therefore counters the WOB. The HMSE equation which they suggested will be valuable during planning and operational phases of selecting and optimizing drilling parameters and is needed to achieve desired ROP when axial and torsional energy are specified.

$$\text{HMSE} = \frac{WOB}{A_b} + \frac{120\pi NT + 1154\eta\Delta P_b Q}{A_b ROP} \qquad (10)$$

2.4 Percussive Drilling

Hustrulid and Fairhurst [21] worked on the theoretical and experimental study of percussive drilling of rock which is developed from analysis of stress-wave

interactions in the drilling system. This study led to the derivation of an expression which allow the prediction of ROP and the amount of impact energy per unit volume of rock broken for particular drill bit and rock type. It was shown that the drilling rate is dependent on the frequency and blow energy, the hole area and also on the energy needed to remove a given volume of rock.

A follow-up study also by Hustrulid and Fairhust [22] was concentrated on force penetration and the determination of specific energy. Continuous forced indentations into the rock were statically utilized to determine static force penetration and energy per unit rock crater volume. A shallow hole was drilled by rotating the bit equally between each indentation. A drop test was also carried out as an accompanying test. Results show that the dynamic energy per unit volume for each rock was much higher than the static energy. In addition, the force penetration curves gradient for smooth surface test were much lower statically than dynamically.

Hustrulid and Fairhst [23] went ahead to apply their model to actual percussive drilling. The drilling experiment involves the use of three different drilling machines which allows the frequency, blow energy, rotary speed, ROP, thrust andstrain waves produced to be measured. The transfer of energy to the rock from the initial analysis [22] was found to vary as much as 15% between the

individual force penetration curves. Also from these experiments, the experimentally observed maximum energy transfer of about 80% of energy of impact matched closely when compared with the theoretically predicted values.

Luiz Fernando et. al. [24] worked on the numerical and experimental study using resonance hammer drilling model with drift. The technique makes use of harmonic loads or impact to generate a greater ROP. The authors generated a new model through the analysis of percussive penetration phenomenon and the model allows for forward motion in stick-slip condition with and without impact. Impact on the bit is found to occur when the excitation frequency is close to the steel mass resonance frequency (Figure 10 & 11). This according to their explanation happens because the steel mass displacement is limited in positive direction by the gap. The authors concluded that the results of the numerical model and those obtained from experiments are qualitatively and quantitatively similar, which validates the model.

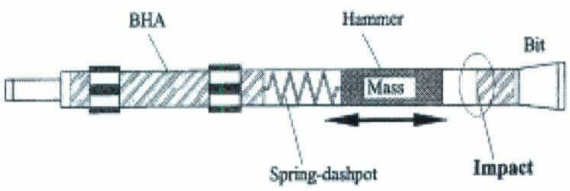

Figure 10. Resonance Hammer Drilling.

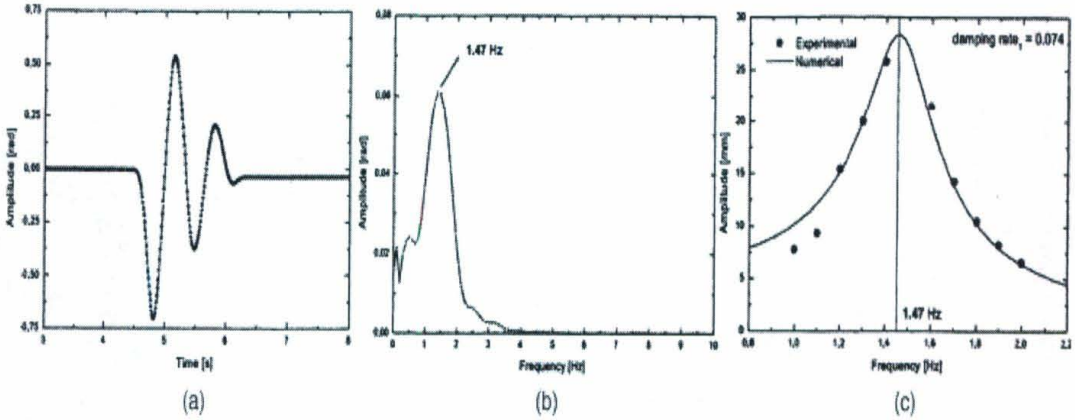

Figure 11. (a) Mass displacement due to impulsive force (b) FFT (c) Max. amplitude vs. frequency

Gang Han et. al. [25] dynamic rock failure model in percussive drilling provided improved understanding of percussion drilling and is forecasted to help facilitate the development of a simulation tool. Mohr –Coulomb model with strain-softening behavior was utilized, a damage algorithm used to update the rock properties due to cyclic loading and a Rayleigh damping used to dissipate excessive oscillation energy. Tensile failure, rock fatigue and compressive failure were all recorded during the study. The authors were convinced that the simulation tool developed will facilitate the study of more efficient and lower cost drilling methods for penetration of hard, brittle rocks.

2.5 Summary

The chapter provides an insight into efforts made in the past to improve petroleum drilling. It summarizes some of the vibro-rotary drilling approaches applied to enhance drilling rate. It emphasizes on the fact that most of these methods have not been developed to a stage of field trial and therefore have not been universally recognized, which has thrown up questions to the applicability of vibration-induced drilling. The chapter also provides information about the concept of mechanical specific energy (MSE) which is used in this work as a measure of drilling efficiency. A new concept of drilling specific energy was also introduced as its application to this work would improve our knowledge of how drilling hydraulics affects penetration rate in vibration-assisted rotary drilling.

Chapter 3

Diamond Drag Bit Drilling

About this chapter: This chapter introduces the basis of the investigation carried out. In order to improve penetration rate, both the frequency and amplitude of vibration were varied at constant rotary speed and flow rate and at different WOB. The chapter provides good conceptual information towards understanding VARD further.

3.1 Introduction

Previous VARD experimental studies were done at 60Hz using a coring bit by varying the amplitude of vibration, showing that ROP increases with increase in vibration amplitude [1]. In order to move a step further in understanding VARD, a set of experiments were designed to provide data for the evaluation of the effects of frequency and amplitude of vibration in rotary drilling using a diamond drag bit. The frequencies were varied at different levels of amplitude, keeping the rotary speed and fluid flow rate constant at multiple WOB. Drilling was done at atmospheric pressure using water as the drilling fluid. Synthetic rock

samples with known unconfined compressive strength (UCS) were drilled with a fully instrumented VARD laboratory drill rig.

3.2 Experimental Setup

The VARD system consists of an instrumented variable rotary-vibration system to apply rotation and vibration to the drill bit. The bit operating conditions for the vibration rotary drilling consists of a combination of static weight, rotary speed, and vibration amplitude and frequency. The drilling system was modified by introducing a frequency controller which enables the generation of a range of frequency. The introduction of a frequency controller modifies the vibrating table characteristics enabling the vibration frequency to be varied between 45Hz and 65Hz. A flow meter and a pressure gauge were installed to ensure proper monitoring and control of fluid flow conditions.

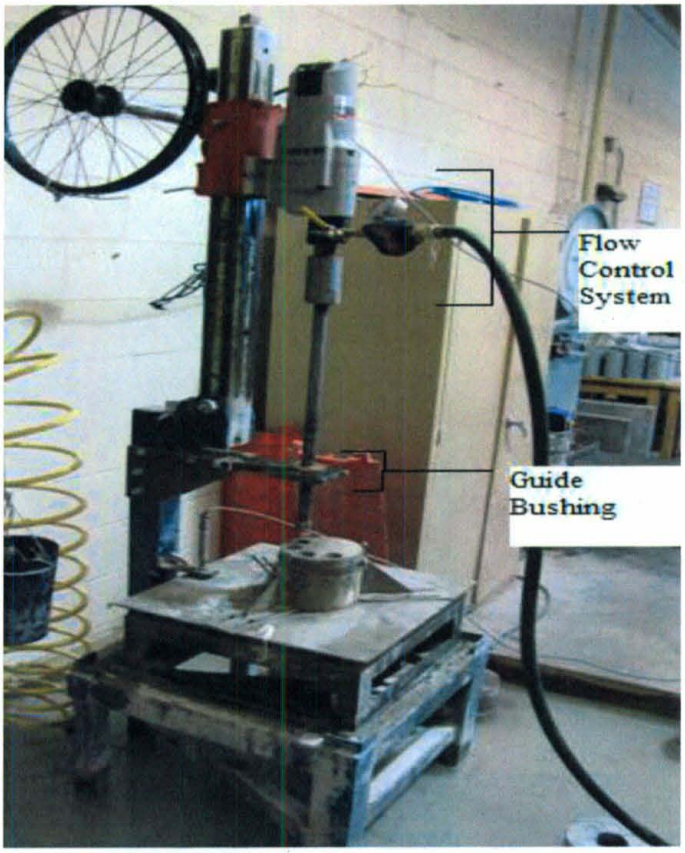

Figure 12. Drilling setup and modified drill string design

3.3 Sample Preparation

The drilled samples used in this experiment were a synthetic rock made from quick-concrete with aggregate greater than 2mm removed (mortar samples). The sample volume composition is made up of approximately 32% cement 58% aggregate and 10% water. These samples were cast in a 6-in cylindrical mould, removed from the mould after setting to a reasonable strength and then properly

cured by immersing them completely in water at room temperature and 100% humidity. This is necessary in order to ensure that samples drilled are of equal strength and prevent varied strength on the different part of each sample. The average UCS, following ASTM D 2938-95, of the drilled samples tested after 64 days of curing was 61MPa.

Table 1. Rock samples UCS

Experiment Number	Frequency (Hz)	Rock UCS (MPa)	Average UCS (MPa)
1	45	59	61.2
2	55	61.5	
3	65	63	

The experiment was designed in such a way that six holes could be drilled on a given surface of a drilled sample due to the small size of the bit (1.25-in). During the experiment, three holes are drilled separated 120° from each other, after which the drilled holes are filled with mortar and allowed to set for at least 24 hours to maintain the confinement of the sample; preventing the effect of near wellbore damage before the sample is drilled again. Core samples were taken from the centre of the samples using a standard coring bit after all the holes had been drilled. These cores are tested to determine the UCS of the samples.

3.4 Experimental Methodology

A 240g, 1.25-in small scale diamond drag bit was used for this experiment as shown in Figure 13. This bit is small enough to enable us produce realistic bit pressures similar to the full scale drill-bit used in the field. The experimental work is aimed at correlating ROP and WOB in conventional drilling and with axial vibration at different frequencies and amplitudes to also study bit wear. The drilling flow rate was fixed at 3gpm and the flow pressure monitored. The rotary speed was fixed at 300 rpm. WOB ranged from 45kg to 129kg.

Figure 13. The 1.25-in diamond drag bit

Three vibration frequencies (45, 55 and 65Hz) were applied, and for each frequency level, three vibration shaker positions (VSP), setting the power to the shaker. As noted also by Li (1), for a given power the vibration amplitude produced in this equipment is a function of WOB. The power settings are

designated low vibration shaker position (LVSP), medium vibration shaker position (MVSP), and high vibration shaker position (HVSP). The various drilling combinations are shown in the following tables.

While WOB is more commonly used in the field, it is also worthwhile to consider the load in terms of apparent bit pressures, i.e. force per unit cutting surface area as projected from the plane perpendicular to the bit axis of rotation. This fixed cutter bit has bit face area of about 775 mm^2, when projected on a plane perpendicular to the bit axis. These include twelve irregular shaped waterways; subtracting this, the projected matrix area reduces to about 700 mm-sq from which the bit pressures at different WOB can be obtained. This bit pressure ranges from 0.63MPa to 1.81MPa.

3.5 Analysis of Results

3.5.1 ROP – WOB Curves

Several plots of the ROP v. WOB for the different drilling combinations have been developed. In earlier VARD experiments reveal that the level of the ROP-WOB curve increases as the vibration power increases.

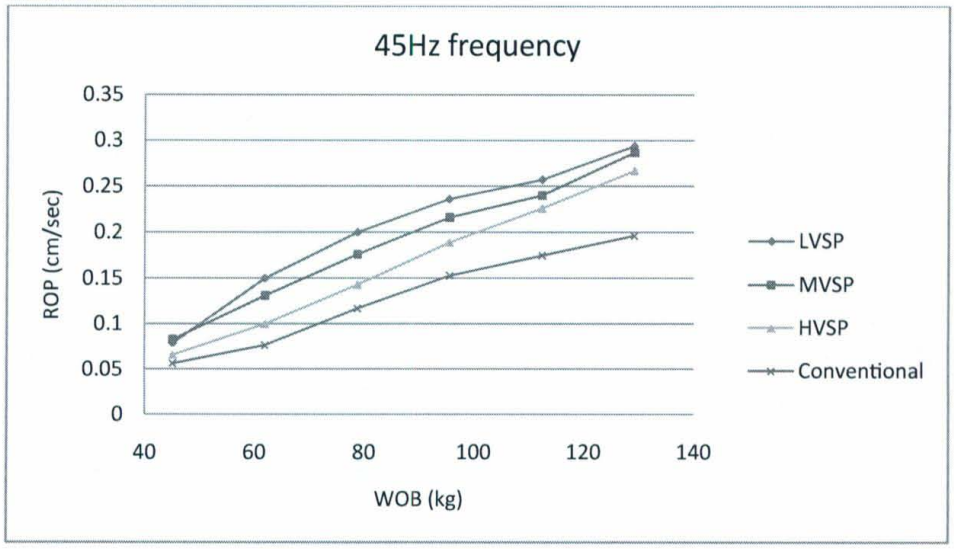

Figure 14. ROP-WOB curves at 45HZ Frequency drilling

The results for the 45 Hz frequency in Figure 14 show a reverse trend. As expected, drilling at all three VSP show a significant ROP increase compared to the conventional drilling. However, the low vibration shaker power unexpectedly produced the highest penetration rate, which is followed in a descending order by the medium vibration shaker power, and the high vibration shaker poweing giving the highest power but the lowest penetration. It was of interest to investigate the effects of frequency and amplitude on ROP for vibration drilling.

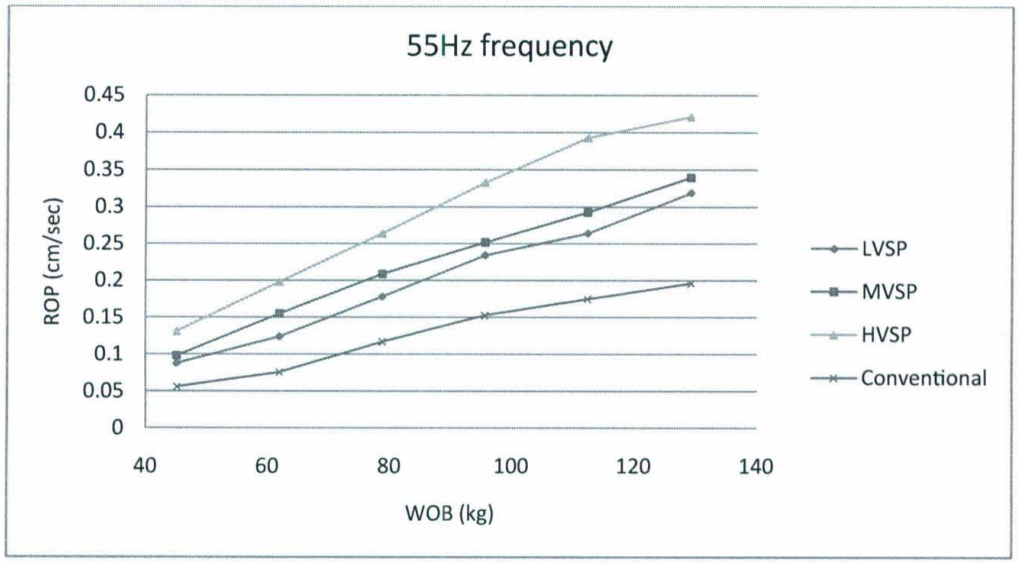

Figure 15. ROP-WOB curves at 55HZ Frequency drilling

At the 55 Hz frequency, the results as shown in Figure 15 are as anticipated from earlier experiments done by Heng Li et. al [6] where ROP increased with increase in vibration power. In this experiment, more than a 100% gain in ROP was obtained at the high vibration shaker power position using 129 Kg WOB in each case, compared to conventional drilling. The same trend was also observed at lower WOB.

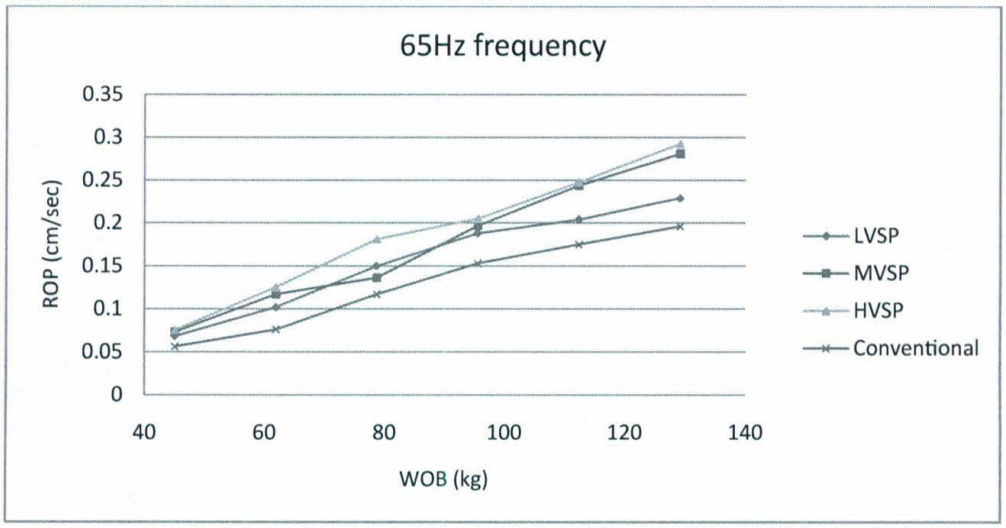

Figure 16. ROP-WOB curves at 65HZ Frequency drilling

The results on Figure 16 above show that although the penetration rates for vibration drilling at 65 Hz are higher than for conventional drilling, there is no significant effect of changing the vibration shaker power on the ROP between 43kg to 60 kg WOB. This is possibly due to the fact that the vibration becomes saturated and there is a reduction in vibration amplitude. The ROP curves for the medium and high vibration shaker power positions also tend to converge at higher WOB. In overall, the gain in ROP is not as significant as those obtained from the 55 Hz drilling, with a maximum increase in this case compared to conventional drilling being about 48%.

In order to study the effectiveness of drilling at the various frequencies at each vibration shaker power level, the data of the previous figures is plotted in Figures 17, 18 and 19 comparing the ROP-WOB curves at different vibration frequencies.

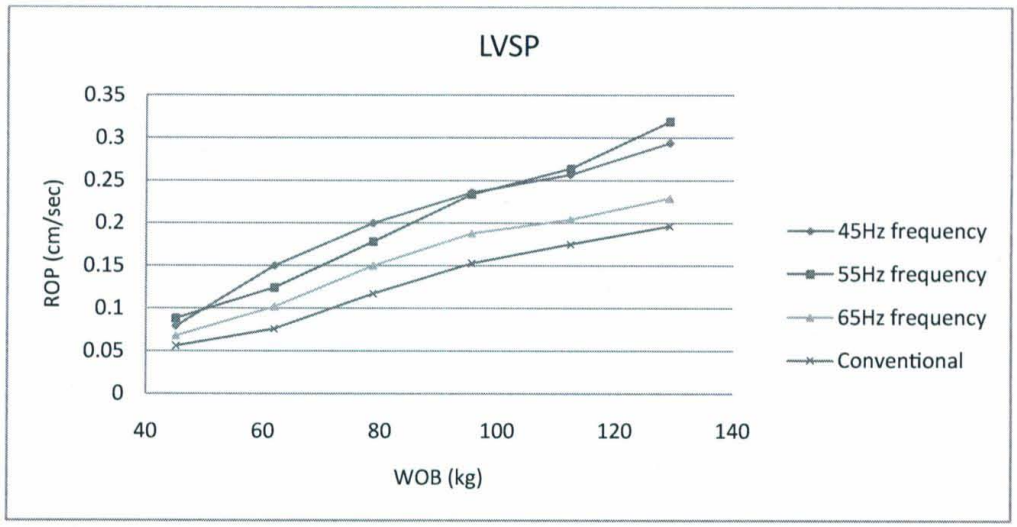

Figure 17. ROP-WOB curves under LVSP at various frequencies

In Figure 17, for the low vibration power, drilling at 45 Hz frequency seems more favourable, but as the WOB increases, the 55 Hz drilling curve overlaps to provide higher ROP. We cannot be sure from this that there is a significant difference between drilling at 45Hz and 55Hz, at least 50% higher ROP than conventional drilling at all WOB up to 106Kg and above that even more.

However drilling at the highest frequency show less gain as only about 12% ROP increase is recorded in comparison with the conventional drilling.

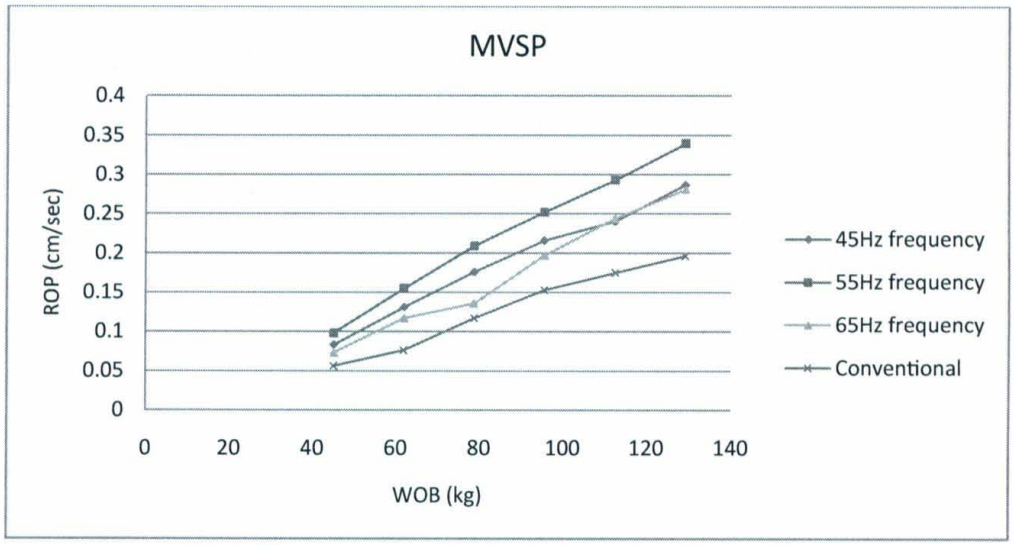

Figure 18. ROP-WOB curves under MVSP at various frequencies

At the middle vibration shaker power position shown on Figure 18, the 55 Hz drilling condition undoubtedly gives the largest ROP gain which is about 75% in relation to conventional drilling and about 20% greater than vibration at the other frequencies.

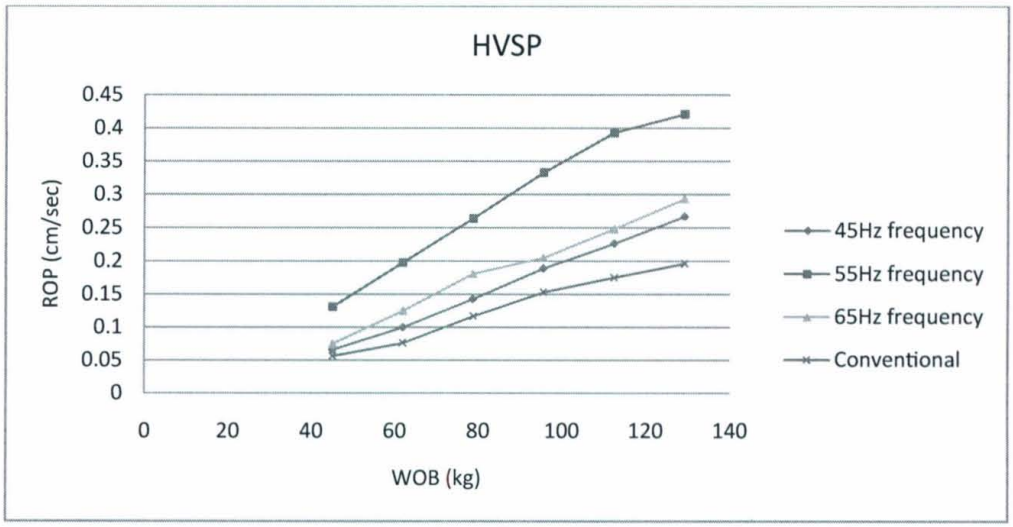

Figure 19. ROP-WOB curves under HVSP at various frequencies

For the high vibration shaker power applied, the lowest frequency has the lowest ROP gains as the WOB increases, but there isn't much diffrence between the 45 Hz and 65 Hz frequency drilling levels, they both do not compare with the very high increase in ROP observed at the 55 Hz frequency which shows more than 100% increase in ROP; about 15m/hour at 130Kg WOB in relation to 7m/hour found in conventional drilling. This value for the 55 Hz frequency though not as high, is close to the ROP common in the industry.

The relationship between ROP and frequency is similar at all WOB values studied. Figures 20-22 shows the various relationships of vibration power and frequencies on ROP at 95 kg WOB. In most instances, the 55 Hz frequency is

the optimum drilling frequency although at LVSP, the 45 Hz frequency provided comparable higher ROP. Drilling at high power is the optimum except at 45 Hz frequency.

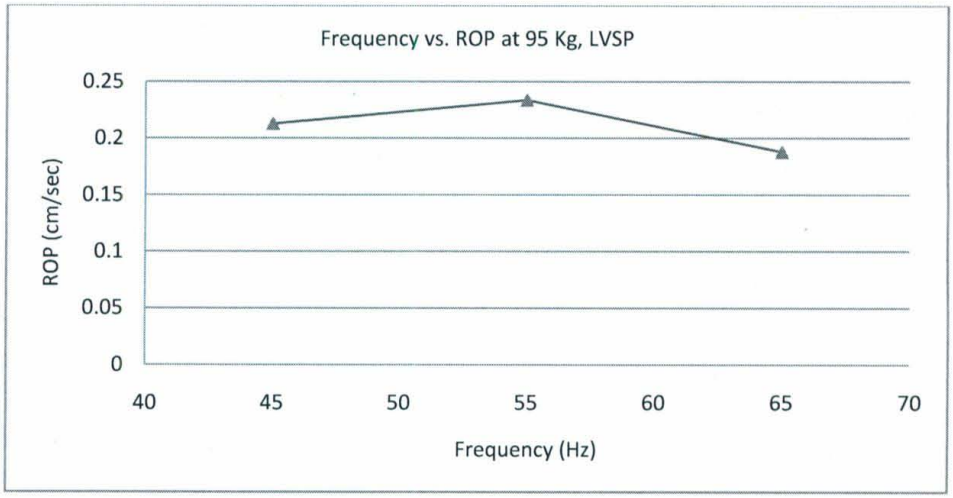

Figure 20. ROP v. Frequency curves at 95Kg and LVSP

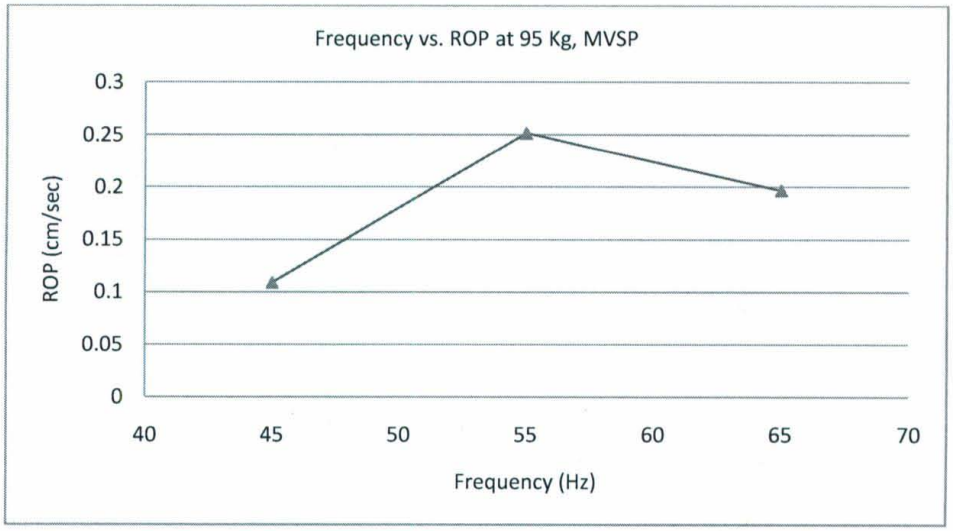

Figure 21. ROP v. Frequency curves at 95Kg and MVSP

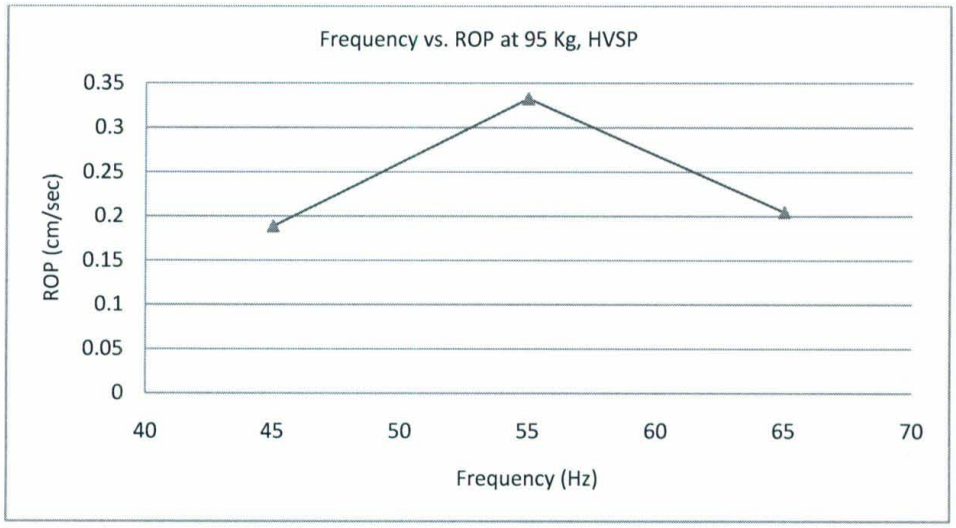

Figure 22. ROP v. Frequency curves at 95Kg and HVSP

These results show anomalous results in that ROP does not vary linearly with vibration amplitude as shown from previous work [Heng Li, 5]. It has been speculated that this is the result of anomalous behavior of vibration mechanism rather than a fundamental penetration mechanism response.

3.5.2 Bit Wear Study

If there is a variable capable of countering the ROP gains in these set of experiments, it will be the bit wear. There is a trade-off between ROP gains and bit wear. However, very little bit wear can be expected in short drill runs, and about the amount of wear can be difficult to measure or detect. Before and

during the course of the experiment, careful investigations of bit wear were done. Replicas of the bit were made during the course of each experiments and investigation is ongoing to study the geometry of the drilled holes. The condition of the bit was examined with optical microscopes. The Figures 23 and 24 below show the condition of the diamond drag bit before and after the experiment. They were taken with a microscope having a magnification of 3.15. The shapes of the individual diamonds were visualized clearly.

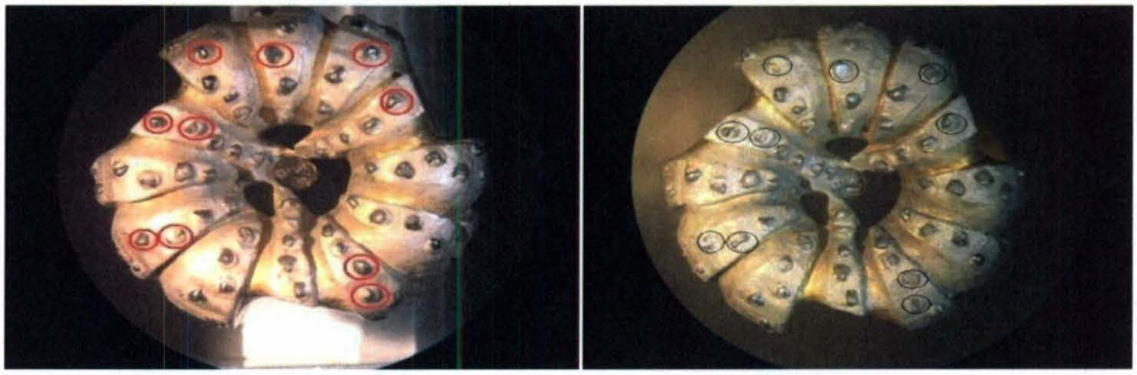

Figure 23. Plan view of diamond drag bit before (1st) and after (2nd) experiment

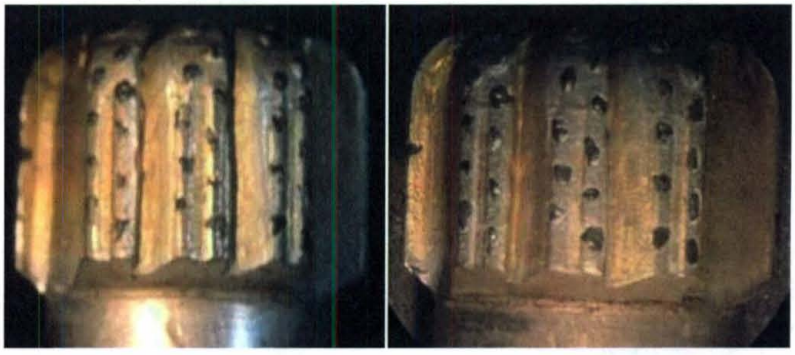

Figure 24. Side view of diamond drag bit before (1st) and after (2nd) experiment

Thorough physical examination of these figures revealed that there were changes on some of the diamond while many diamond do not seem to have worn significantly.

Some cutters i.e. diamonds show more wear than others. It is unlikely that some are weaker than others since same kind of diamonds are observed on the bit. Another important observation is that diamonds protruding from the bit do not protrude from the matrix by the same distance. At low loads it is likely that the force between the bit and the rock, i.e. the WOB, acts primarily through the diamonds but is distributed unequally between the diamonds. Some diamonds do not carry much load, or even any load, if they protrude less than other diamonds traveling in the same path. It could be that some diamonds bear the brunt of the cutting action at any one moment, perhaps because they protrude most in their "circle of travel" as the bit rotates - i.e. that at any one time in the drilling process just a portion of all the diamonds do most of the work, especially at lighter bit pressures (relative to the optimum pressure where ROP is a maximum). In the case of the embedded diamond bits, the cutters under the most stress will eventually wear and fall out, transferring the cutting process to other diamonds

At low loads there may be little or no direct contact between the matrix and the rock, perhaps only some three-body contact, i.e. through rock debris particles.

Comparing the two pictures, taken before the bit was used and after, there are clear signs of wear on about 10 cutters, out of about 50 visible. All the worn ones are on the "crown" of the segments, i.e. at about R/2 from the centre, where the surface is more or less perpendicular to the bit axis. There are two or three cutters in that position on each of the twelve segments, so the wear, such as it is, affects between 1/3 to 1/2 of those cutters. Some cutters do appear to show change due to wear, but not so many or so much that the total amount of wear can be said to be of concern in terms of a change in the performance of the bit. This is investigated further in the next chapter.

3.6 DSE - MSE

Several plots of the ROP v. WOB for the different drilling combinations have been considered to further understand the specific energy concept in VARD. Drilling with VARD Phase I setup has produced series of results which are now serving as the basis for which the final instrument to be developed will be based. The following analysis discussed the concept of DSE and MSE as applied to the current VARD instrument. The experimental data obtained from the drilling experiment done using the diamond drag bit are utilized for this analysis. The idea behind this analysis is to evaluate the contribution to ROP made by bit-

hydraulic interaction (water as drilling fluid in this case) and the possible contribution made by the vibration energy. Each drilling was started at 10mm below the surface of the concrete (i.e. in a 1.0 cm pre-drilled hole). The drilling were done in ascending order for all conditions varied (WOB, vibration frequency, vibration energy).

3.6.1 Bit Hydraulic Contribution

Conventional drilling and drilling at 45 Hz, 55 Hz and 65 Hz frequency were analyzed. MSE values for conventional drilling, (axial and torsion) and for vibration drilling, (axial, torsion and vibration) were calculated from equation 2. DSE values were obtained from equation 9.

The value of the hydraulic power HP_B was obtained from equation 11 below:

$$HP_B = \frac{\Delta P_b}{1714} * q \qquad (11)$$

$$\Delta P_b = 8.311 * 10^{-5} * \rho * \frac{q^2}{C_d^2 A_t^2} \qquad (12)$$

ρ is the density of water (Lb/gal), q is the flow rate (GPM) used, C_d is a dimensionless number having a value of 0.95. A_t is the flow area of all nozzles (in^2).

ΔP_b was calculated from equation 12 and used in equation 11 to calculate the hydraulic power. The flow rate q fluctuates by 0.2 gpm. The evaluation of hydraulic contribution to rock cutting and cuttings removal in this study shows it is very small and therefore this fluctuation of q is negligible.

A_t was calculated from the three nozzles of the diamond drag bit by measuring the diameters. Hence,

$$HP_B = 0.003853 \text{ hp}$$

The MSE was calculated directly from equation 2 in chapter 2. But for the DSE, we still require a value for lambda which is a dimensionless bit-hydraulic factor depending on bit diameter. From the figure given below by Armenta [13], the curve was re-plotted and extrapolated to obtain the value of λ. With these, the DSE values were calculated.

$$\lambda = 0.8$$

λ is very sensitive to bit diameter for small bits as shown in figure 25 below. However in this case, the contribution to DSE is very small and therefore the uncertainty in λ is not of concern.

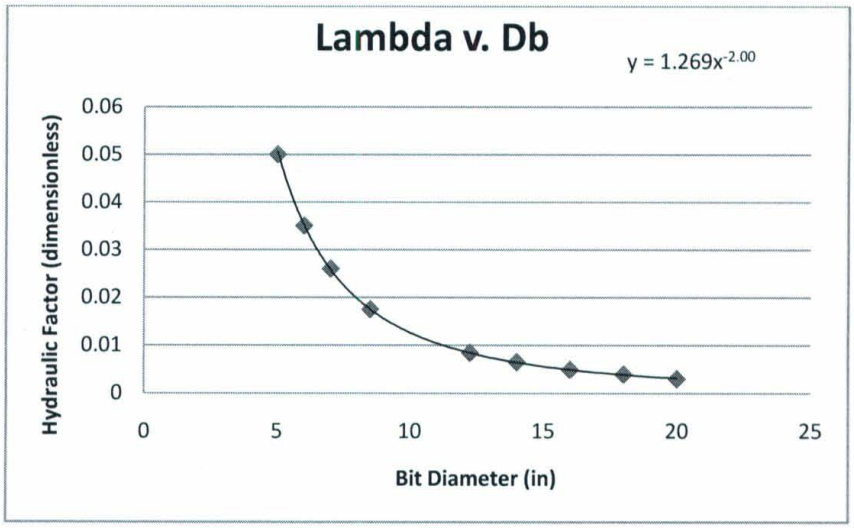

Figure 25. Hydraulic Factor conversion chart

Other parameters used include WOB which range from 99.4 Ib (45 Kg) to 284.8 Ib (129 Kg), rotary speed which is constant at 300 rpm, A_b which is calculated and have a value of 1.23 in^2. The torque was calculated from the value of induced current obtained from the current sensor during the experiment. Initially, we aren't able to get the current values directly; however the current was calculated from voltage display values obtained from LabVIEW signal express (National Instrument) using the impedance of the motor. All voltage measurements were taken only while drilling. The torque is calculated using a derived the basic formula below which is based on sensor current (Appendix A):

$$T = 527.12\frac{I}{N} \qquad (13)$$

Where I is the induced motor current and N is the rotary speed.

Having calculated the values of DSE and MSE, there is need to calculate the bit hydraulic contribution to the specific energy correlation. This is given as the ratio of the bit hydraulic-energy contribution as a function of the mechanical energy contribution and was calculated from equation 14 shown below.

$$Bit\ Hydraulic\ Contribution = \left\{\frac{MSE-DSE}{MSE}\right\} * 100 \qquad (14)$$

The values of MSE, DSE and bit hydraulic-energy contribution were obtained for conventional and vibration (45 Hz, 55 Hz, 65 Hz) drilling. The following plots were obtained (Figure 26 and 27). The plots show the MSE, DSE versus ROP plotted for conventional and 55Hz (High vibration power) drilling conditions.

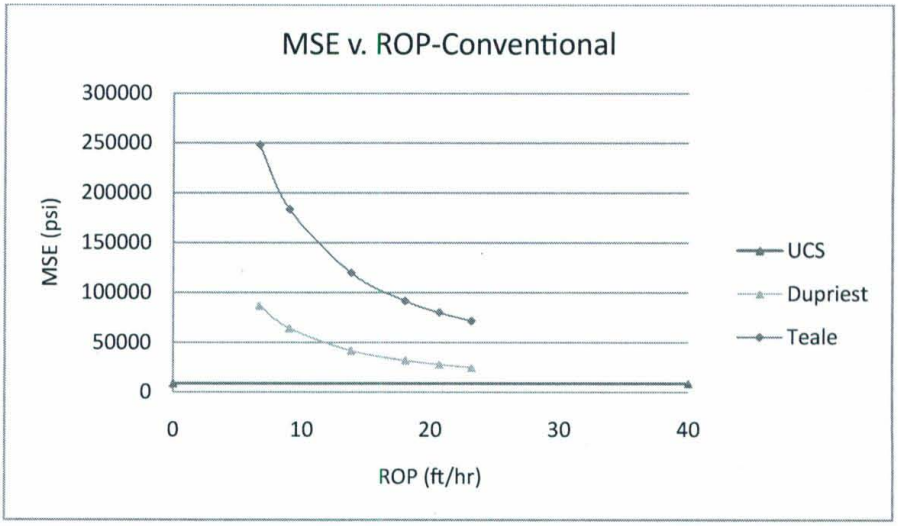

Figure 26. MSE v. ROP for conventional drilling

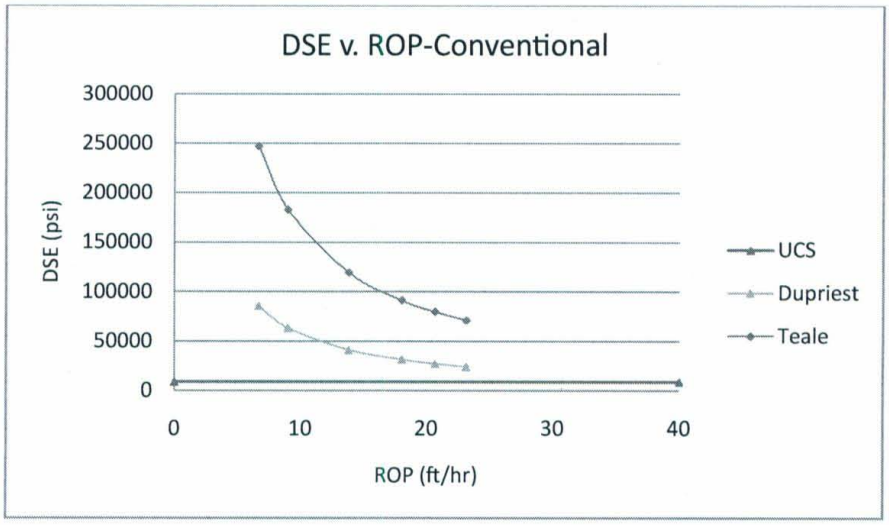

Figure 27. DSE v. ROP for conventional drilling

The charts above show estimated curves of MSE and DSE by applying both Teale's original MSE equation and Dupriest's equation. Teale's equation shows

that drilling at higher WOB for this particular case is still in the transition region, while Dupriest's shows that at higher WOB, drilling is already approaching the efficient drilling region as the curve is getting closer to the UCS value as a result of 35% efficiency applied as he argued that bits are about 30% efficient even at peak performance.

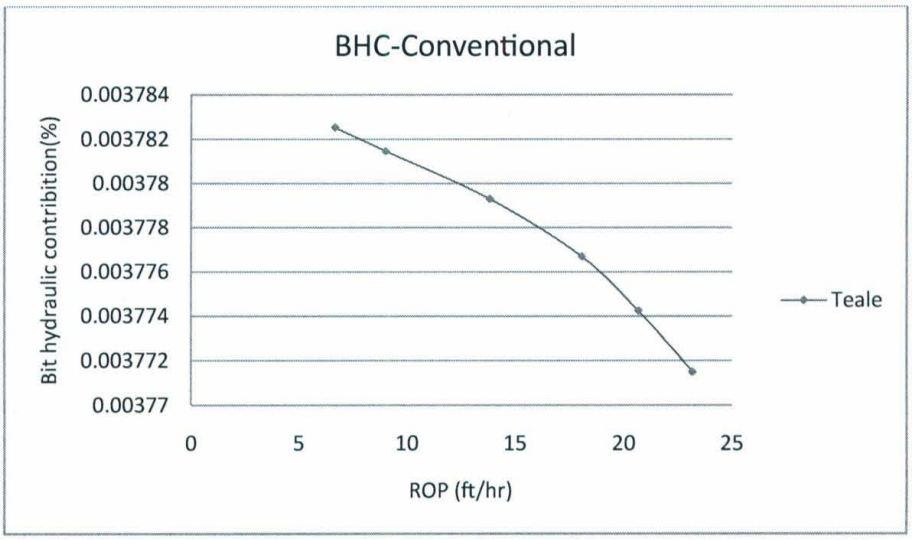

Figure 28. Bit Hydraulic Contribution v. ROP for conventional drilling using Teale's equation

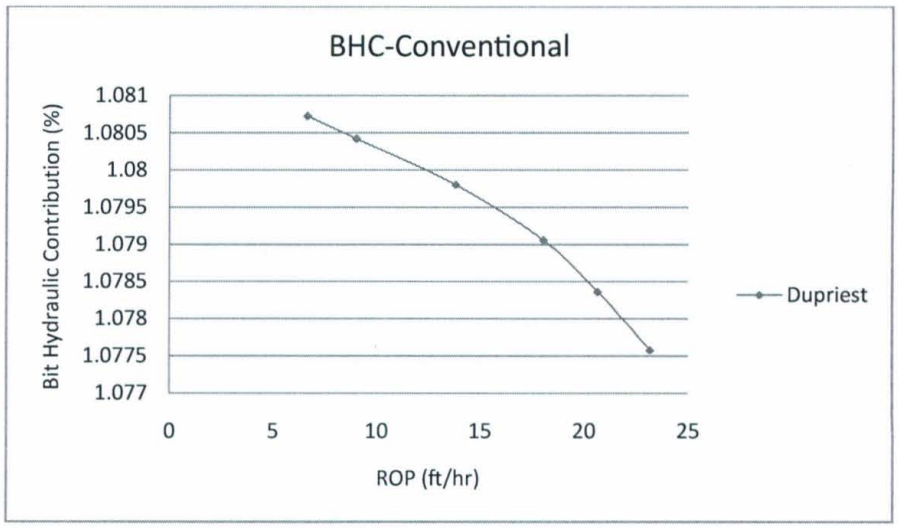

Figure 29. Bit Hydraulic Contribution v. ROP for conventional drilling using Dupriest equation

Figure 28 and 29 compares bit hydraulic contribution using Teale's and Dupriest's equation. As expected, BHC is higher using the later equation, though it decreases generally as the ROP increases for both scenarios.

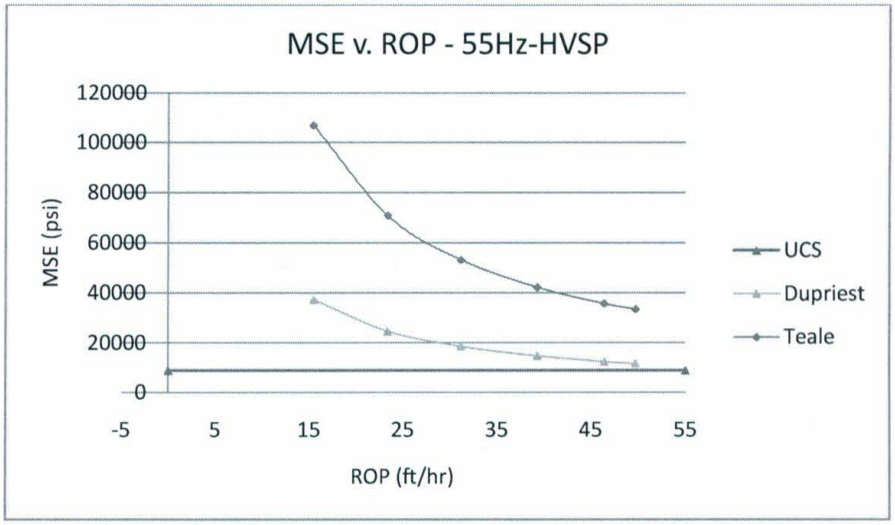

Figure 30. MSE v. ROP for 55HZ - HVSP drilling

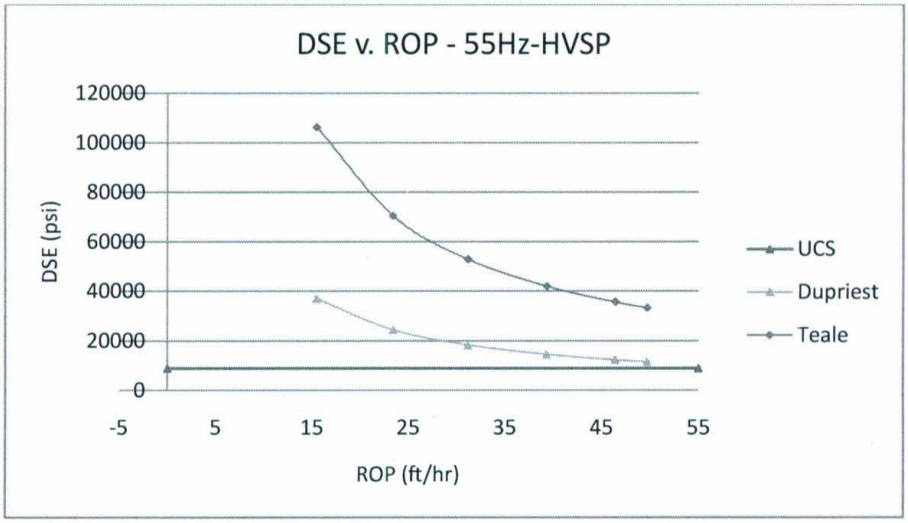

Figure 31. DSE v. ROP for 55HZ - HVSP drilling

The above figures (30 and 31) show similar MSE and DSE plots for drilling at 55HZ – HVSP. In this particular case, both methods revealed drilling at higher

WOB is approaching efficient region. This is as a result of the application of vibration during drilling to help improve the ROP. This also has influence on the BHC plots shown in figure 32 and 33 as the BHC in this case becomes lower compared to that observed for Conventional drilling.

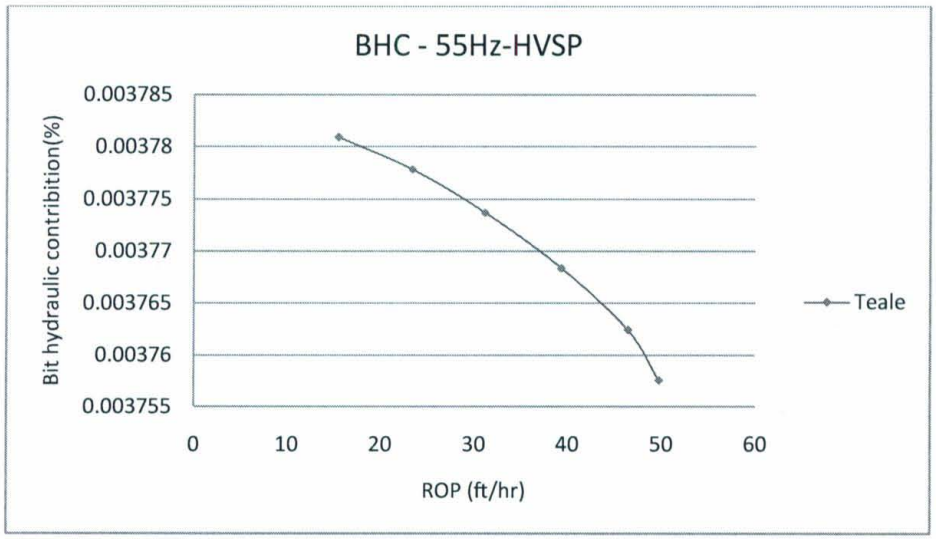

Figure 32. Bit Hydraulic Contribution v. ROP for 55HZ - HVSP drilling using Teale's equation

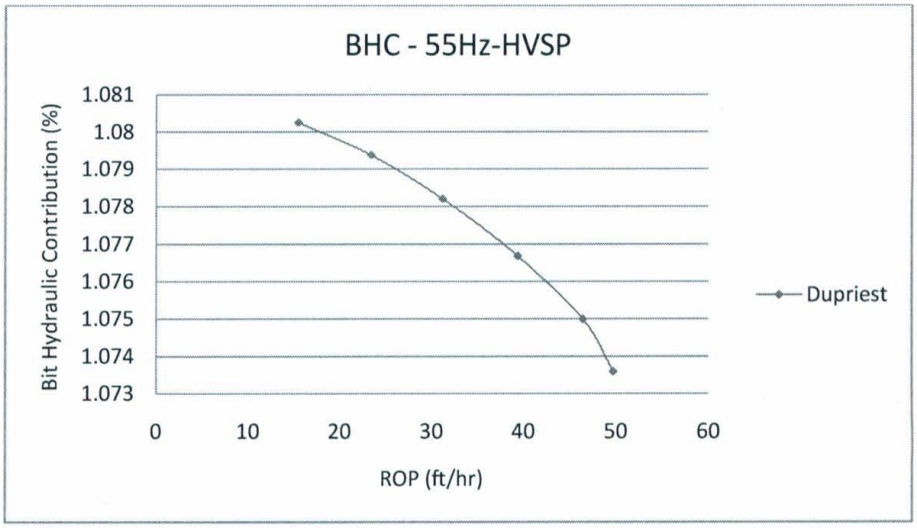

Figure 33. Bit Hydraulic Contribution v. ROP for 55HZ - HVSP drilling using Dupriest's equation

3.6.2 Vibration Energy Contribution

From the analysis done thus far, it is clear that from these set of experiments carried out on the VARD system, the contribution of fluid energy to the breakage and removal of rock is very small. Most of the energy employed is either from axial, torsion or vibration. It therefore will be imperatively important to estimate the portion of this energy produced by vibration. Applying similar concept as in the DSE, the vibration energy contribution is calculated as shown below:

$$VEC = \frac{MSE_C - MSE_V}{MSE_C} * 100 \qquad (15)$$

Where MSE_V is the mechanical specific energy from vibration drilling and MSE_C is the mechanical specific energy from conventional drilling. To show this, data from conventional drilling and vibration drilling at 55 Hz frequency were utilized.

Table 2. Vibration Energy Contribution Analysis at 55 Hz and LVSP

Conventional MSE X 10^3 (psi)	Vibration 55 Hz, LVSP MSE X 10^3 (psi)	(MSE_C - MSE_V) X 10^3 (psi)	Vibration-Energy Contribution (MSE_C - MSE_V)/ MSE_C X 100
125	80	45	36
93	57	36	39
60	40	20	33
46	30	16	35
40	27	13	33
36	22	14	39
			35.83

Table 3. Vibration Energy Contribution Analysis at 55 Hz and MVSP

Conventional MSE X 10^3 (psi)	Vibration 55 Hz, MVSP MSE X 10^3 (psi)	(MSE_C - MSE_V) X 10^3 (psi)	Vibration-Energy Contribution (MSE_C - MSE_V)/ MSE_C X 100
125	72	53	42
93	46	47	51
60	34	26	44
46	28	18	39
40	24	16	40
36	21	15	42
			43.1

Table 4. Vibration Energy Contribution Analysis at 55 Hz and HVSP

Conventional MSE X 10^3 (psi)	Vibration 55 Hz, HVP MSE X 10^3 (psi)	(MSE_C - MSE_V) X 10^3 (psi)	Vibration-Energy Contribution (MSE_C - MSE_V)/ MSE_C X 100
125	54	71	57
93	36	57	62
60	27	34	56
46	21	25	54
40	18	22	55
36	17	19	53
			56.17

The three tables shown above display values of the vibration energy (%) contribution to the overall MSE applied in drilling. The MSE values are for different WOB, 99.41 Lb to 284.8 Lb. Results show that at low vibration shaker power position, an average of 36% of the MSE is supplied from vibration while the remaining energy are from axial force and torsion. At medium vibration shaker position, we have an average of 43%, while 56% of the total energy at high vibration shaker power position is from vibration.

3.6.3 Drilling Efficiency

The percent drilling efficiency is calculated from Equation 3. The tables and plots shown below illustrates the trend for conventional and vibration drilling at 55 Hz. The average UCS of the drilled rock which is 62 MPa (9000 psi) was used. The trend shows drilling efficiency increases with increase in ROP.

As can be seen on comparing efficiencies at the same ROP, the relationship of drilling efficiency to ROP is virtually identical in all cases, while the ranges of ROP, and hence efficiency, achieved varied. Comparing the drilling efficiency for vibration drilling and conventional drilling in this case, more than 80 % (about 100% at HVSP) increase in drilling efficiency was observed for vibration drilling. This again confirms the importance of the VARD concept.

Table 5. Drilling Efficiency for Conventional Drilling

WOB (lbf)	MSE (psi) x 10^3	UCS/MSE	Drilling Eff.(%)	ROP (ft/hr)
99.4	13	0.072	7.18	6.66
136.5	93	0.097	9.70	9.01
173.6	60	0.149	14.89	13.82
10.7	46	0.194	19.44	18.06
247.8	40	0.222	22.24	20.67
284.8	36	0.249	24.93	23.18

Table 6. Drilling Efficiency for 55 Hz, LVSP Drilling

WOB (lbf)	MSE (psi) x 10^3	UCS/MSE	Drilling Eff. (%)	ROP (ft/hr)
99.4	80	0.111	11.20	10.39
136.5	57	0.157	15.73	14.6
173.6	40	0.226	22.63	21.02
210.7	30	0.297	29.74	27.64
247.8	27	0.335	33.52	31.18
284.8	22	0.405	40.47	37.68

Table 7. Drilling Efficiency for 55 Hz, MVSP Drilling

WOB (lbf)	MSE (psi) x 10^3	UCS/MSE	Drilling Eff. (%)	ROP (ft/hr)
99.4	72	0.125	12.47	11.57
136.5	46	0.197	19.72	18.31
173.6	34	0.266	26.57	24.68
210.7	28	0.320	32.01	29.76
247.8	24	0.372	37.20	34.61
284.8	21	0.431	43.13	40.16

Table 8 Drilling Efficiency for 55 Hz, HVSP Drilling

WOB (lbf)	MSE (psi) x 10^3	UCS/MSE	Dilling Eff. (%)	ROP (ft/hr)
99.4	54	0.167	16.67	15.47
136.5	36	0.252	25.19	23.39
173.6	27	0.335	33.55	31.18
210.7	21	0.423	42.28	39.33
247.8	18	0.498	49.84	46.42
284.8	17	0.534	53.34	49.72

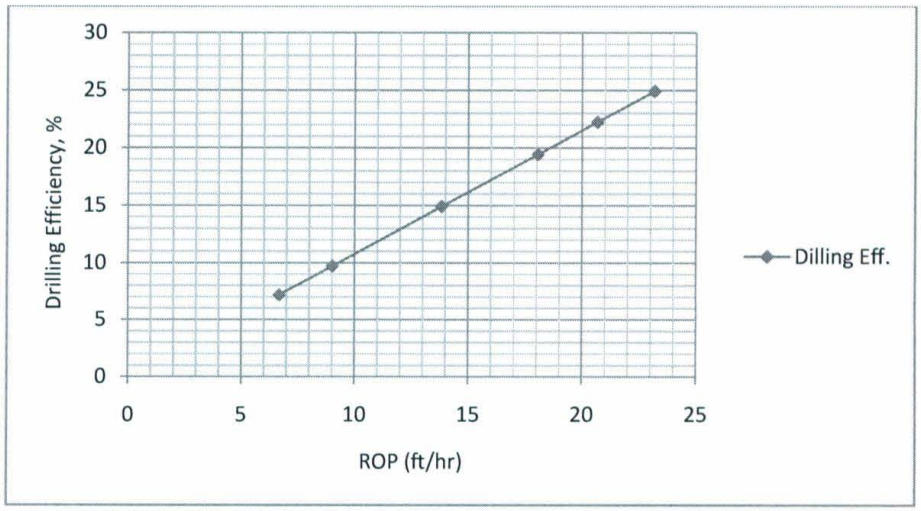

Figure 34. Drilling Efficiency for Conventional Drilling

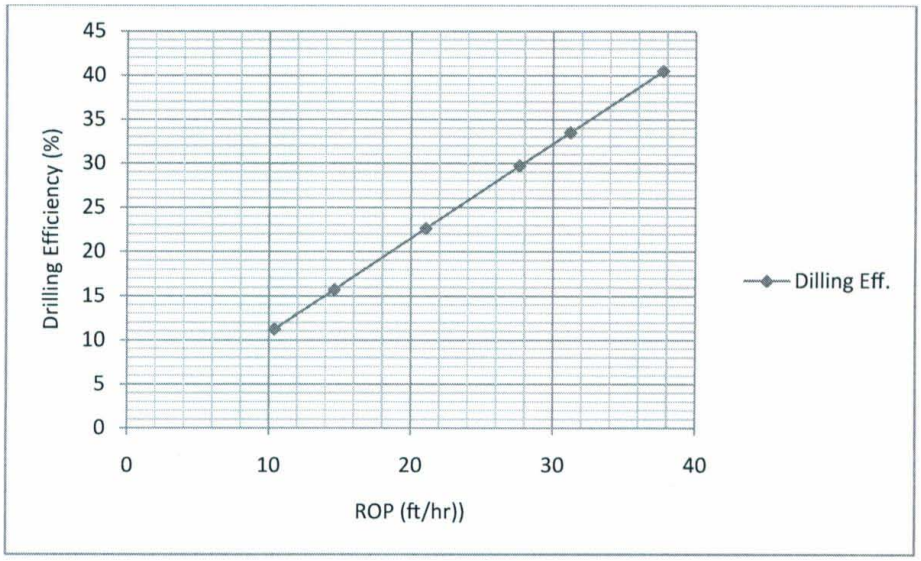

Figure 35. Drilling Efficiency for 55HZ - LVSP Drilling

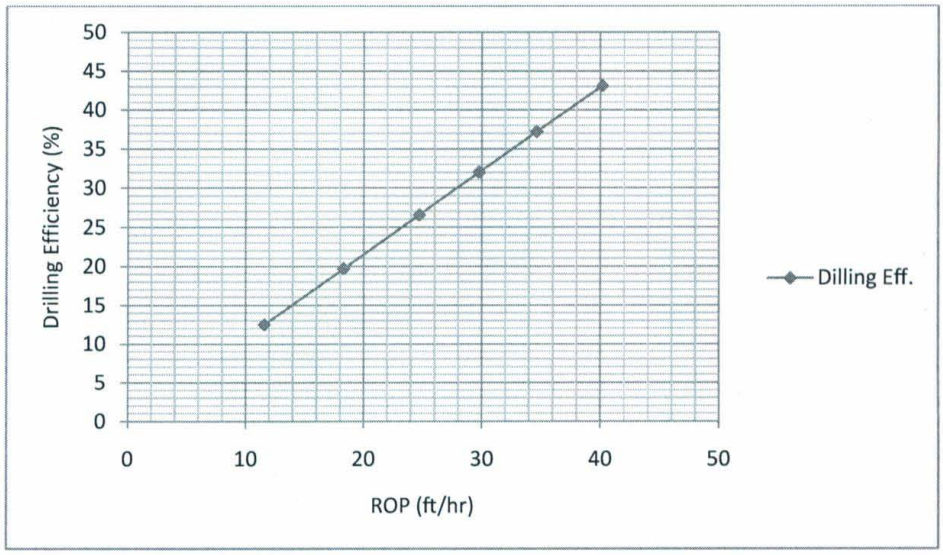

Figure 36. Drilling Efficiency for 55HZ - MVSP Drilling

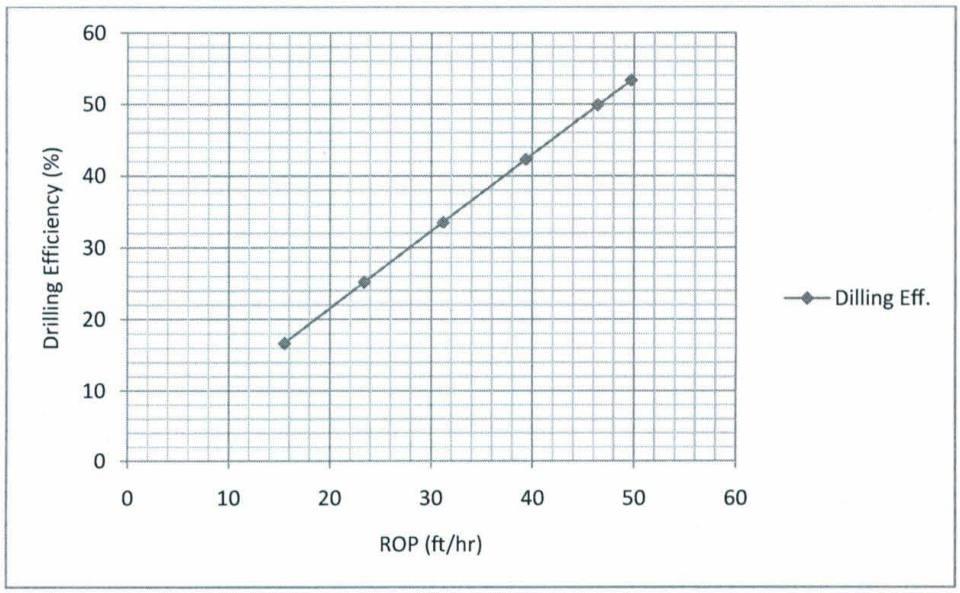

Figure 37. Drilling Efficiency for 55HZ - HVSP Drilling

3.7 Summary

The chapter is a study of the effect of varying the frequency and amplitude of vibration during vibration drilling by using a diamond drag bit. It was observed that drilling with vibration at higher WOB could produce significant increase in ROP ranging from about 25% to more that 100%, depending on the drilling combinations applied. The 55HZ frequency appears to be the optimum frequency of drilling and generally, for most drilling combination, the higher the amplitude of vibration, the higher the ROP. There was little evidence of bit wear not enough to affect the overall drilling efficiency. A more quantitative and comprehensive study of bit wear is suggested for future work.

A study of vibration characteristics revealed that the hydraulic contribution to breaking and removal of cuttings is minute and that a higher percentage of the energy required are supplied by vibration as this seems to increase proportionally with the vibration shaker power position utilized. Overall, the drilling efficiency was good with MSE reduction (improved efficiency) increasing with vibration amplitude.

Chapter 4

PDC Bit Drilling

About this chapter: This chapter introduces a more elaborate drilling investigation carried out using polycrystalline diamond compact bit. Some modifications were made to the drilling setup to aid real-time vibration and drilling data acquisition. As in the previous experiment, both the frequency and amplitude of vibration were varied at constant rotary speed and flow rate using different values of WOB. The chapter provides a better understanding of the response and behavior of PDC bit to optimizing VARD.

4.1 Introduction

Previous VARD experimental studies were done at 60Hz by varying the amplitude of vibration, showing that ROP increases with increase in vibration amplitude. In order to move a step further in understanding VARD, a set of experiments was designed to provide data for the evaluation of the effects of

frequency and amplitude of vibration in rotary drilling using a diamond drag bit. The frequencies were varied at different levels of amplitude, keeping the rotary speed and fluid flow rate constant at different values of WOB. Drilling was done at atmospheric pressure using water as the drilling fluid. Rock samples with known unconfined compressive strength (UCS) were drilled with a fully instrumented VARD laboratory drill rig. Real-time drilling and vibration data were obtained.

4.2 Drill Rig Modification

As in the previous work, this experiment was also performed using the instrumented variable rotary-vibration system which applies rotation and vibration to the drill bit. The experimental drill rig was modified in order to understand better the vibration characteristics and also to obtain real time drilling and vibration data. The modification included addition of more sensors and an additional data acquisition (DAQ) system.

4.2.1 PDC Bit

The polycrystalline diamond compact bit used for this experiment has a diameter of 1.00-in. The bit consists of two cutting blades and two nozzles.

Figure 38. The 1.00-in diameter PDC Bit

4.2.2 Instrumentation and DAQ System

Additional sensors were connected to the drilling system to obtain more comprehensive readings which might help explain the drilling characteristics better. Below are list of sensors and DAQ systems with their functions:

- **Load Cell :** in the drillstring rotating with the drill bit with its power and data pack. It measures the force variation during vibration drilling

- **Current Sensor:** in the power leads to the drillstring motor measures the current output required to obtain bit rotation torque
- **LPDT:** in contact with the motor and gear box mounted on the rig post provides consistent records of the distance drilled which is plotted against time and from which the ROP can be estimated.
- **LVDT:** two of these mounted on the rig frame where used, one near the base connected to the vibrating table and the other on the holder for a guide bearing and placed on each drilled sample, to measure vibration displacement.
- **Flow Sensors:** sensors in the water supply line connected to measure the flow rate and flow pressure during drilling.
- **LABVIEW Signal Express:** used to acquire ROP, rock displacement, vibrating table displacement, flow rate and flow pressure measurements as well as motor induced current measurement; all acquired in real time.
- **AGILE LINK:** provided non-contact data transmission to obtain the rotating load cell readings in real time.

More details on the characteristics and usage of these instruments and DAQ systems can be found in Li [5].

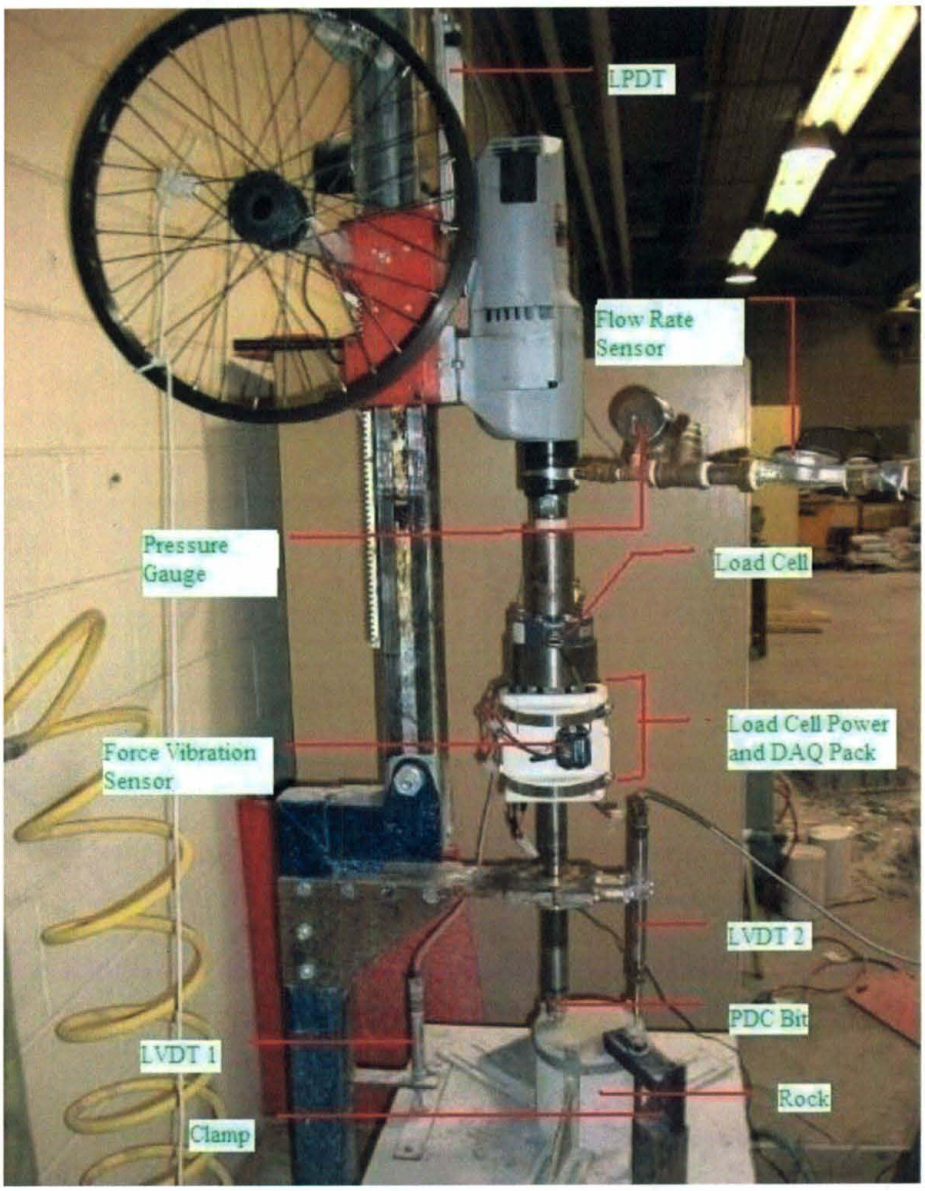

Figure 39. Modified Drilling Setup

4.3 Drilling Procedure

The drilling procedure used in this experiment is similar to that used for the Drag bit experiment. The rock sample was set in place and in this case, a clamp was introduced to hold the sample firmly in place in order to ensure that the sample vibrates along with the vibrating table. Vibration was set to the desired frequency and amplitude and the fluid flow turned on. Weight was applied and rotation was turned on. The rock was initially drilled to a depth of 10mm to create a platform for the drilling proper. Each drilling lasted an average of 1.5 minutes. In order to stop drilling, the weight was first lifted, the bit disconnected from the rock before rotation and vibration was turned off. The acquired measurements with the DAQ systems were saved and ready for processing and analysis. The average UCS of the rock after 68 days of curing was 65.29 MPa.

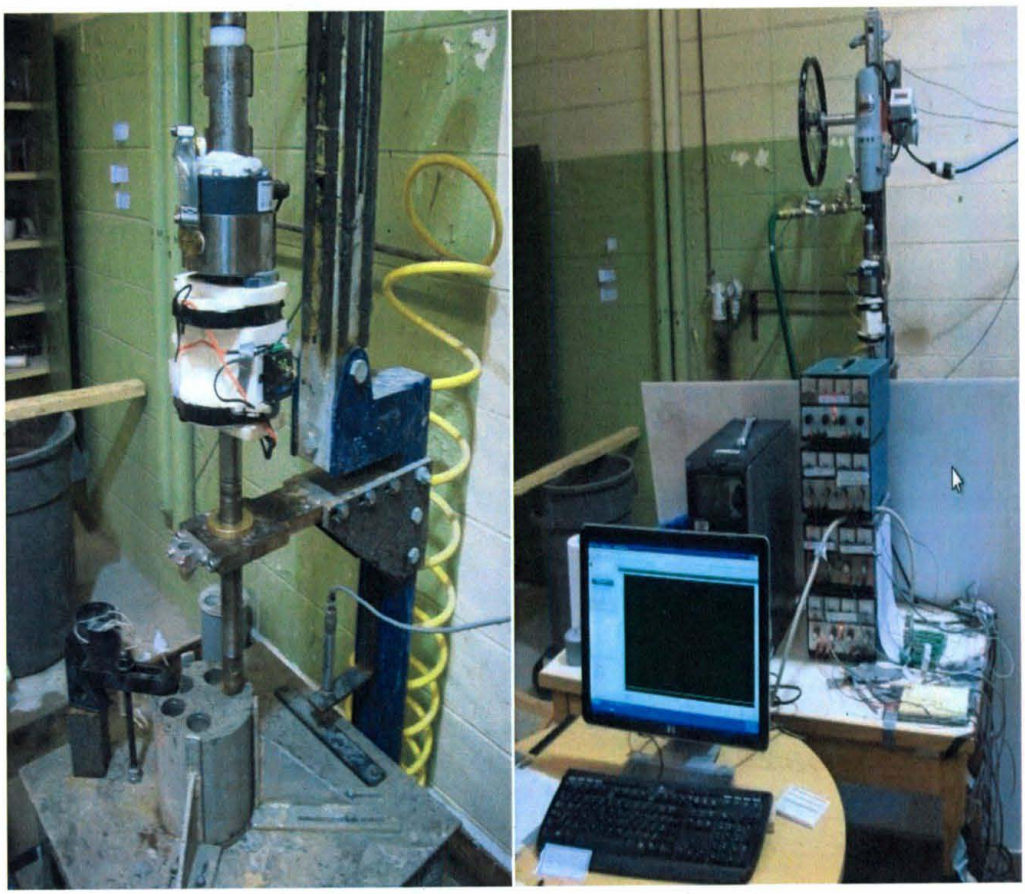

Figure 40. Drilling Setup after a drilling run and the DAQ System

4.4 Experimental Results

4.4.1 ROP v. WOB Curves

The plots below shows ROP-WOB curves plotted for the different drilling combinations.

At 45 HZ frequency, as the WOB increases, the ROP initially increase as seen in Figure 41. This trend continues from lower WOB to a WOB of about 106Kg,

after which the ROP seems to be dropping. This drilling condition also shows that at most value of WOB, the higher the vibration energy supplied to the drilling system, the higher the ROP at a fixed WOB. If the dip at 120kg WOB is an anomalous result, the overall trend at medium power is the same as at low power.

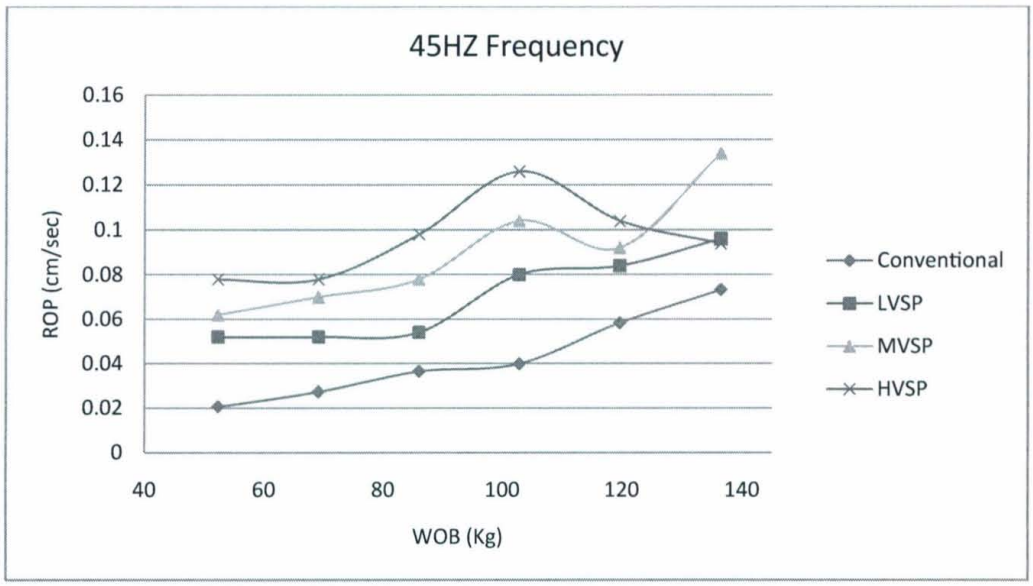

Figure 41. 45HZ PDC Bit Drilling

Figure 42 shows the results of drilling at 55HZ frequency. In this case, the pattern is the same at all vibration powers including no vibration i.e. ROP increasing with increasing WOB generally more steeply at higher WOB than at lower WOB. At lower WOB, there isn't much difference in the ROP recorded

and the ROP values increase insignificantly from of about 69Kg to 120Kg. As the WOB increases to 136Kg, the ROP values increases significantly. This gives a clue that in order to obtain a significant ROP increase at this condition using the PDC bit, higher WOB will be required. Unfortunately, the current VARD setup can't take higher WOB.

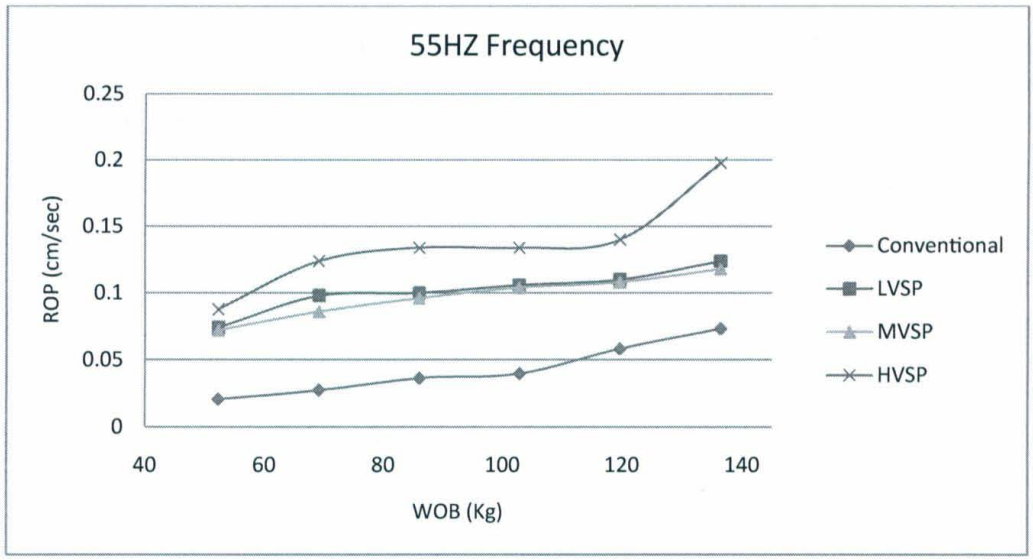

Figure 42. 55HZ PDC Bit Drilling

At 65HZ drilling, Figure 43, it is interesting to see that there is a significant rise in ROP at lower WOB until 86Kg before the values start to level out at low and medium power and drop at high power. This result is of interest as it shows that vibration at lower WOB can be utilized to obtain significant rise in ROP.

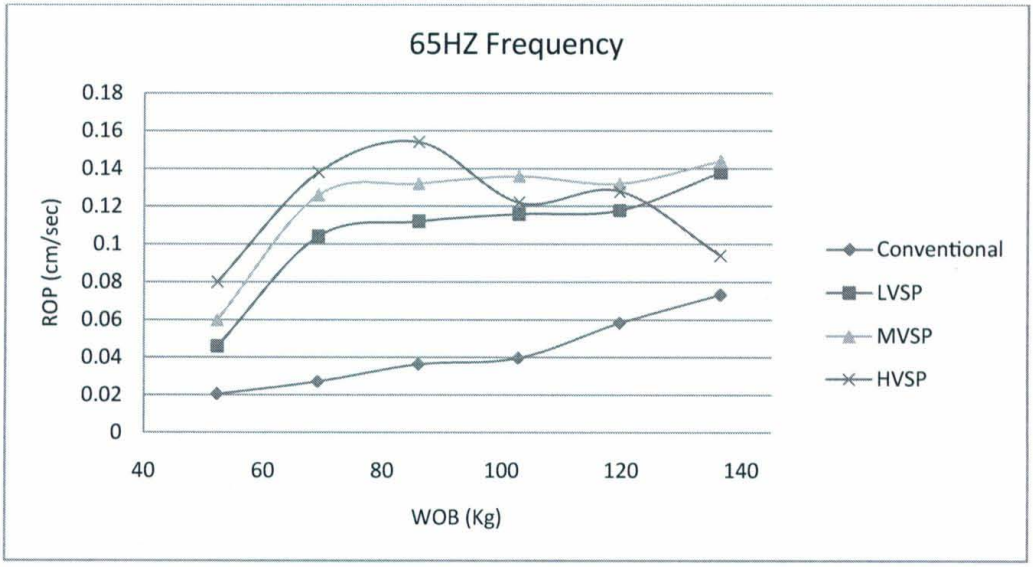

Figure 43. 65HZ PDC Bit Drilling

Figures 44 to 46 can help to choose a particular drilling frequency that could be applied at various vibration power shaker positions. For the LVSP and MVSP cases, the better frequency is in the order 65HZ > 55HZ > 45HZ, but at HVSP, the 55HZ frequency looks the better drilling frequency especially while drilling at higher WOB.

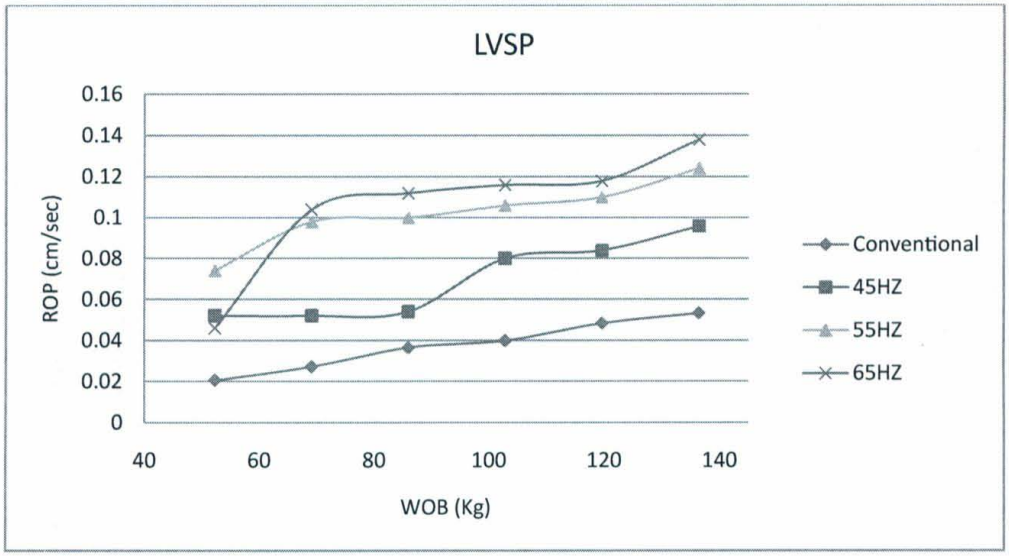

Figure 44. PDC Bit Drilling at LVSP

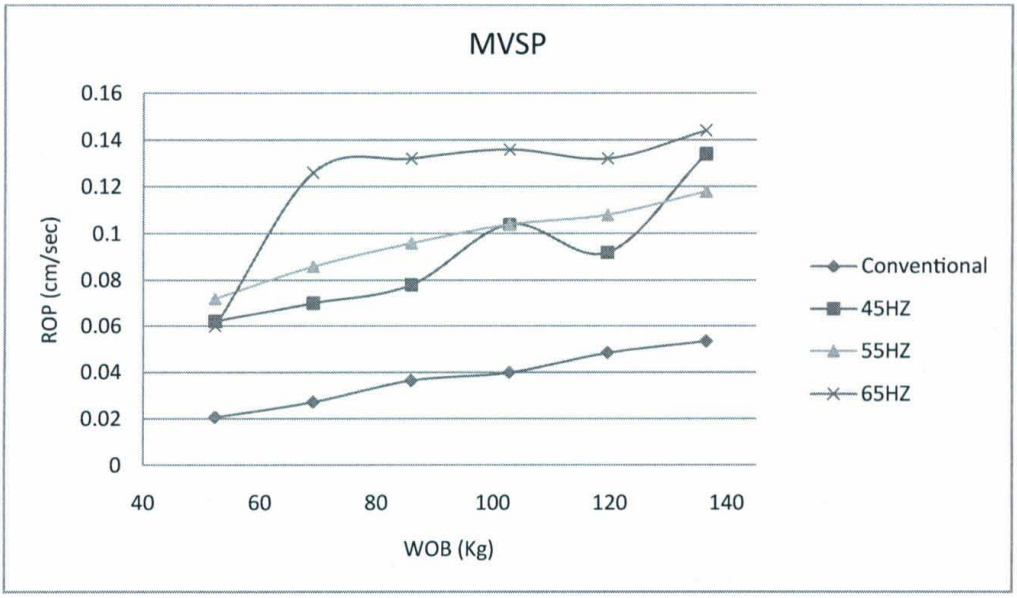

Figure 45. PDC Bit Drilling at MVSP

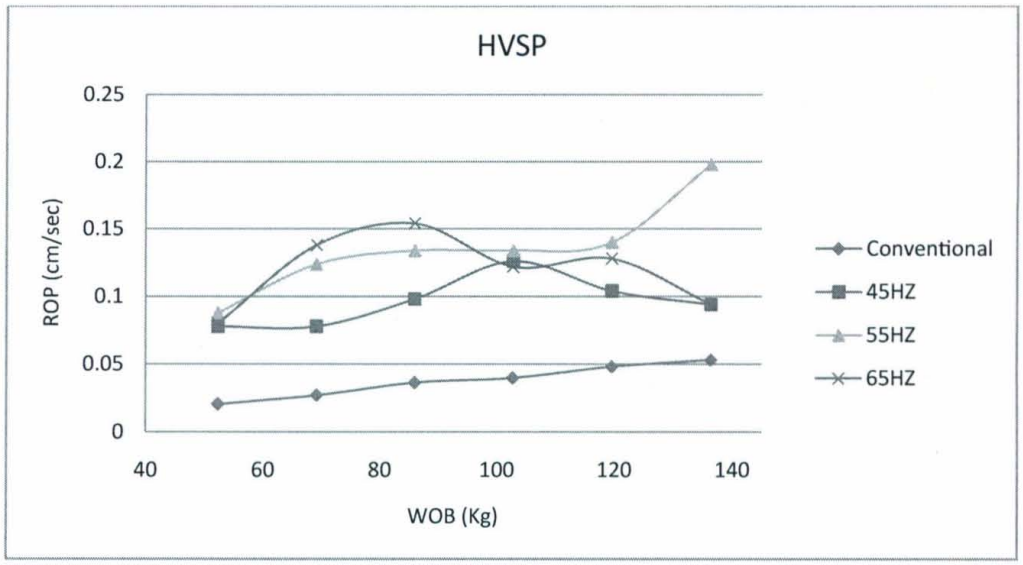

Figure 46. PDC Bit Drilling at HVSP

4.4.2 Displacement Amplitude Data Analysis

In order to understand the vibration characteristics better, several plots (Figures 47 - 61) are shown. These plots show that the higher the WOB applied, the lower the vibration amplitude. There is a similar trend observed for all drilling conditions and combinations. The non-linearity observed in certain cases signify that though the amplitude reduces as the WOB increases, these reduction might not be due to the increase in WOB alone.

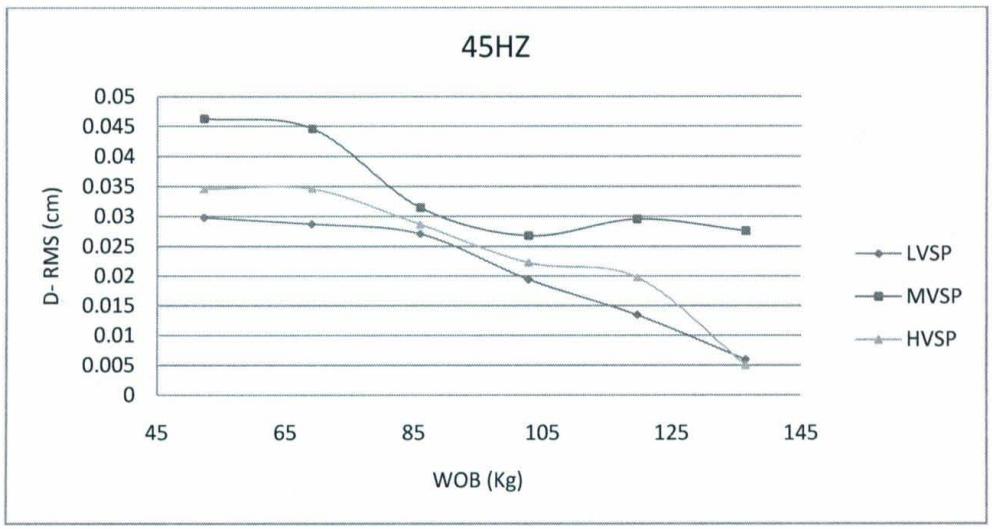

Figure 47. D-RMS v. WOB at 45HZ Frequency

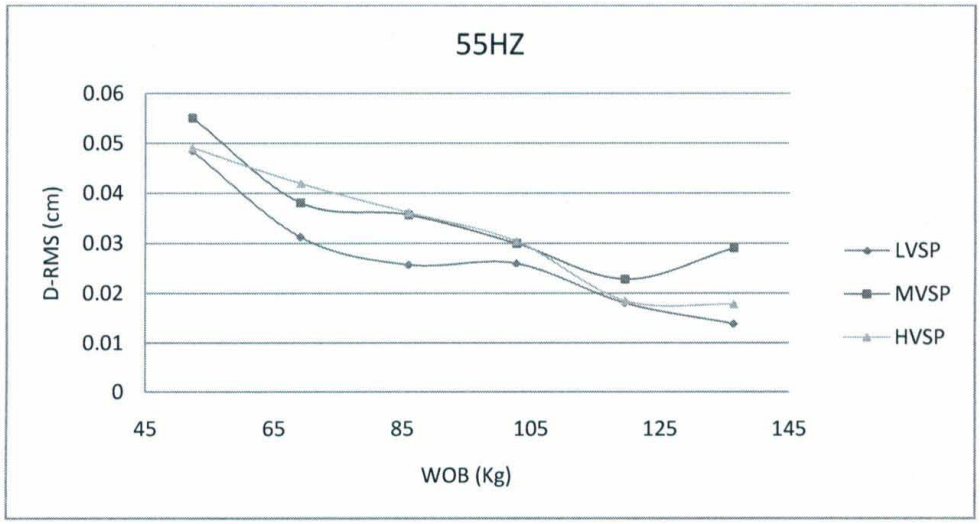

Figure 48. D-RMS v. WOB at 55HZ Frequency

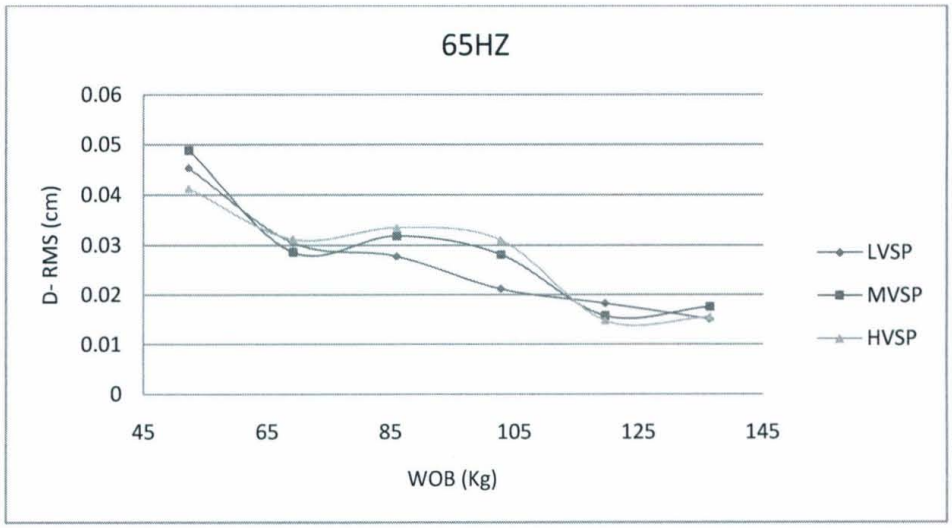

Figure 49. D-RMS v. WOB at 65HZ Frequency

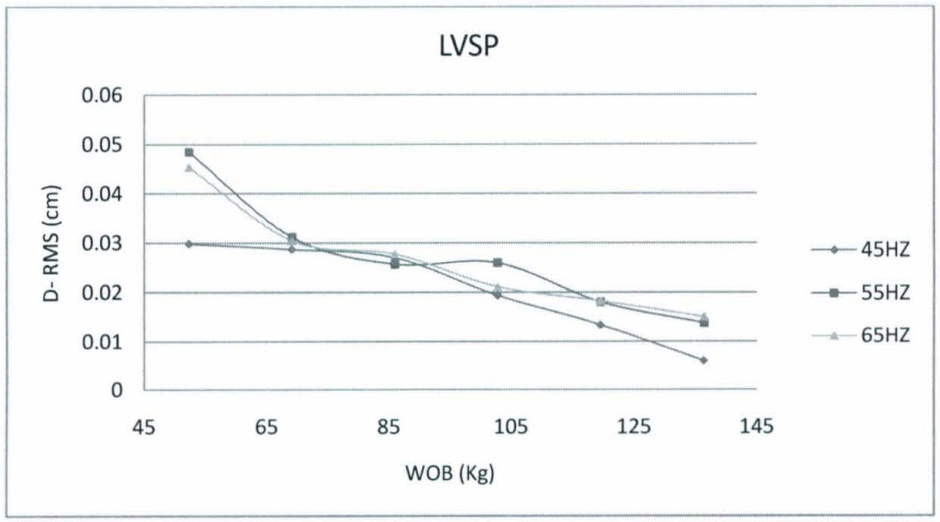

Figure 50. D-RMS v. WOB at LVSP

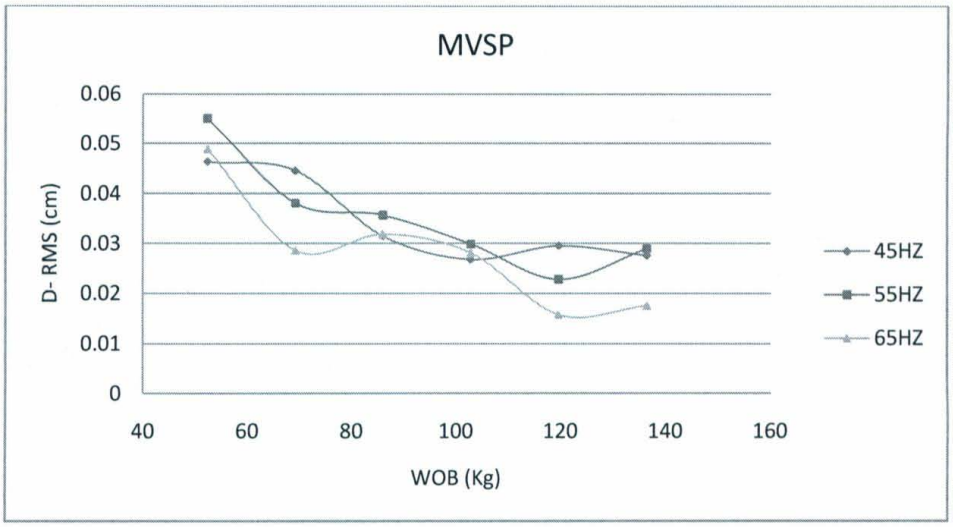

Figure 51. D-RMS v. WOB at MVSP

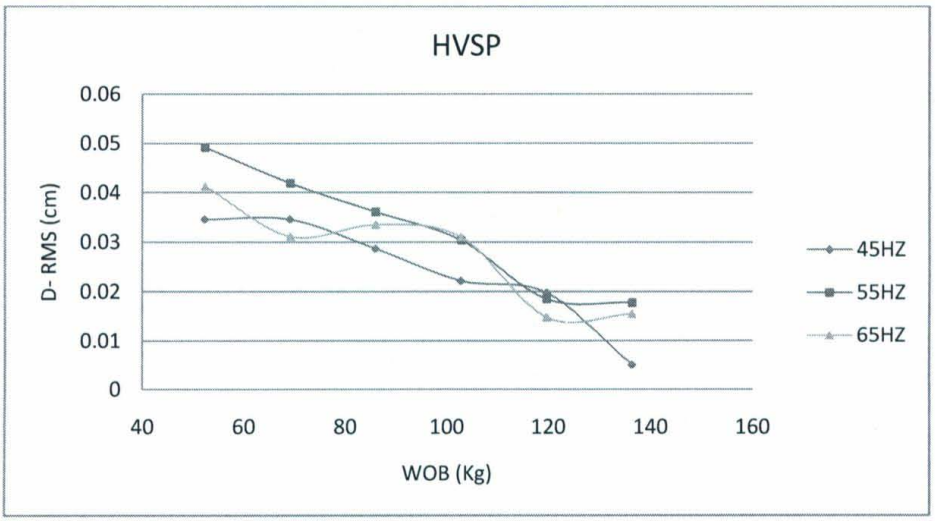

Figure 52. D-RMS v. WOB at HVSP

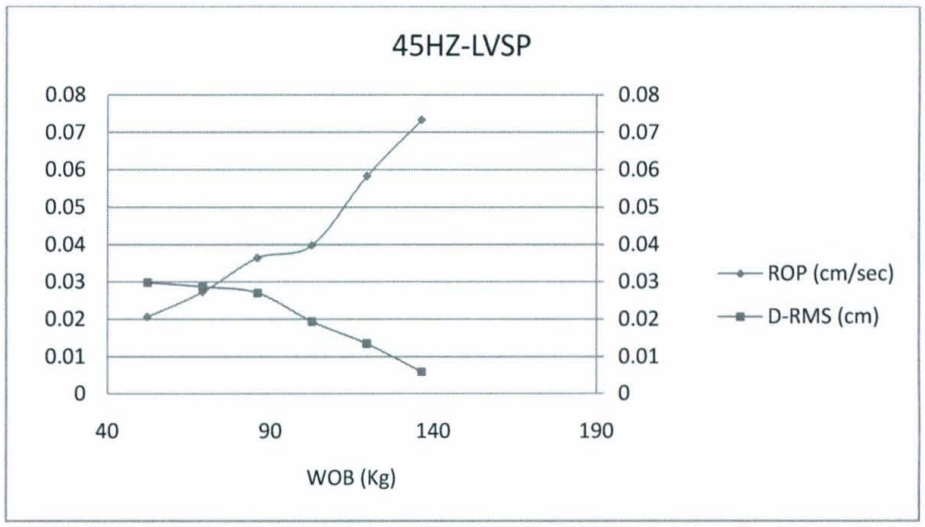

Figure 53. D-RMS and ROP v. WOB at 45 – LVSP

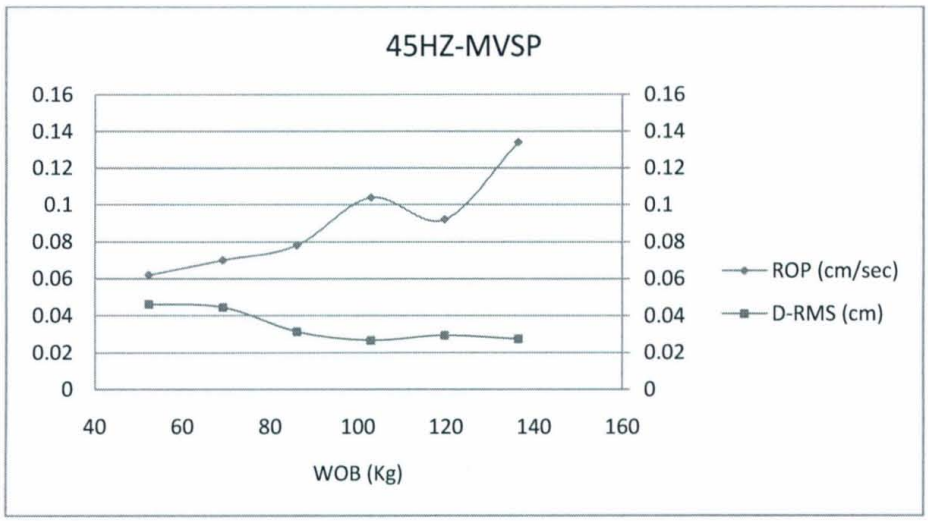

Figure 54. D-RMS and ROP v. WOB at 45 - MVSP

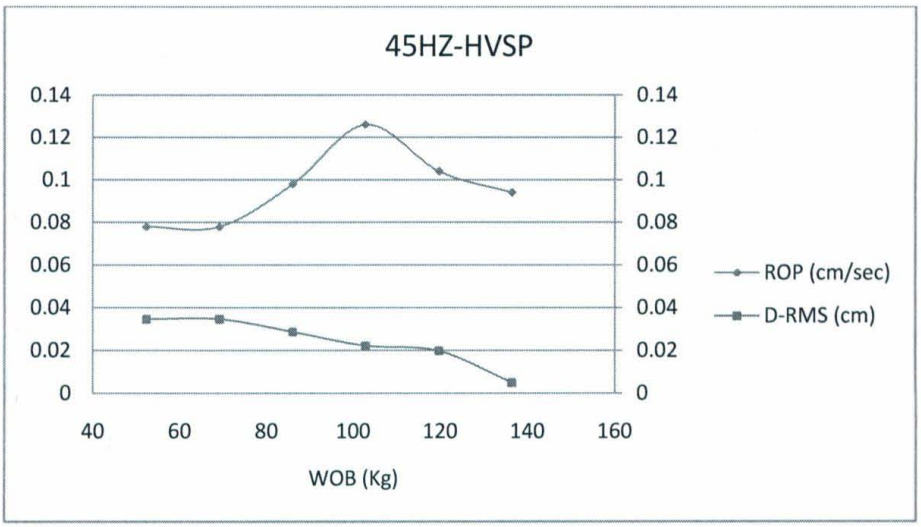

Figure 55. D-RMS and ROP v. WOB at 45 - HVSP

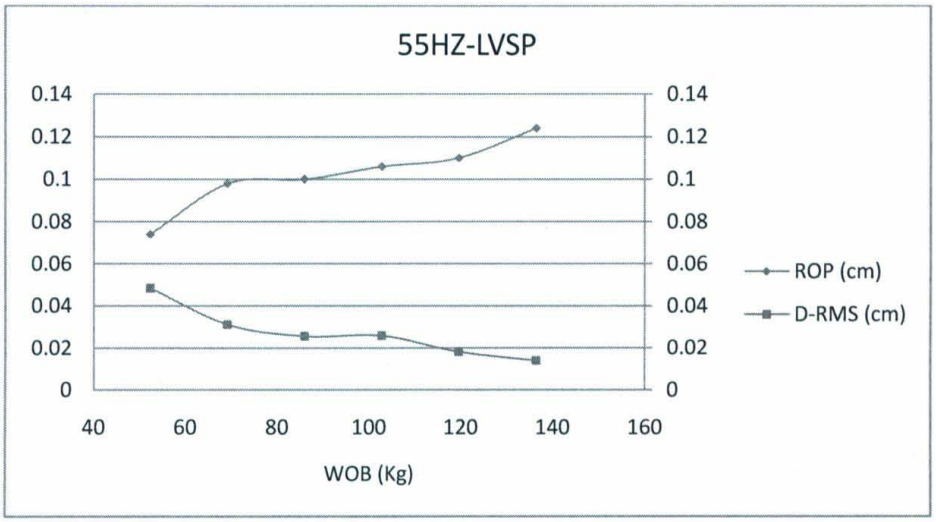

Figure 56. D-RMS and ROP v. WOB at 55 - LVSP

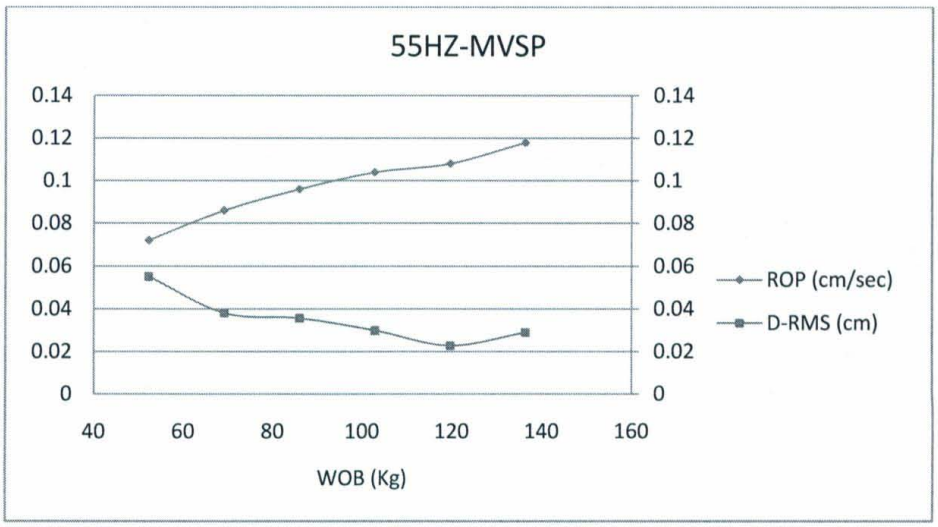

Figure 57. D-RMS and ROP v. WOB at 55 - MVSP

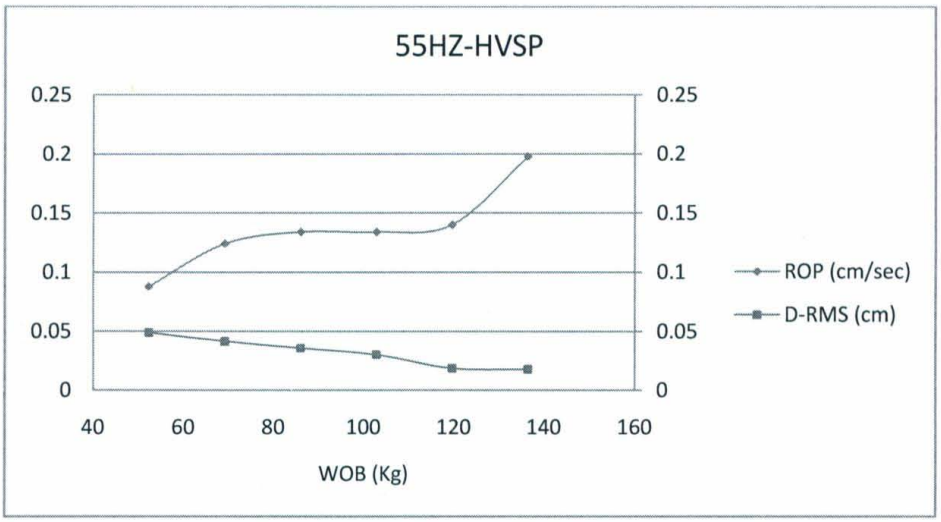

Figure 58.D-RMS and ROP v. WOB at 55 - HVSP

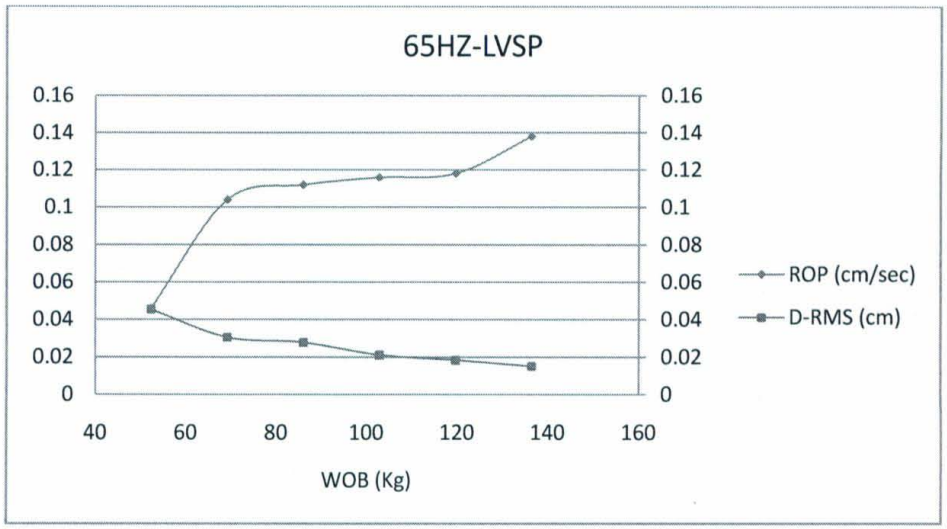

Figure 59. D-RMS and ROP v. WOB at 65 - LVSP

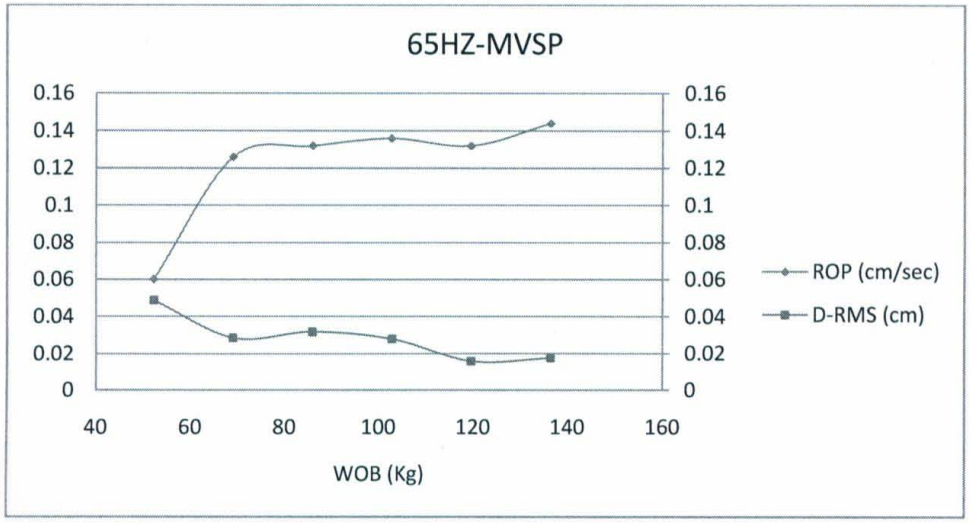

Figure 60. D-RMS and ROP v. WOB at 65 - MVSP

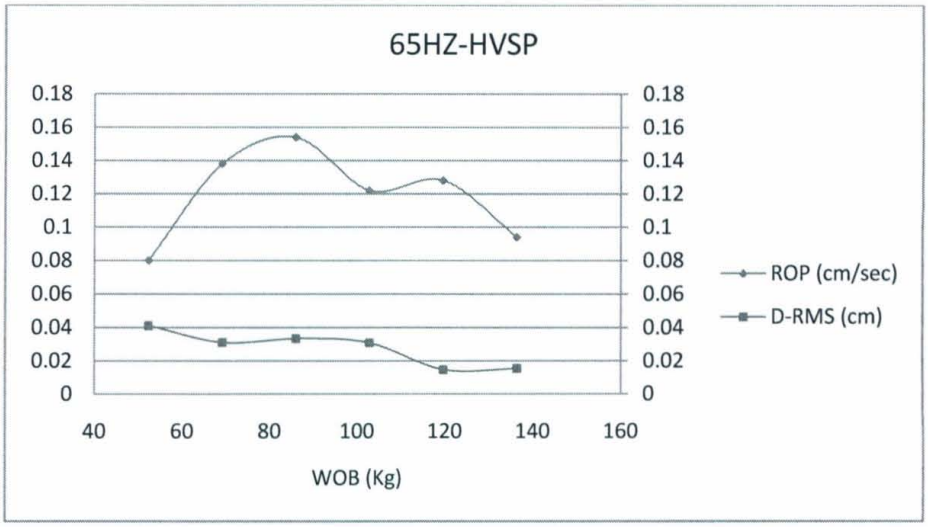

Figure 61. D-RMS and ROP v. WOB at 65 - HVSP

Normalizing with respect to RMS displacement (Figures 62, 63, 64) of the sample changes the shape of the ROP v WOB PLOTS. In all cases normalizing brings the curves closer together, i.e. less dependent on vibration power, at least up to about 106 kg WOB, to the extent that it may be reasonable to conclude that there is little dependence on vibration frequency (in the range studied) up to 106 kg WOB, only a dependence on vibration displacement amplitude of the sample. This agrees with earlier findings by Li et al. [6] that increase in ROP due to vibration is proportional to the vibration amplitude. Above 120 kg the relationship of ROP to WOB, normalized to displacement amplitude, is different at the different vibration power settings used.

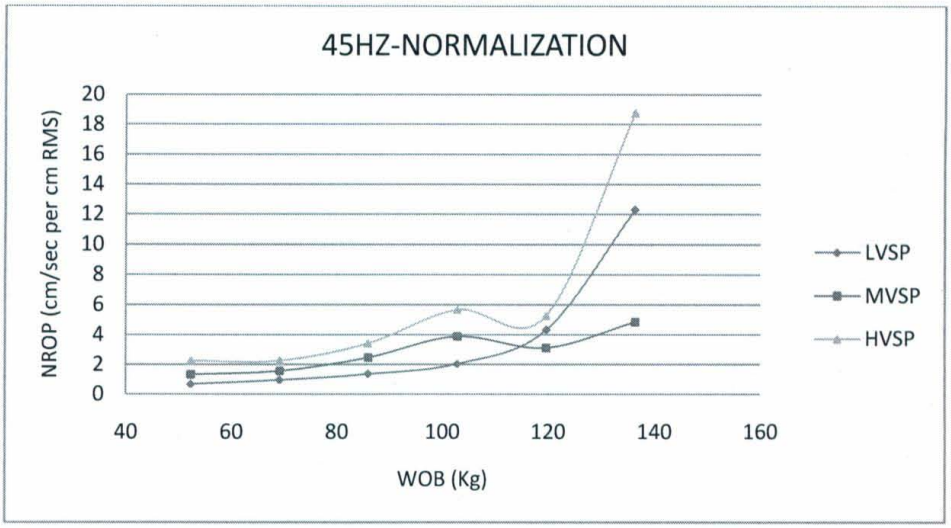

Figure 62. NROP v. WOB at 65HZ Frequency

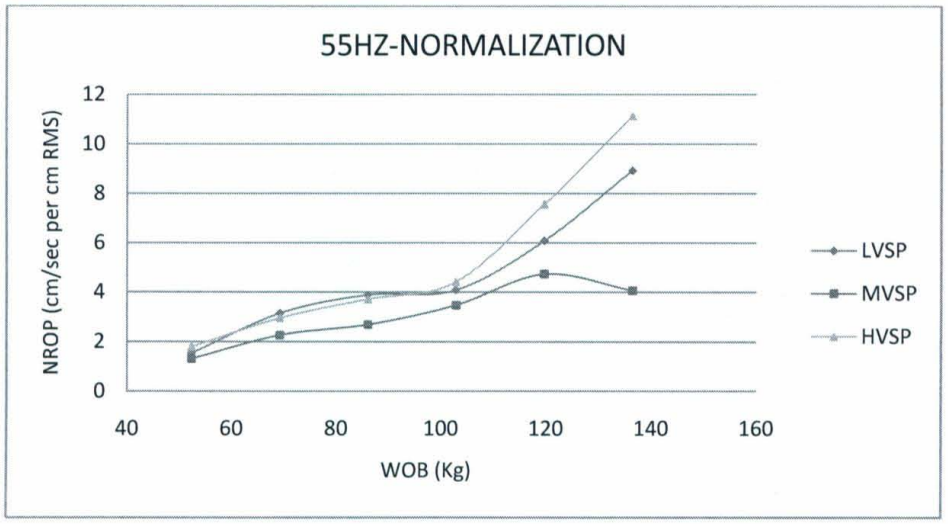

Figure 63. NROP v. WOB at 55HZ Frequency

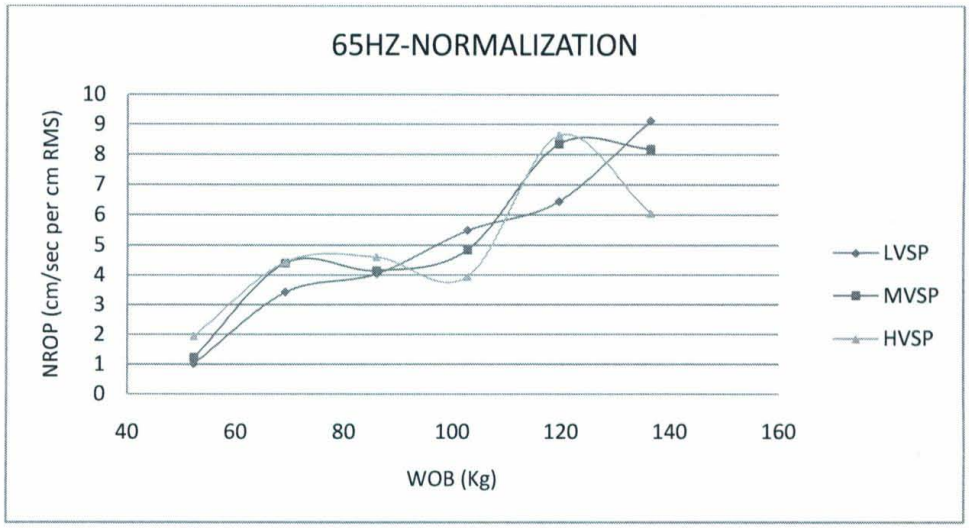

Figure 64. NROP v. WOB at 65HZ Frequency

4.4.3 Force Amplitude Data Analysis

Similar analysis done with the displacement amplitude data is also done using the force amplitude data. In all cases, the RMS does not change much with changing WOB, and does not depend much on vibration power at 45Hz and 65Hz but was much higher at 65Hz than at 45Hz. However at 55Hz, the F-RMS at high power was more than double than at low and medium power, about the same as 65Hz where it was about the same as at 45Hz.

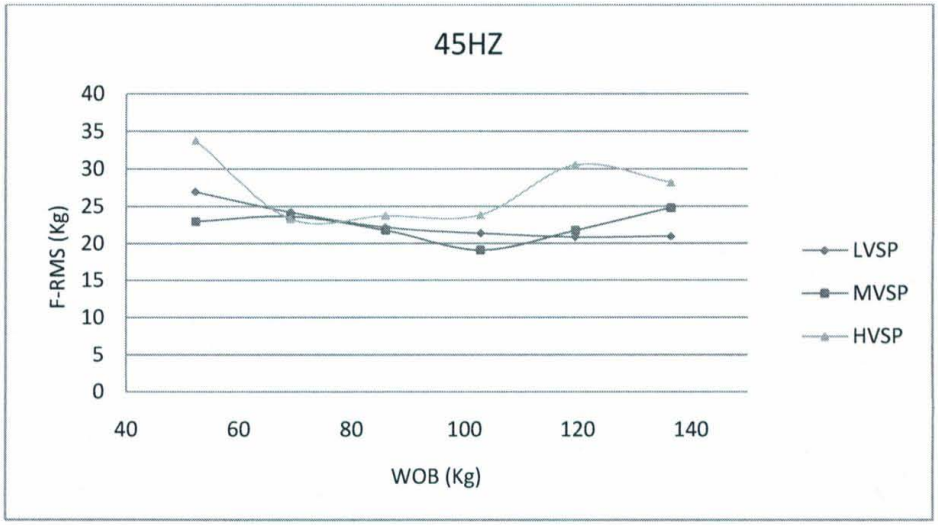

Figure 65. F-RMS v. WOB at 45HZ Frequency

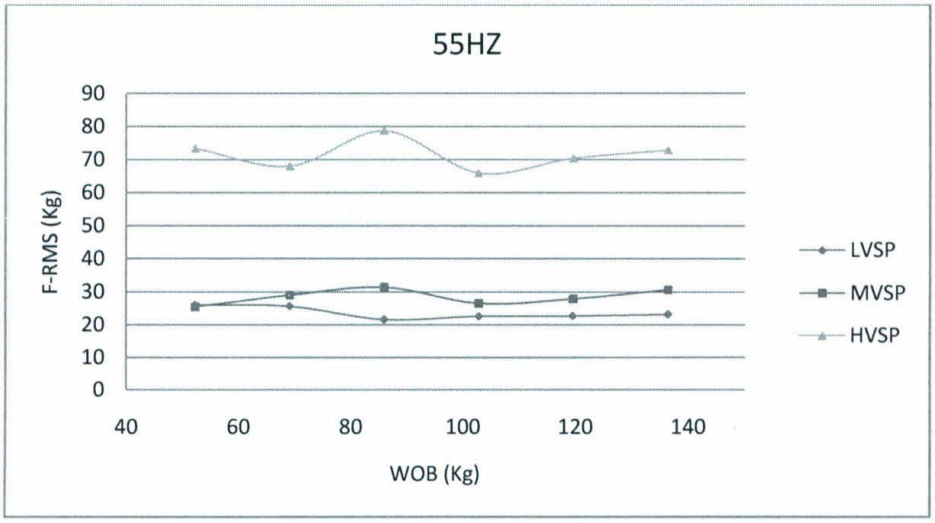

Figure 66. F-RMS v. WOB at 55HZ Frequency

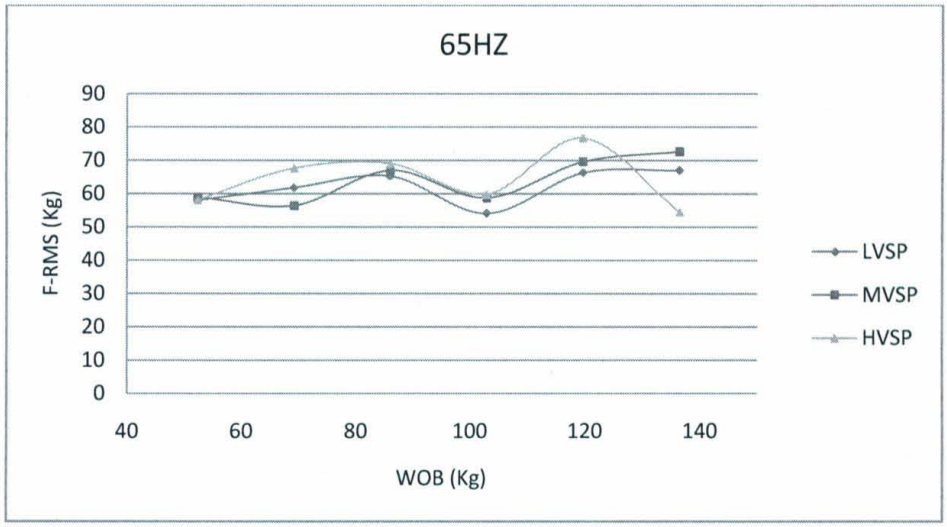

Figure 67. F-RMS v. WOB at 65HZ Frequency

Normalizing with respect to RMS force sensed in the drill string, has no consistent effect. At 65 Hz the curves are closer together than those that are not normalized in this way, all three showing similar trends. At 55 Hz the normalized curves are further apart than the corresponding data that is not normalized, with NROP inversely related to vibration power. At 45 Hz the normalized curves for the medium and high power settings are closer together than the un-normalized data up to 106 kg WOB. Otherwise there is little difference between the original data and the data normalized to RMS force.

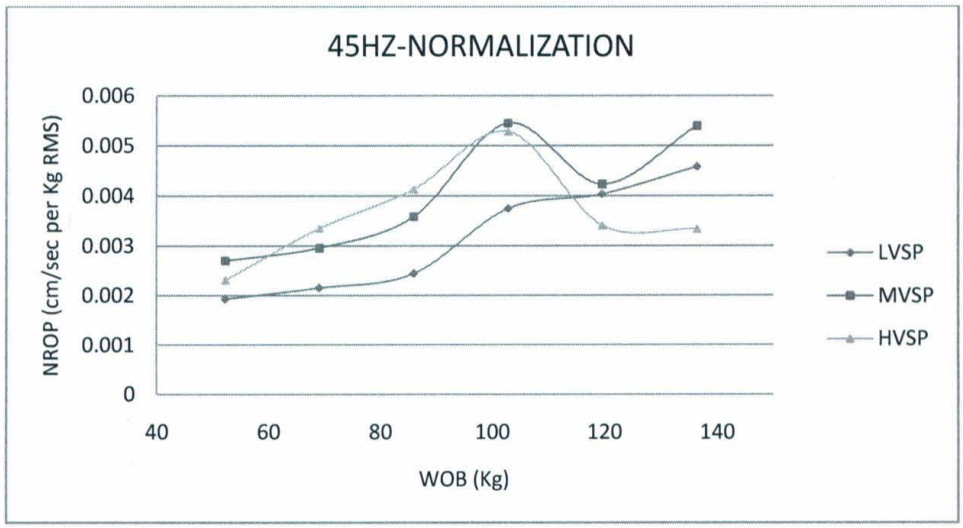

Figure 68. NROP v. WOB at 45HZ Frequency using F-RMS

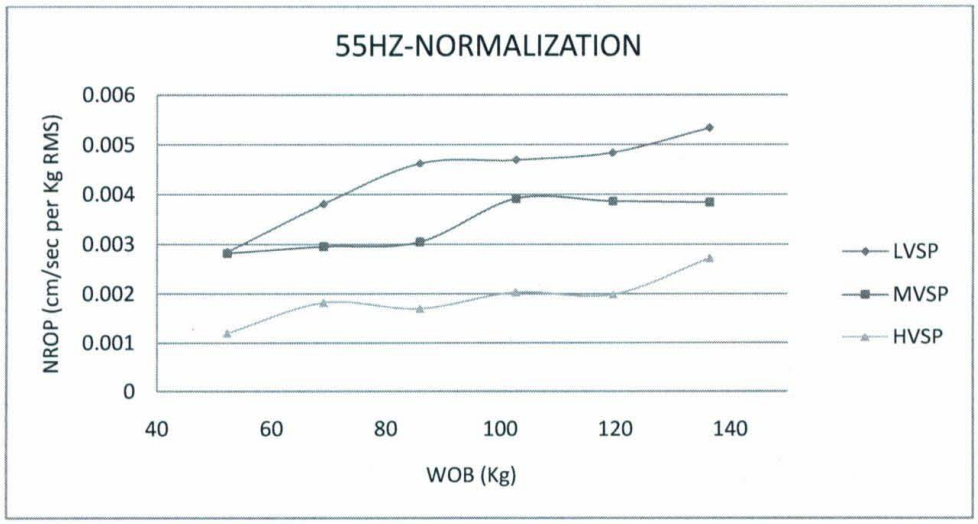

Figure 69. NROP v. WOB at 55HZ Frequency using F-RMS

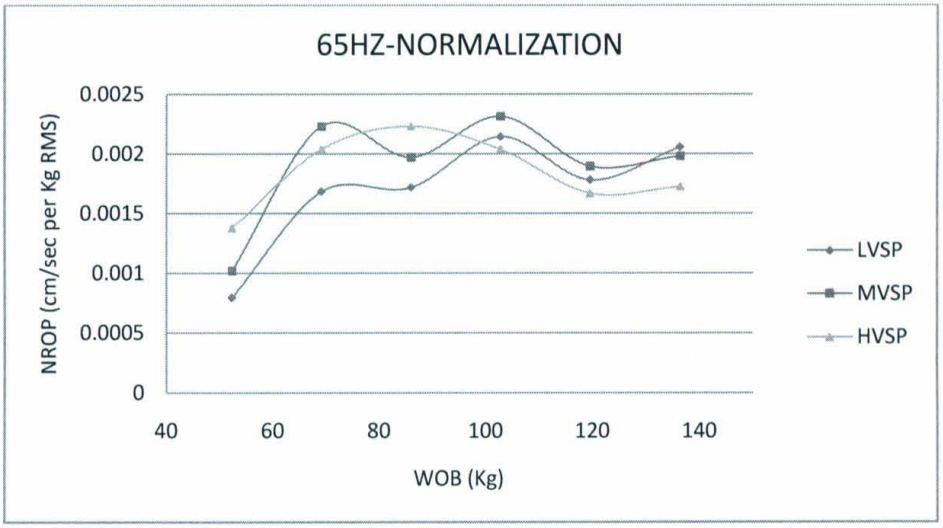

Figure 70. NROP v. WOB at 65HZ Frequency using F-RMS

4.5 Vibration Fast Fourier Transform (FFT)

In order to better understand the connection between force and displacement vibration data in describing the ROP, amplitude spectra are determined from FFT's for both data are plotted. At all the drilling combinations, both the force and displacement spectra are showing other peaks in addition to the drilling frequency peak. Observed peaks at the vibration frequencies confirm that there is an agreement between vibration data recorded by the load cell and that recorded by the LVDT. The various spectra can be found in Appendix 2.

Section 4.4.2 and 4.4.3 provide plots of normalized ROP (N-ROP) plotted against WOB. These plots show linear increment for lower WOB up to 120 Kg after which the linearity disappears. In order to better understand this phenomenon, there is a guess that the sudden change in behavior might be due to some resonance at multiples of natural vibration frequencies occurring during drilling. A part of the linear and non-linear section was analyzed for resonance at multiples of natural vibration frequencies, just to check if the sudden rise was due to reverberation at higher WOB by comparing it with a plot at lower WOB (where there is linearity) under same condition. This is achieved by plotting the force and displacement vibration data on same graph for the sample sections in the two regions at the three vibration frequencies applied.

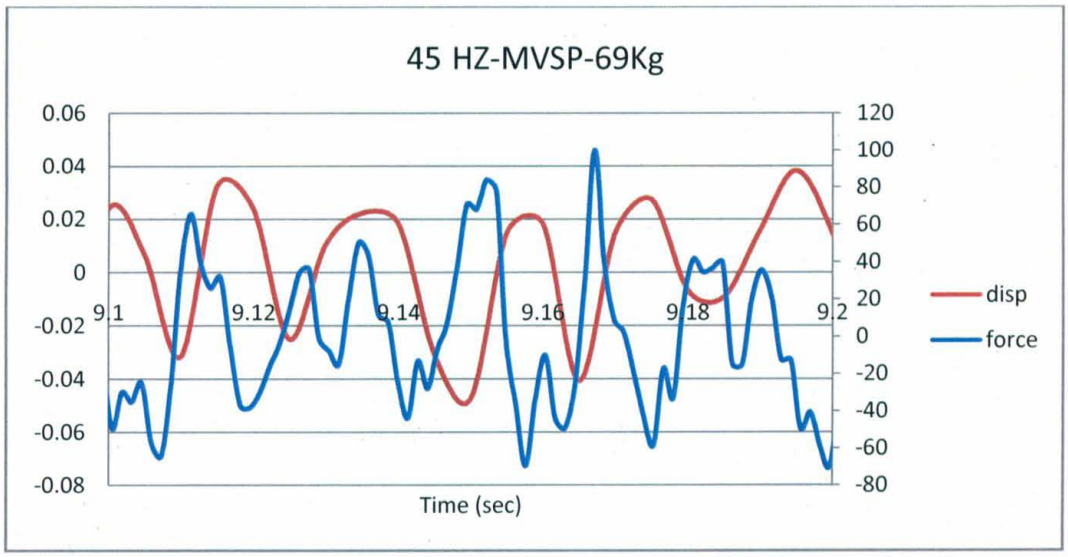

Figure 71. Reverberation check at 45Hz-MVSP-69Kg

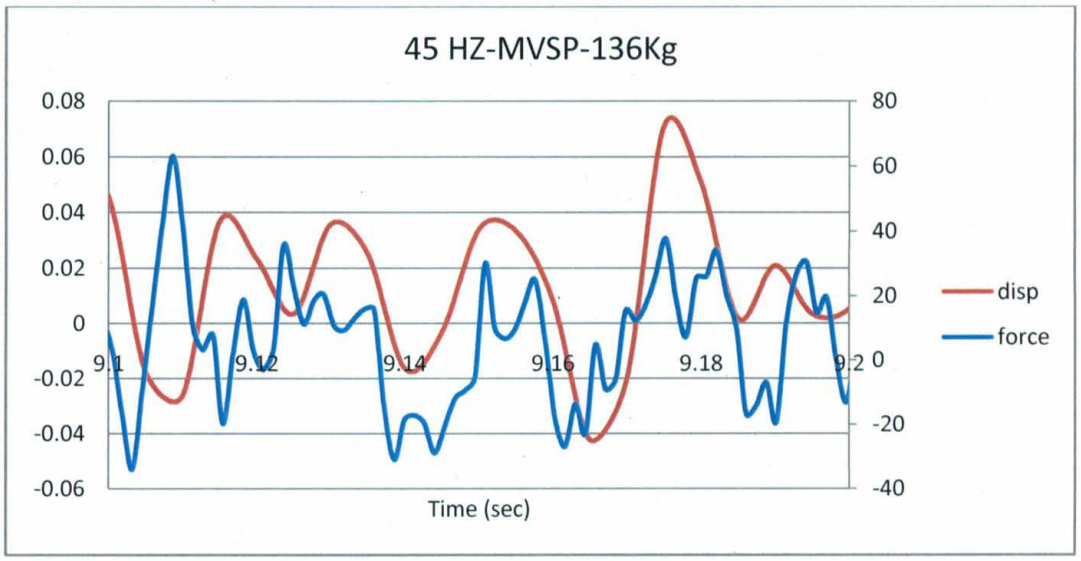

Figure 72. Reverberation check at 45Hz-MVSP-136Kg

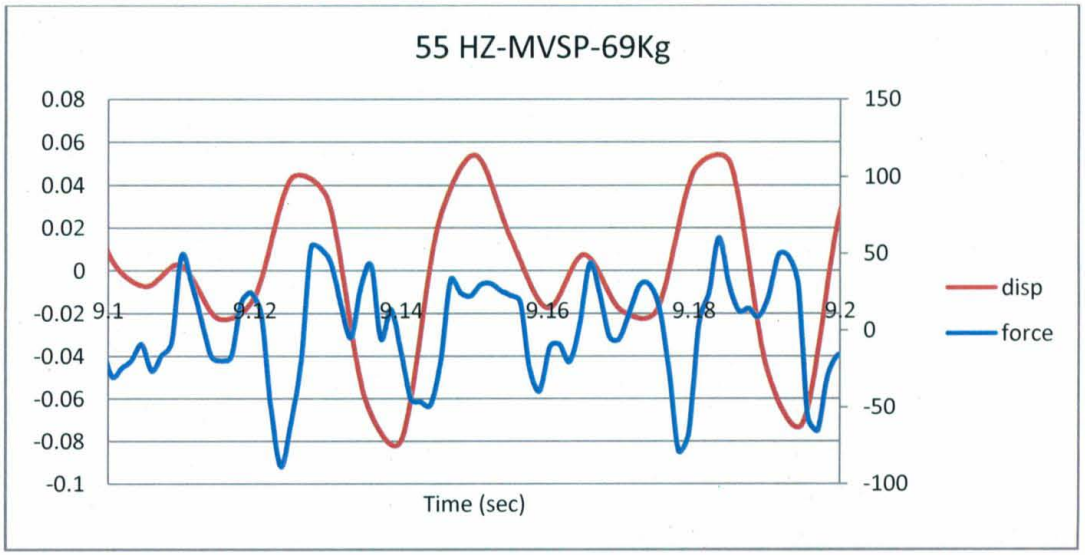

Figure 73.Reverberation check at 55Hz-MVSP-69Kg

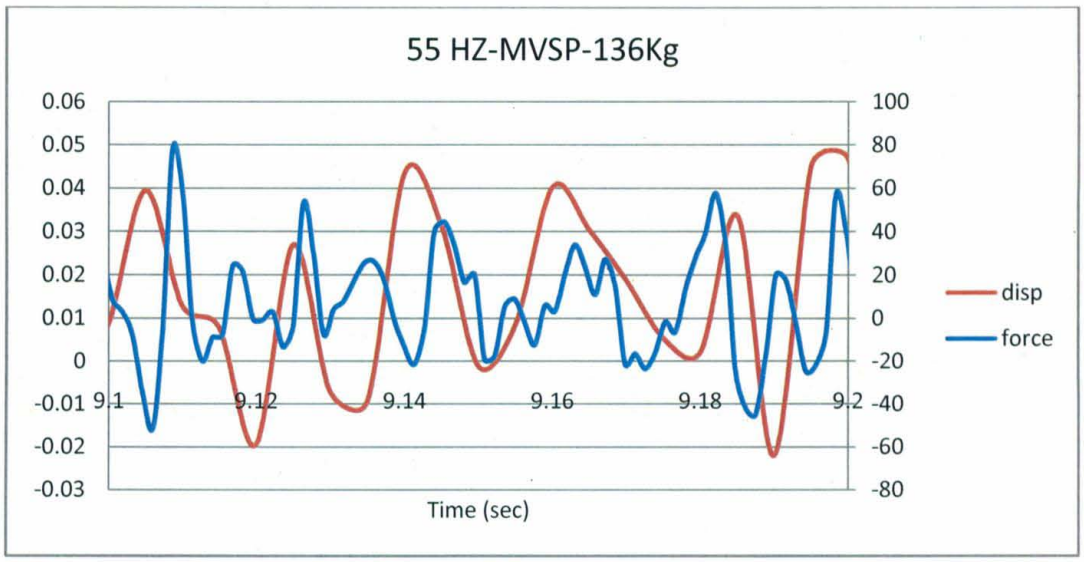

Figure 74. Reverberation check at 55Hz-MVSP-136Kg

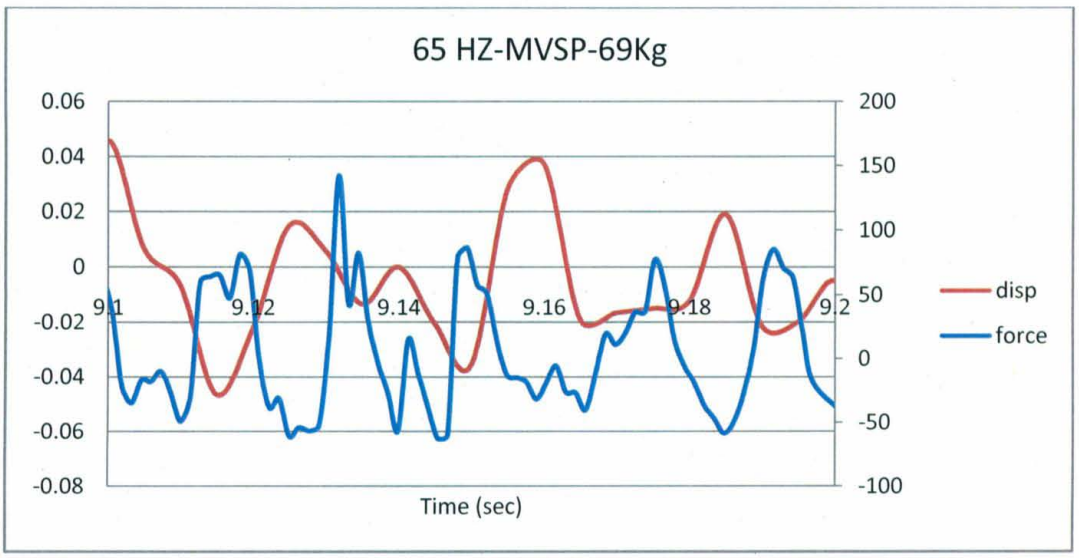

Figure 75. Reverberation check at 65Hz-MVSP-69Kg

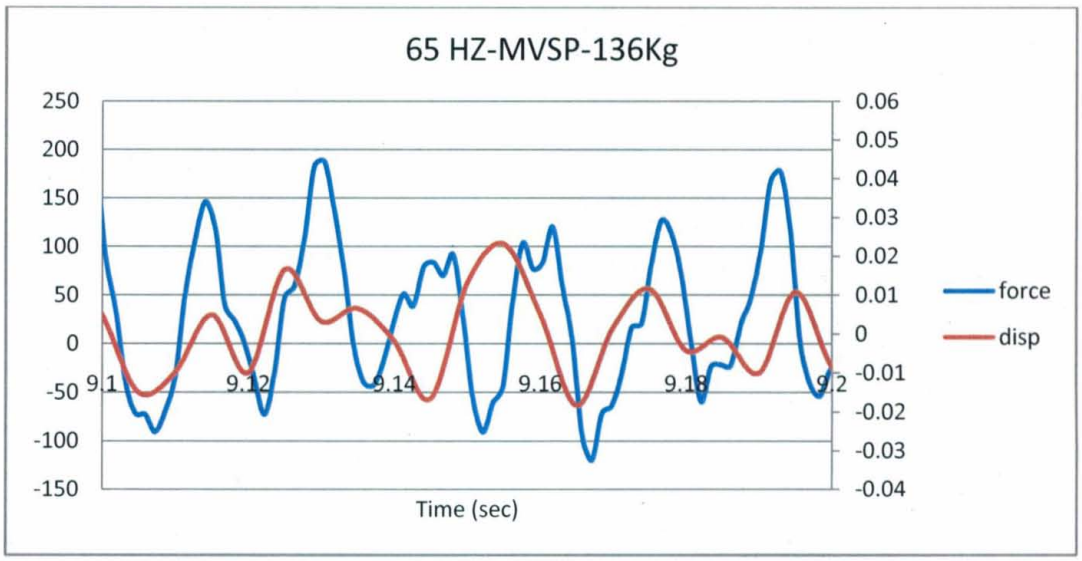

Figure 76. Reverberation check at 65Hz-MVSP-136Kg

Looking at the plots thoroughly, it could be generally said that, both force and displacement vibration data follow similar trend. However, as far as resonance at multiplies of natural vibration frequencies check is concern, 45 Hz frequency plots show some evidence of resonance at the high WOB. Meanwhile, at 55 Hz frequency, evidence of resonance is seen at low and high WOB but more frequently at high WOB while 65 Hz frequency shows little evidence at high WOB. A follow-up analysis is considered using amplitude spectra from FFT for both the low and high WOB selected. The plots below show spectra for both force and displacement vibration data on same graph. It is observed that for the linear section, peaks for the force and displacement spectra align properly with each other. Considering the same observation for the non-linear region, we

found out that the peak for the force FFT to a little extent overlaps that for the displacement FFT. It is therefore seen clearly that the sudden rise in NROP at high ROP is caused by change in vibration force behavior which is attributed to resonance occurring at higher WOB applied. In addition to resonance from the shaker frequency, there could also be resonance caused by influence of rotating frequency of the cutters which was found to roughly match 9.2 Hz.

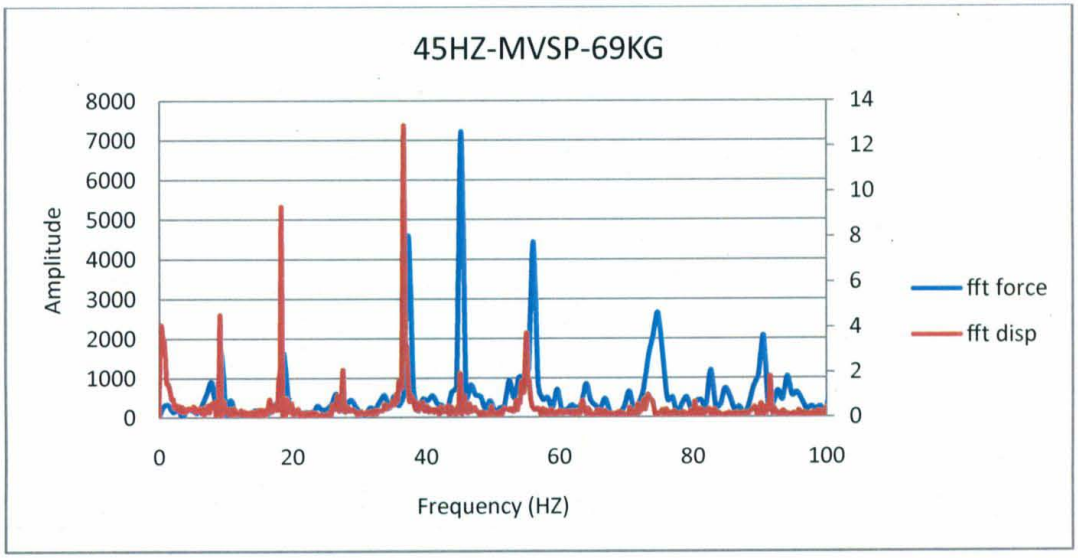

Figure 77. Force and Displacement FFT at 45Hz-MVSP-69Kg

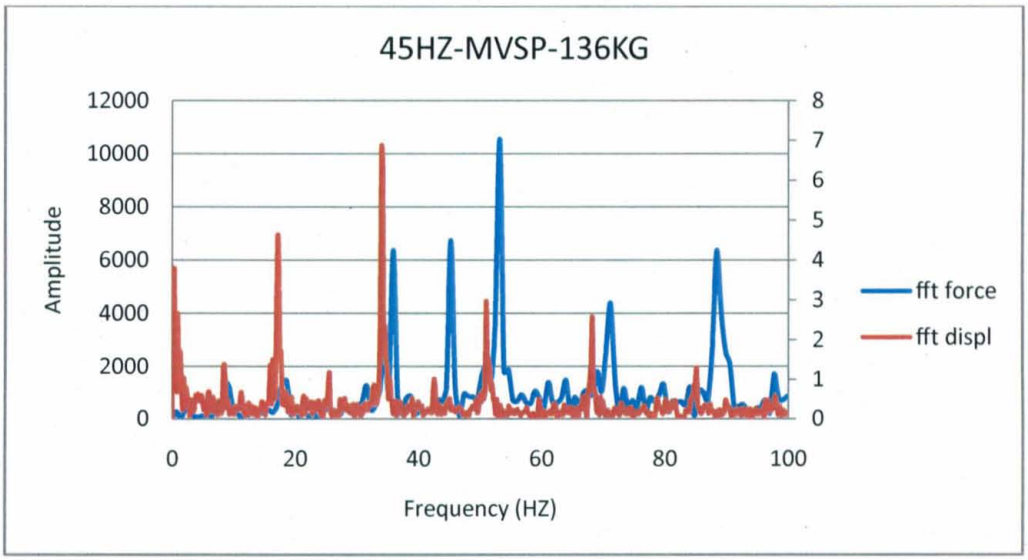

Figure 78. Force and Displacement FFT at 45Hz-MVSP-136Kg

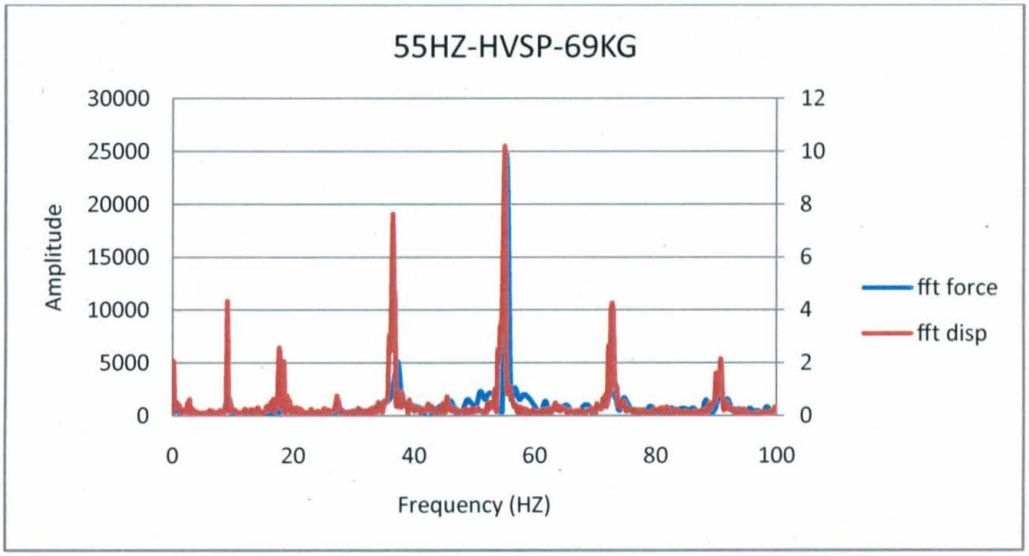

Figure 79. Force and Displacement FFT at 55Hz-MVSP-69Kg

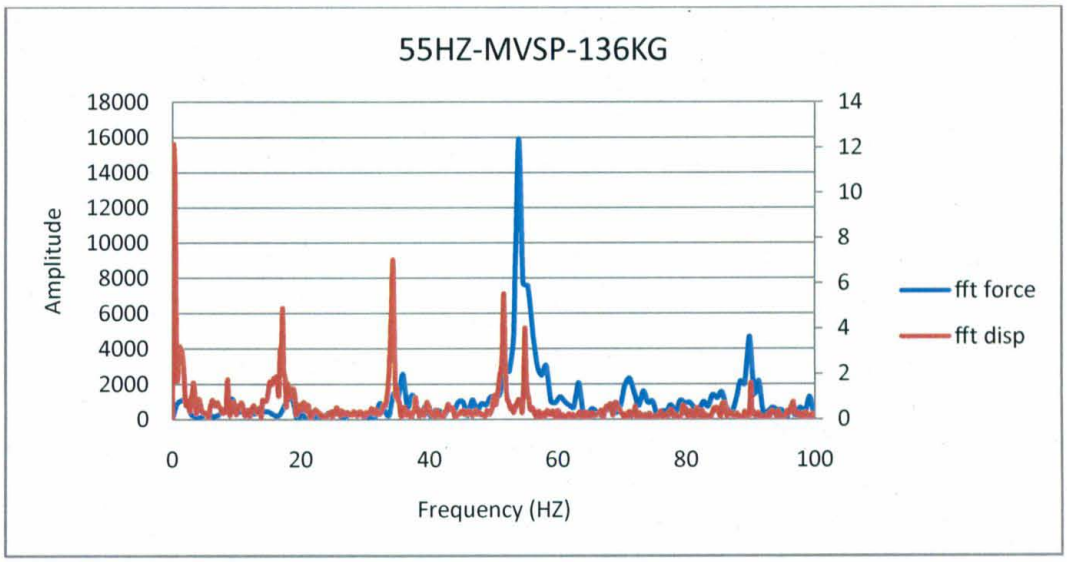

Figure 80. Force and Displacement FFT at 55Hz-MVSP-136Kg

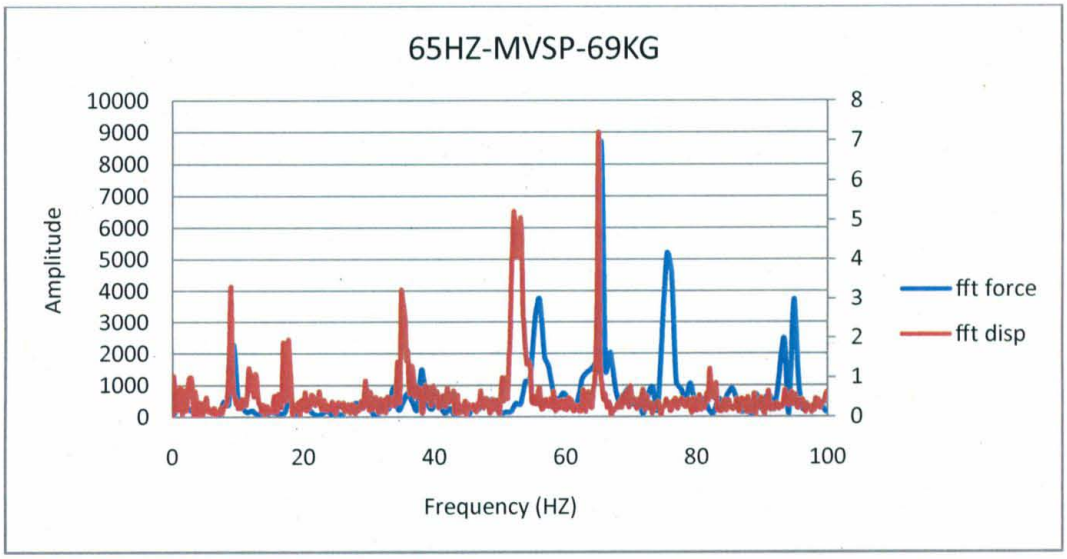

Figure 81. Force and Displacement FFT at 65Hz-MVSP-69Kg

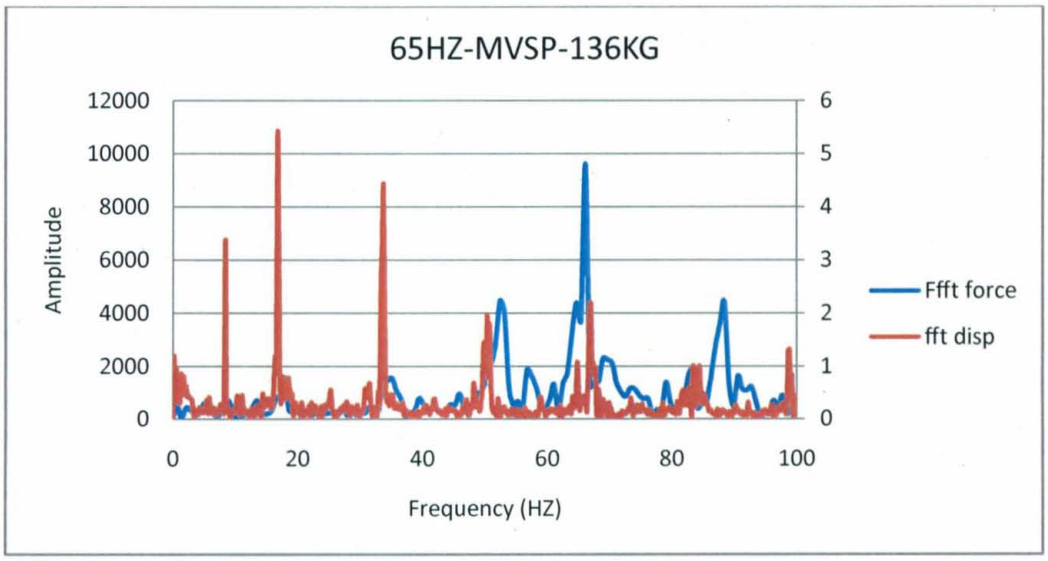

Figure 82. Force and Displacement FFT at 65Hz-MVSP-136Kg

4.6 DSE – MSE

4.6.1 Bit Hydraulic Contribution

Plots of MSE and DSE for conventional and vibration drilling are compared using Teale's and Dupriest's equations, and the BHC in both cases estimated. In both cases, drilling done can be said to be in the transition region, and applying higher WOB would possibly provide a situation of getting close to the efficient drilling region. For both cases, the BHC is minute and decreases with increase in ROP.

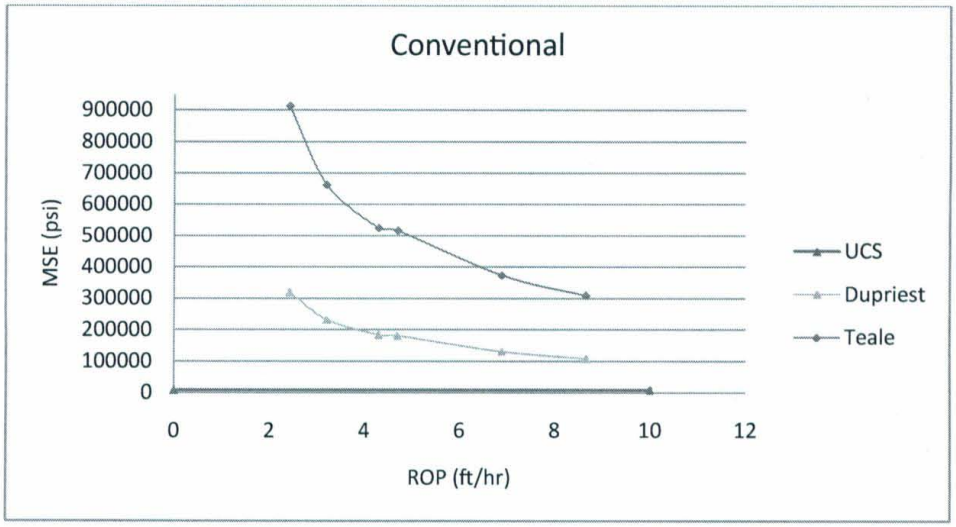

Figure 83. MSE v. ROP for PDC Conventional Drilling

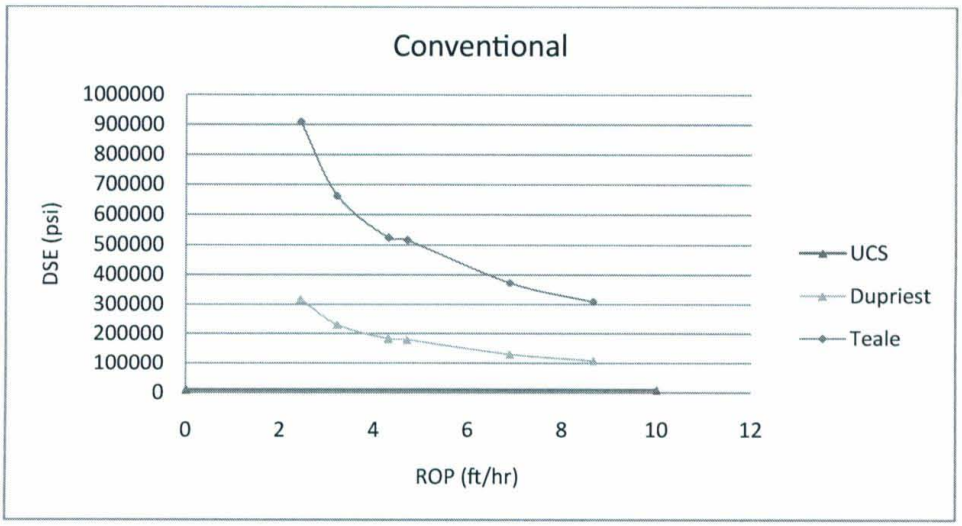

Figure 84. DSE v. ROP for PDC Conventional Drilling

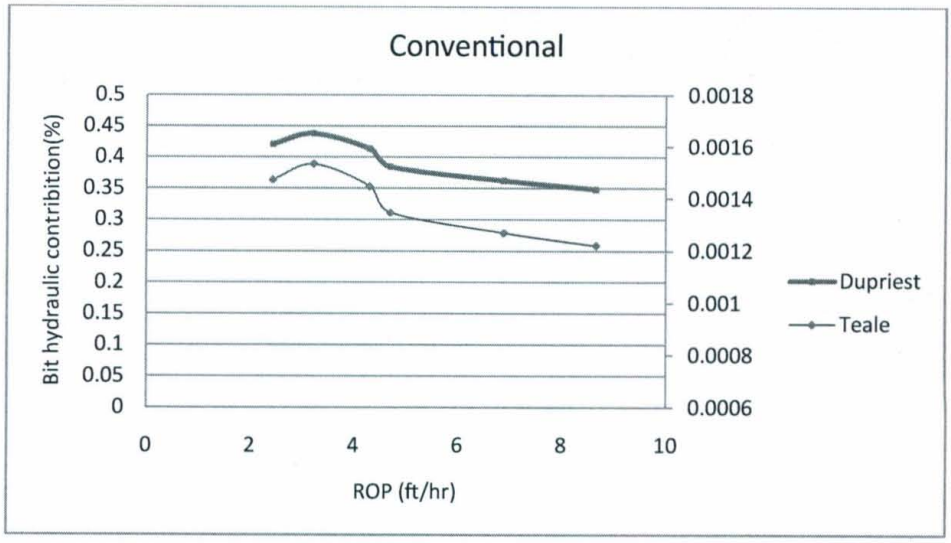

Figure 85. BHC v. ROP for PDC Conventional Drilling – Teale/Dupriest

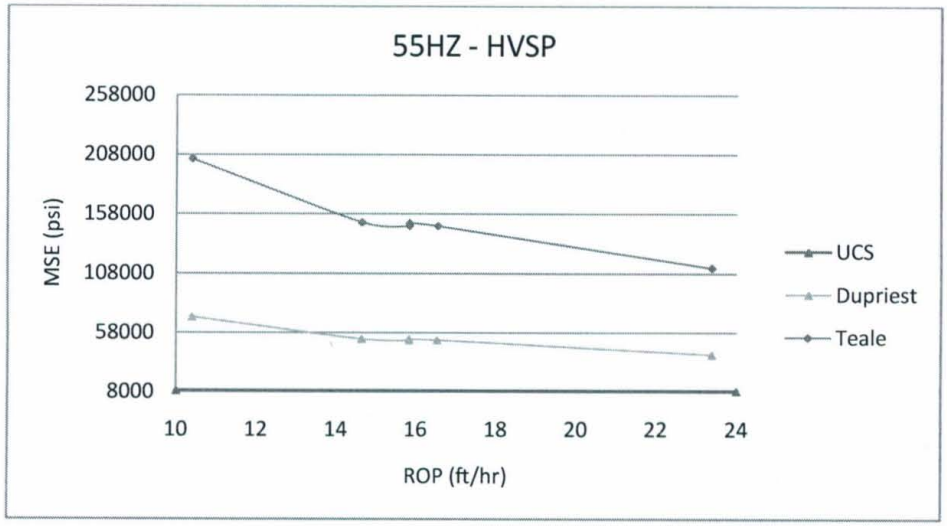

Figure 86. MSE v. ROP for PDC 55HZ - HVSP Drilling

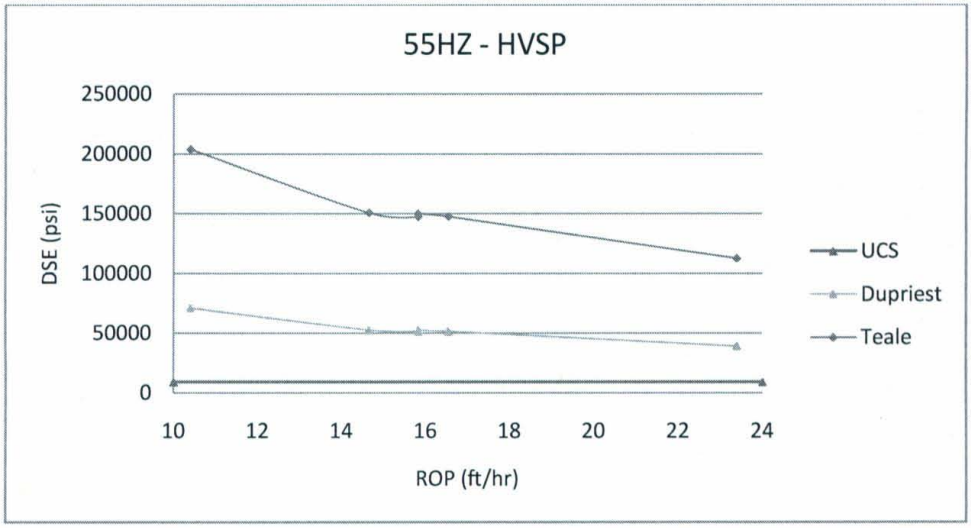

Figure 87. DSE v. ROP for PDC 55HZ - HVSP Drilling

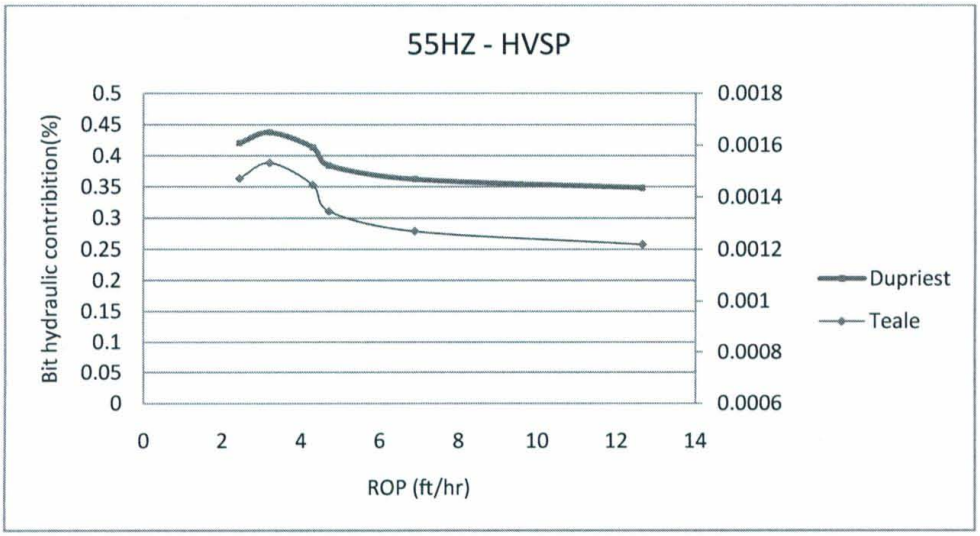

Figure 88. BHC v. ROP for PDC 55HZ - HVSP Drilling – Teale/Dupriest

4.6.2 Vibration Energy Contribution

As shown on tables 9, 10 and 11, the vibration energy contribution to rock drilling is 59.33% at 55HZ – LVSP, 59.4% at 55HZ – MVSP and 70.25% at 55HZ – HVSP. This creates an understanding that higher axial force would be required for improved performance with the PDC bit.

Table 9. Vibration Energy Contribution at 55HZ – LVSP PDC Drilling

Conventional MSE X 10^3 (psi)	Vibration 55 Hz, LVSP MSE X 10^3 (psi)	$MSE_C - MSE_V$ X 10^3 (psi)	$(MSE_C - MSE_V)/ MSE_C$ X 100
912	258	653	72
663	209	454	68
524	192	332	63
516	194	322	62
373	191	183	49
309	181	128	41
			59.17

Table 10. Vibration Energy Contribution at 55HZ – MVSP PDC Drilling

Conventional MSE X 10^3 (psi)	Vibration 55 Hz, MVSP MSE X 10^3 (psi)	MSE_C - MSE_V X 10^3 (psi)	$(MSE_C - MSE_V)/ MSE_C$ X 100
912	256	655	72
663	220	443	67
524	207	317	61
516	188	328	64
373	181	193	52
309	179	130	42
			59.67

Table 11. Vibration Energy Contribution at 55HZ – HVSP PDC Drilling

Conventional MSE X 10^3 (psi)	Vibration 55 Hz, HVSP MSE X 10^3 (psi)	MSE_C - MSE_V X 10^3 (psi)	$(MSE_C - MSE_V)/ MSE_C$ X 100
912	204	707	78
663	151	512	77
524	147	377	72
516	150	366	71
373	148	226	60
309	113	196	64
			70.33

4.6.3 Drilling Efficiency

The tables below show drilling efficiency estimation at various WOB for conventional drilling and vibration drilling. These drilling efficiency values are low compared with those obtained while drilling with the diamond drag bit, which produces drilling efficiency which are about five times those shown below for the PDC bit.

Table 12. Drilling Efficiency at Conventional PDC Drilling

WOB (lbf)	MSE X 10^3 (psi)	UCS/MSE	Drilling Eff.(%)
115	912	0.0104	1.04
152	663	0.0143	1.43
189	524	0.0181	1.81
227	516	0.0183	1.83
264	373	0.0254	2.54
301	309	0.0306	3.06

Table 13. Drilling Efficiency at 55HZ - LVSP PDC Drilling

WOB (lbf)	MSE X 10^3 (psi)	UCS/MSE	Drilling Eff. (%)
115	258	0.0366	3.66
152	209	0.0452	4.52
189	192	0.0493	4.93
227	194	0.0487	4.87
264	191	0.0496	4.96
300	181	0.0522	5.22

Table 14. Drilling Efficiency at 55HZ - MVSP PDC Drilling

WOB (lbf)	MSE X 10^3 (psi)	UCS/MSE	Drilling Eff. (%)
115	256	0.0369	3.69
152	220	0.043	4.30
189	207	0.046	4.60
227	188	0.0504	5.04
264	181	0.0524	5.24
300	179	0.0528	5.28

Table 15. Drilling Efficiency at 55HZ - HVSP PDC Drilling

WOB (lbf)	MSE X 10^3 (psi)	UCS/MSE	Drilling Eff. (%)
115	204	0.0463	4.63
152	151	0.0627	6.27
189	147	0.0642	6.42
227	150	0.0630	6.30
264	148	0.0640	6.40
301	113	0.0839	8.40

4.7 Summary

The chapter discuses the effect of varying the frequency and amplitude of vibration during vibration drilling using a PDC bit. It was observed that drilling with this bit produces higher ROP at lower WOB at 65HZ frequency regardless of the vibration shaker position applied. As the WOB increases, it will be better to switch to the 55HZ frequency as this provides higher ROP. A study of vibration characteristics revealed that the hydraulic contribution to breaking and removal of cuttings in this case is also minute and that a higher percentage of the energy required are supplied by vibration which seems to increase proportionally with the vibration shaker power position utilized. The drilling efficiency estimated in this case is low compared with those obtained with drilling using the diamond drag bit. In general, drilling with vibration has once again proved to be vital in terms of ROP gain, in this case, using a PDC bit.

Vibration behavior was fully analyzed using force and displacement amplitude data. Force and displacement RSM used to obtain NROP. The analysis reveals that increase in N-ROP with WOB is linear at low WOB and the linearity changes drastically at high WOB.

Chapter 5

Conclusions and Recommendations

5.1 Conclusions

In this thesis, two major vibration-assisted rotary drilling experiments were carried out; one with diamond drag bit and the other with PDC bit to study and understand vibration drilling optimization with industry-type bits. The diamond drag bit experiment provided the basis for the modification of the drill rig used for the PDC experiment. The PDC bit experiments provided real-time drilling and vibration data, from which the rig's vibration behavior was properly understood. Detailed analysis were also done on mechanical specific energy and drilling specific energy in order to be able to understand percent energy contribution made by application of vibration to the drilling setup and also to quantify how efficient the drilling is. All the experiments are run at atmospheric pressure with no confining pressure.

The following conclusions can be drawn from the study:

- Vibration-assisted rotary drilling provides significant improvement in ROP compared to the conventional rotary drilling, using diamond drag bit and PDC bit at different vibration frequency and amplitude.
- Diamond full face drag bit produced more overall efficient drilling in terms of ROP enhancement when compared with the PDC bit for the present VARD setup.
- In every case, it was found that the largest specific energy applied to drilling comes from vibration. Other energy inputs are from torsion, axial and hydraulics. The percent contribution from hydraulics in all drilling combination is minute and highly insignificant.
- From our monitoring of the impregnated diamond bit, in this work wear is not very pronounced after drilling and could be said not to have much effect on the overall drilling efficiencies observed with the drag bit.
- No particular combination of vibration frequency and amplitude can be categorically said to be the optimum applicable to every situation. Obtaining real-time drilling data for continuous monitoring of vibration, MSE and DSE can assist to know when ROP increases or decreases; in which case drilling variables such as vibration frequency, vibration amplitude, WOB and fluid flow rate can be adjusted accordingly for improved performance or optimization.

5.2 Recommendations

The following are recommended for future work:

- A separate and elaborate study should be carried out on bit hydraulics by applying higher flow rates and flow pressure to study their impact on drilling specific energy.
- A qualitative numerical analysis should be done to confirm the percent energy contribution from vibration. This should be compared with the experimentally obtained results.
- The voltage supply to the load cell should be measured before every drilling run as this is very essential in processing the force amplitude data obtained.
- Progressive bit wear should be studied with both the impregnated diamond bit and the PDC bit. In both cases, drilling run should be longer for the study to be compared with field work.

Publication

Y. Babatunde, S. Butt, J. Molgaard and F. Arvani. "Investigation of the Effects of Vibration Frequency on Rotary Drilling Penetration Rate Using Diamond Drag Bit". 45th US Rock Mechanics Symposium, San Francisco, USA, June 26-29, 2011.

Appendix A

Torque Formula Derivation and Motor Current Chart

Full load motor torque (braking torque)

$$T = \frac{5252\ X\ HP}{RPM}$$

T = full load motor torque (Ib-ft)

HP = motor power

RPM = speed of motor shaft

Calculating Horsepower

$$HP = \frac{V\ x\ I\ x\ \eta\ x\ PF}{746}$$

V = voltage, I = current, η = efficiency, PF = power factor

Calculating power

P = V x I x η x PF

$$T = \frac{P}{w} = \frac{V\ x\ I\ x\ \eta\ x\ PF}{2\pi} = \frac{60\ x\ V\ x\ \eta\ x\ PF}{2\pi}\ x\ \frac{I}{N}$$

Approximately, $K = \frac{60\ x\ 115\ x\ 0.6\ x\ 0.8}{2\pi} = 527.12$

V - 115 (5V drop considering)

η = 0.6. PF = 0.8

$$T = 527.12\frac{I}{N}$$

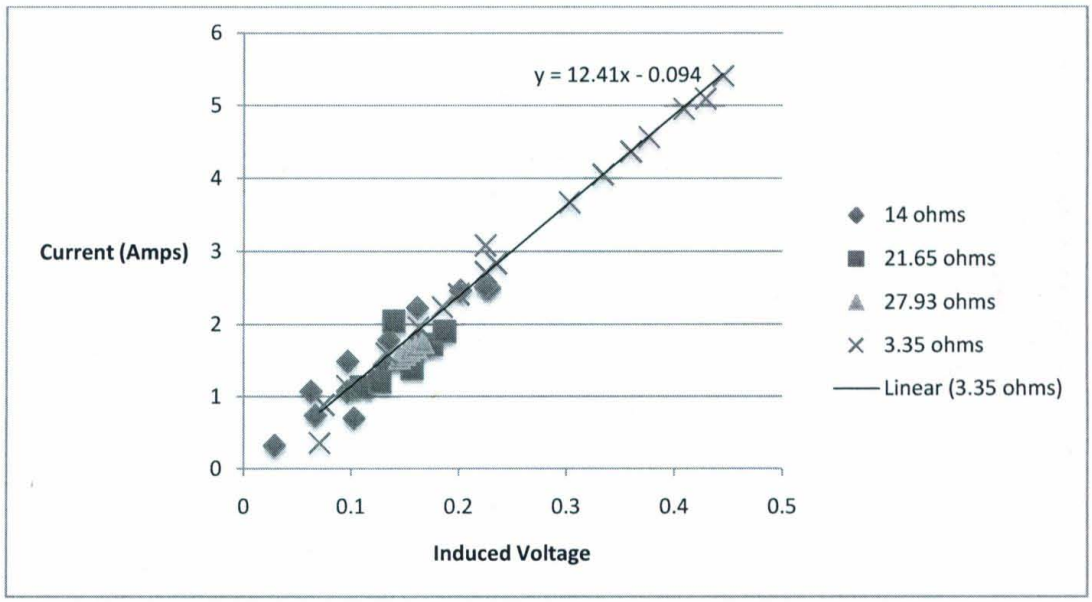
y = 12.41x - 0.094
Current (Amps)
Induced Voltage
0
1
2
3
4
5
6
0
0.1
0.2
0.3
0.4
0.5
14 ohms
21.65 ohms
27.93 ohms
3.35 ohms
Linear (3.35 ohms)

Appendix B

Vibration Fast Fourier Transform

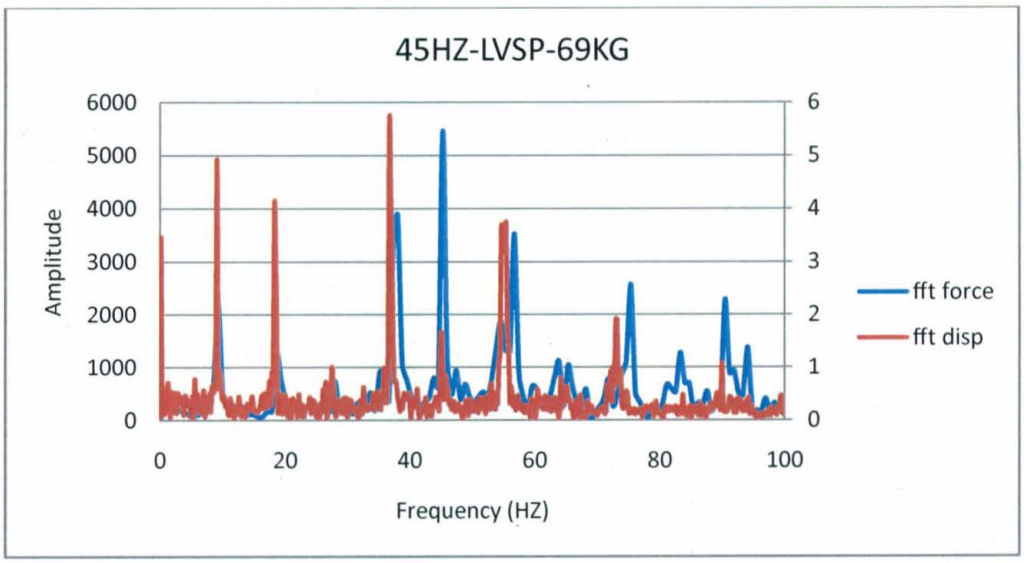

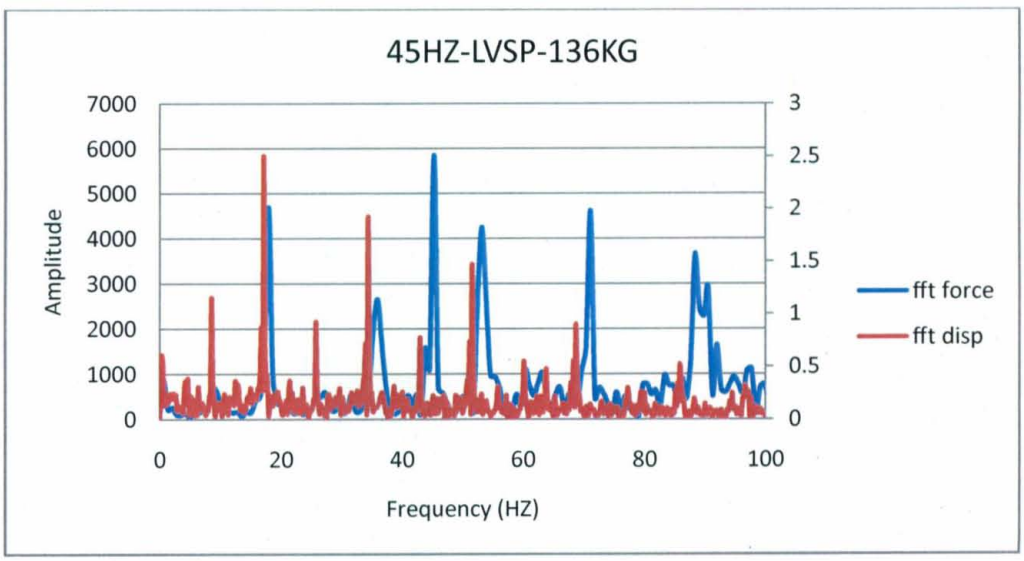

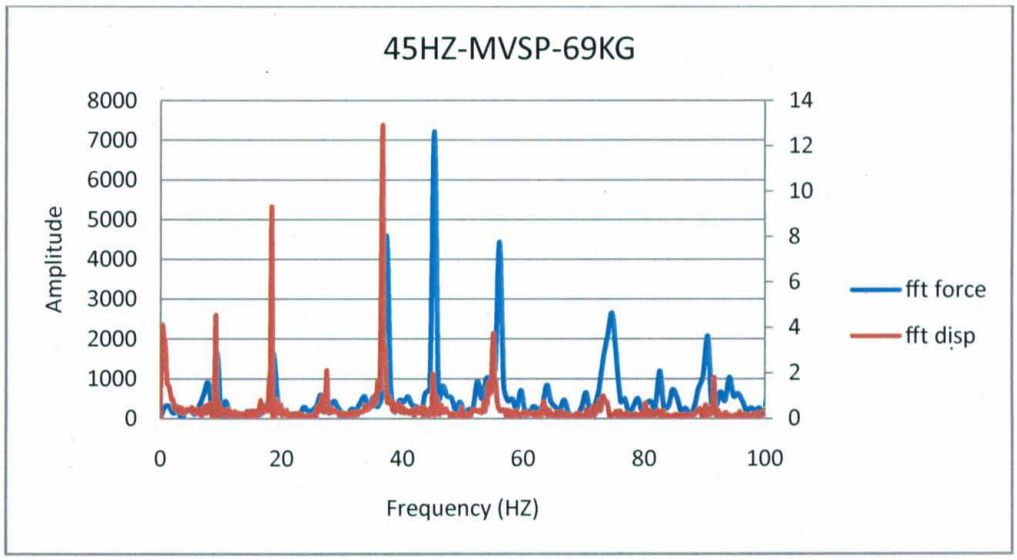
45HZ-MVSP-69KG
Amplitude
8000
7000
6000
5000
4000
3000
2000
1000
0
14
12
10
8
6
4
2
0
0
20
40
60
80
100
Frequency (HZ)
fft force
fft disp

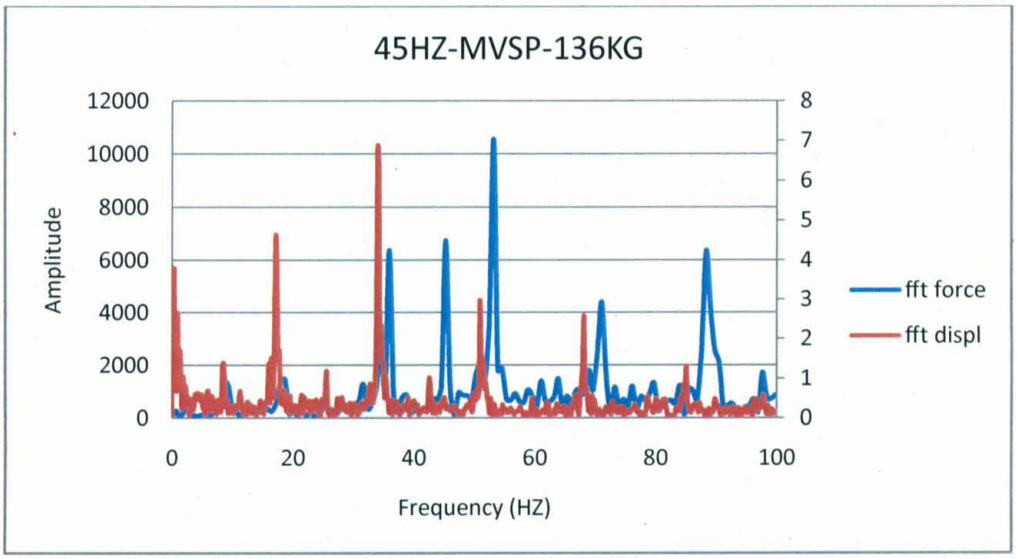
45HZ-MVSP-136KG
Amplitude
12000
10000
8000
6000
4000
2000
0
8
7
6
5
4
3
2
1
0
0
20
40
60
80
100
Frequency (HZ)
fft force
fft displ

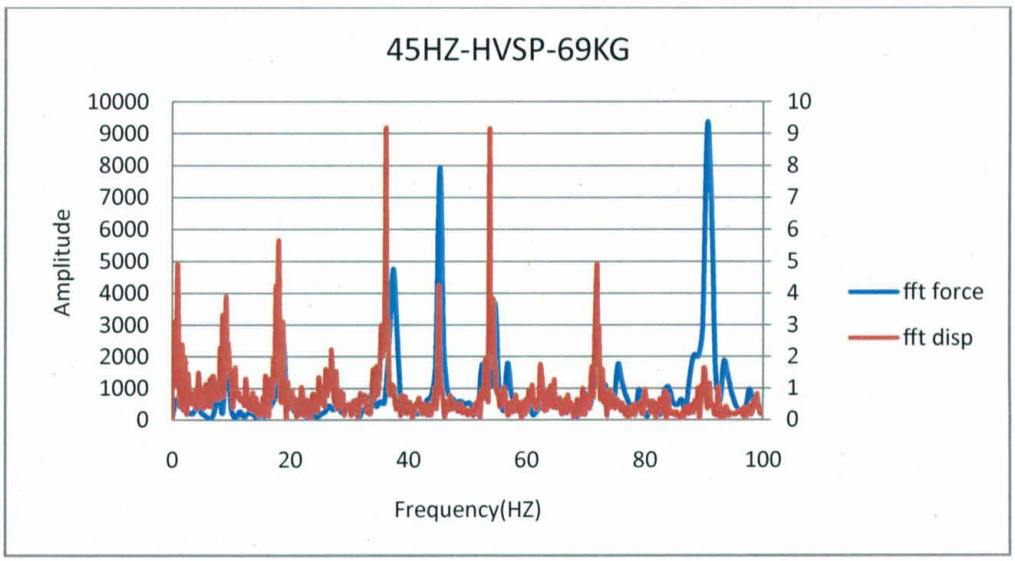
45HZ-HVSP-69KG
Amplitude
10000
9000
8000
7000
6000
5000
4000
3000
2000
1000
0
10
9
8
7
6
5
4
3
2
1
0
0
20
40
60
80
100
Frequency(HZ)
fft force
fft disp

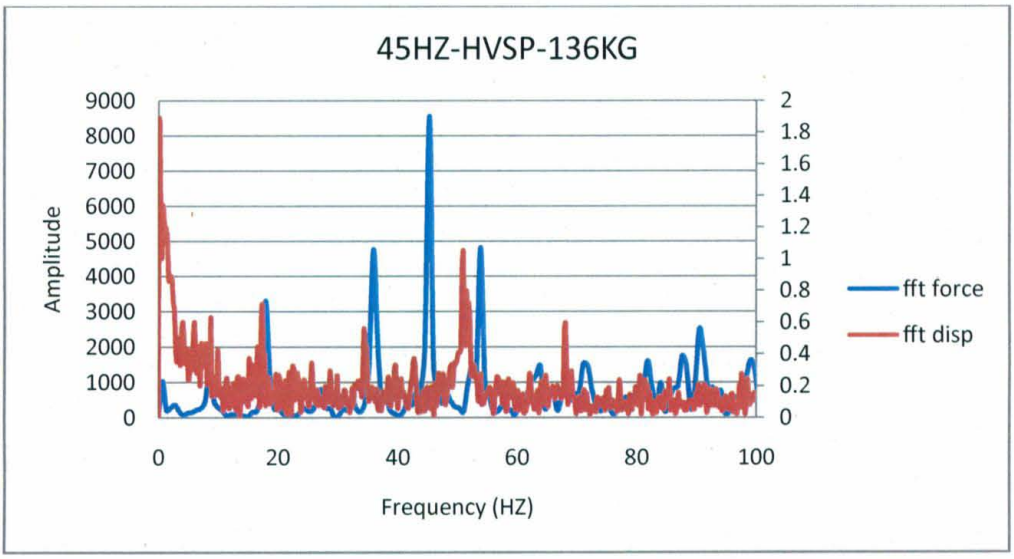
45HZ-HVSP-136KG
Amplitude
9000
8000
7000
6000
5000
4000
3000
2000
1000
0
2
1.8
1.6
1.4
1.2
1
0.8
0.6
0.4
0.2
0
0
20
40
60
80
100
Frequency (HZ)
fft force
fft disp

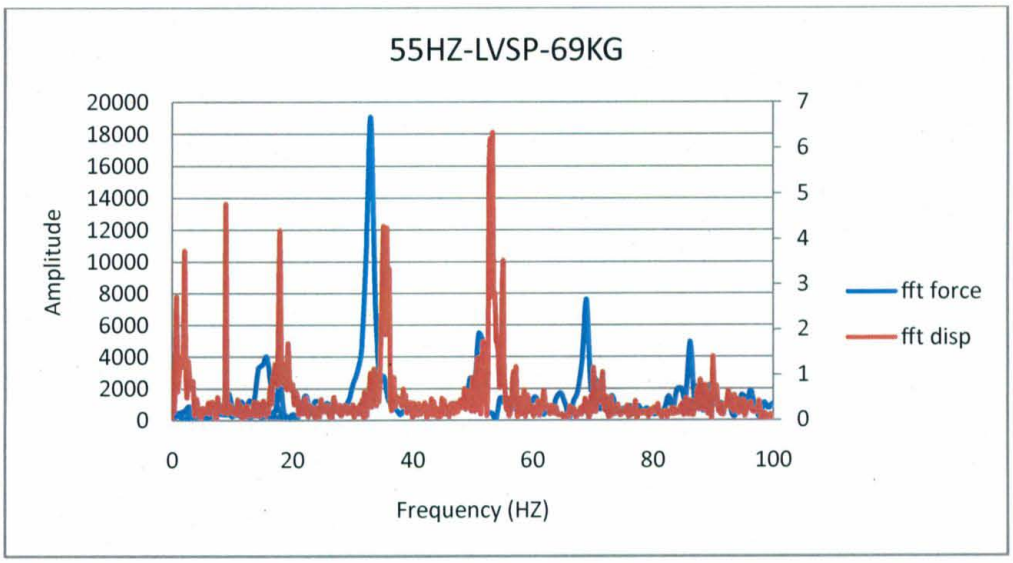
55HZ-LVSP-69KG
Amplitude
20000
18000
16000
14000
12000
10000
8000
6000
4000
2000
0
7
6
5
4
3
2
1
0
0
20
40
60
80
100
Frequency (HZ)
fft force
fft disp

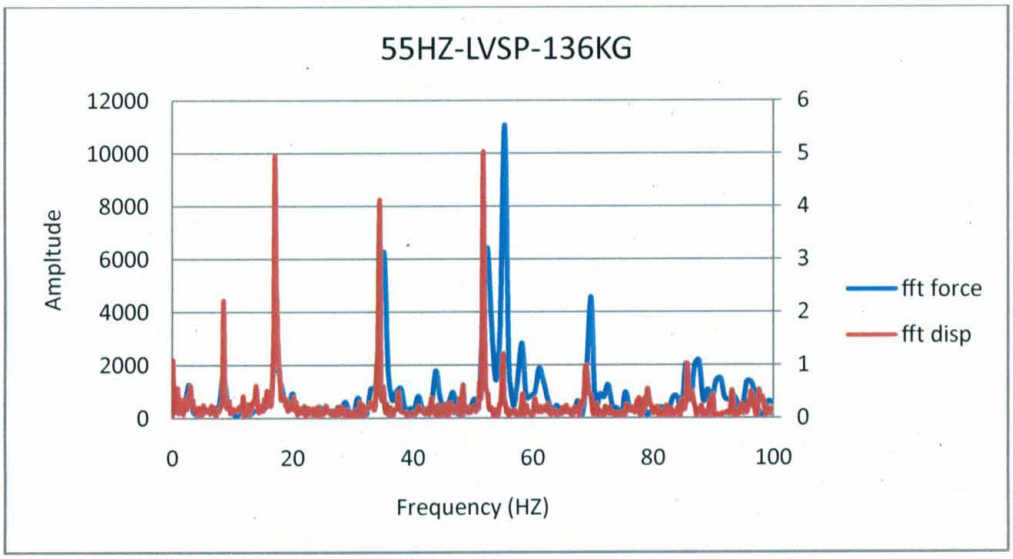
55HZ-LVSP-136KG
Amplitude
12000
10000
8000
6000
4000
2000
0
6
5
4
3
2
1
0
0
20
40
60
80
100
Frequency (HZ)
fft force
fft disp

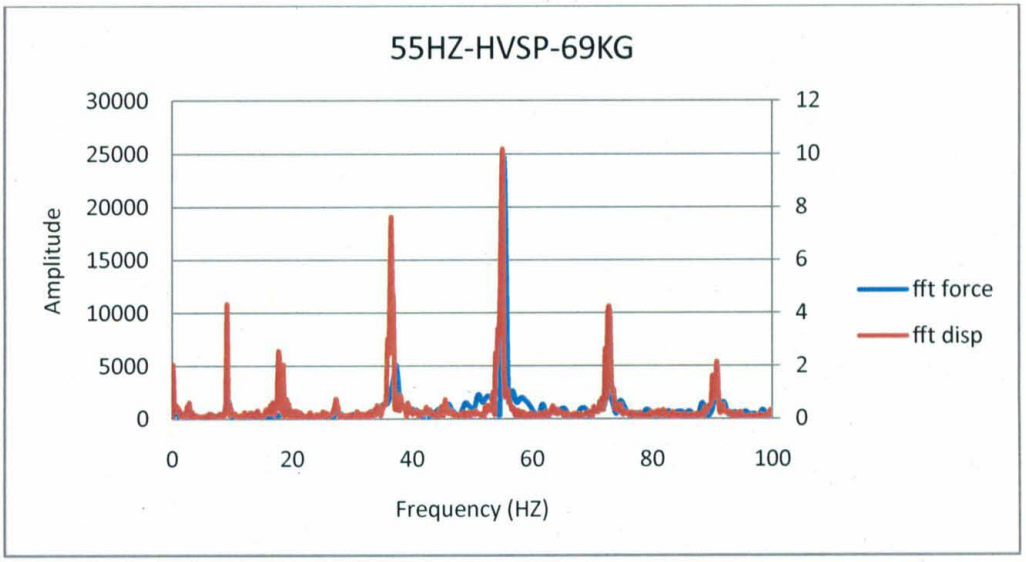
55HZ-HVSP-69KG
Amplitude
30000
25000
20000
15000
10000
5000
0
12
10
8
6
4
2
0
0
20
40
60
80
100
Frequency (HZ)
fft force
fft disp

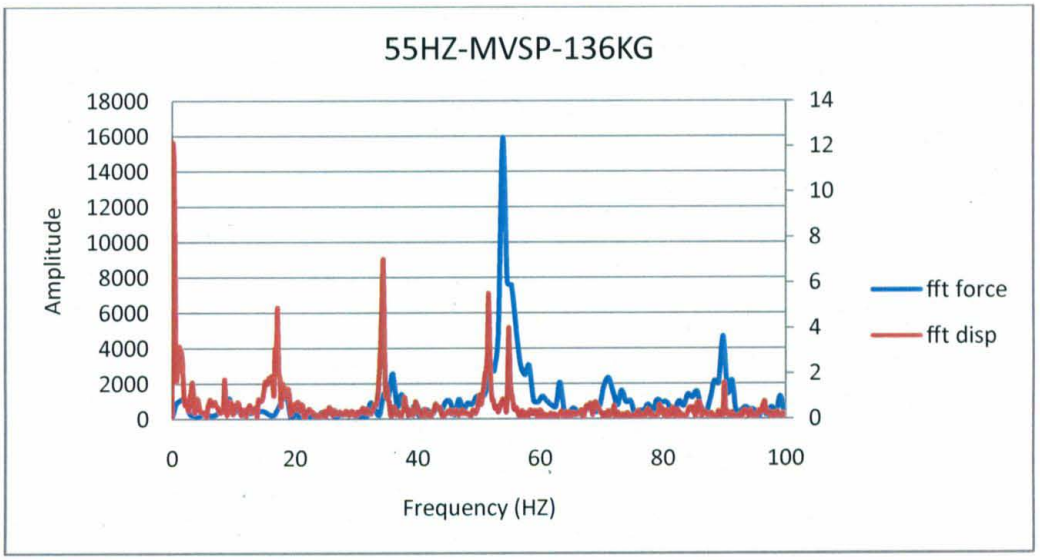
55HZ-MVSP-136KG
Amplitude
18000
16000
14000
12000
10000
8000
6000
4000
2000
0
14
12
10
8
6
4
2
0
0
20
40
60
80
100
Frequency (HZ)
fft force
fft disp

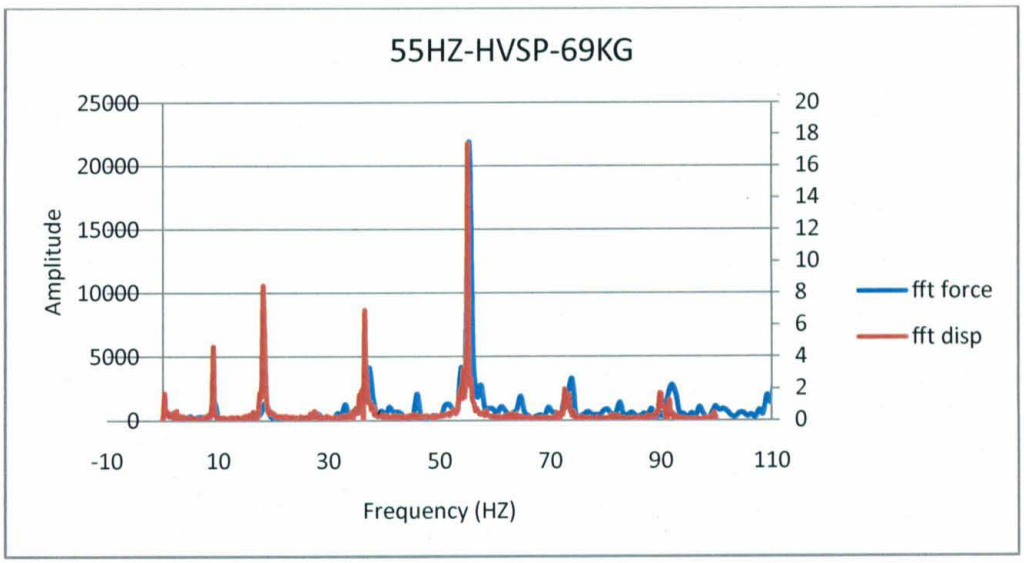
55HZ-HVSP-69KG
Amplitude
25000
20000
15000
10000
5000
0
20
18
16
14
12
10
8
6
4
2
0
-10
10
30
50
70
90
110
Frequency (HZ)
fft force
fft disp

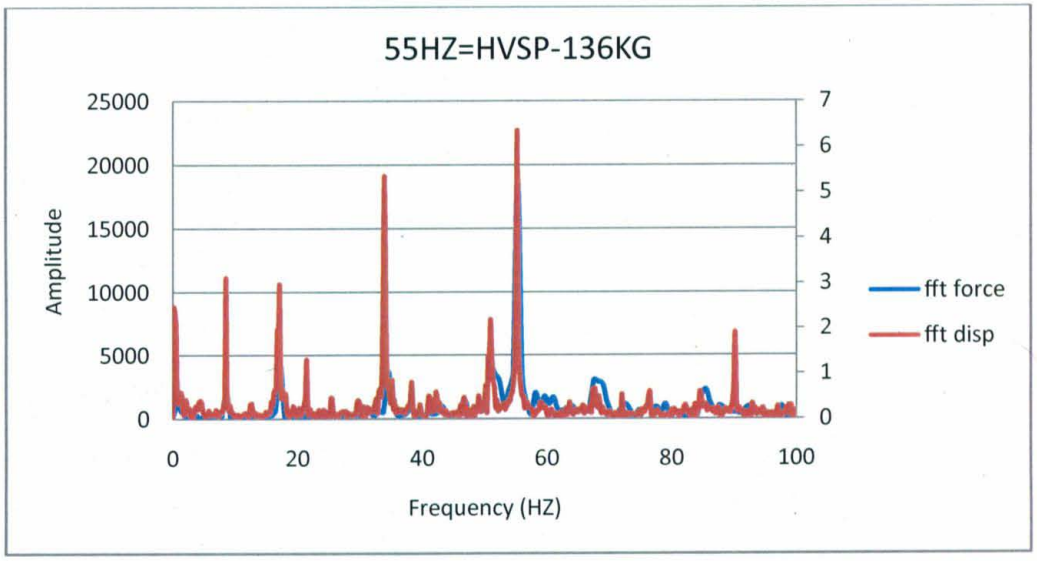
55HZ=HVSP-136KG
Amplitude
25000
20000
15000
10000
5000
0
7
6
5
4
3
2
1
0
0
20
40
60
80
100
Frequency (HZ)
fft force
fft disp

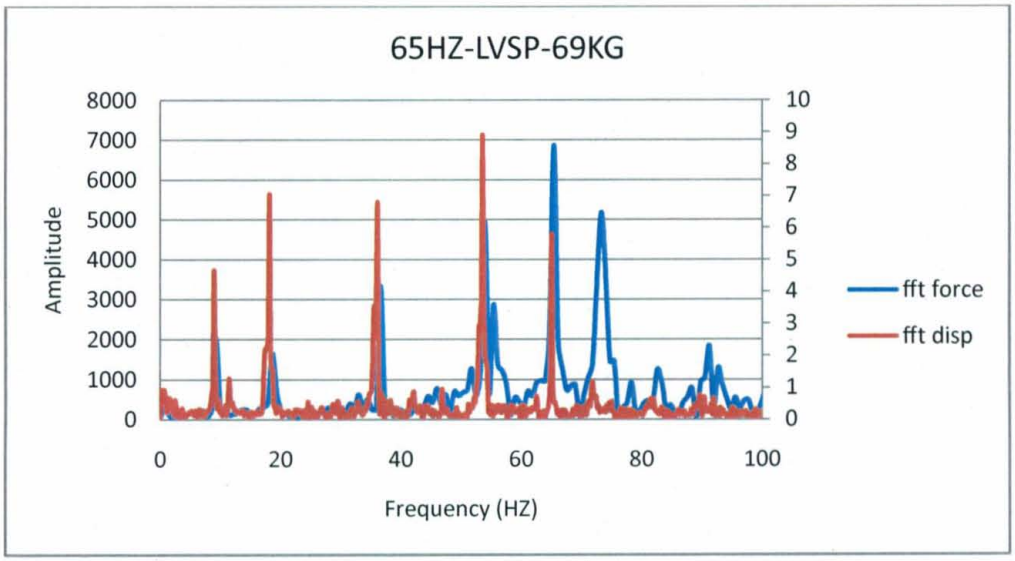
65HZ-LVSP-69KG
Amplitude
8000
7000
6000
5000
4000
3000
2000
1000
0
10
9
8
7
6
5
4
3
2
1
0
0
20
40
60
80
100
Frequency (HZ)
fft force
fft disp

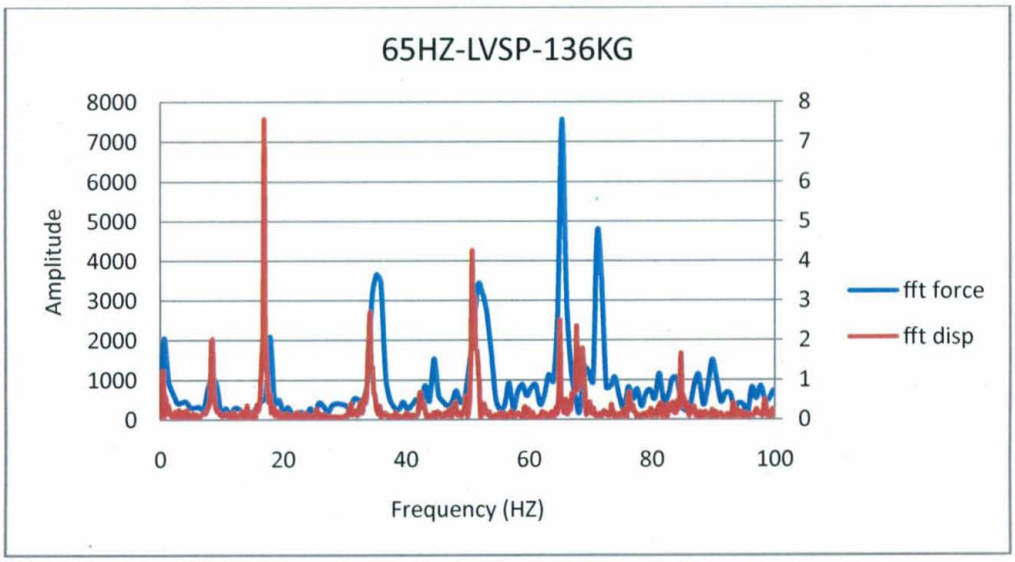
65HZ-LVSP-136KG
Amplitude
8000
7000
6000
5000
4000
3000
2000
1000
0
8
7
6
5
4
3
2
1
0
0
20
40
60
80
100
Frequency (HZ)
fft force
fft disp

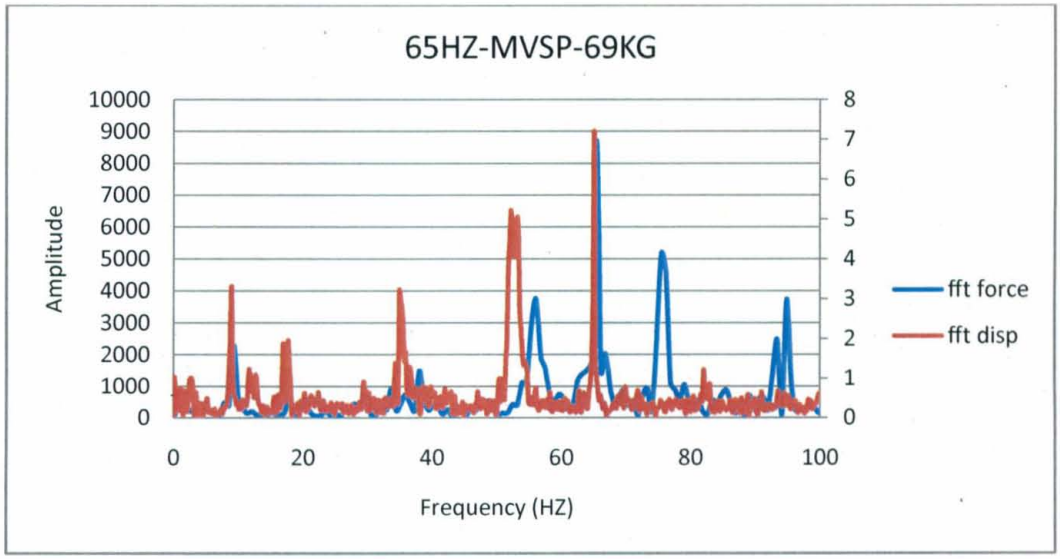
65HZ-MVSP-69KG
Amplitude
10000
9000
8000
7000
6000
5000
4000
3000
2000
1000
0
8
7
6
5
4
3
2
1
0
0
20
40
60
80
100
Frequency (HZ)
fft force
fft disp

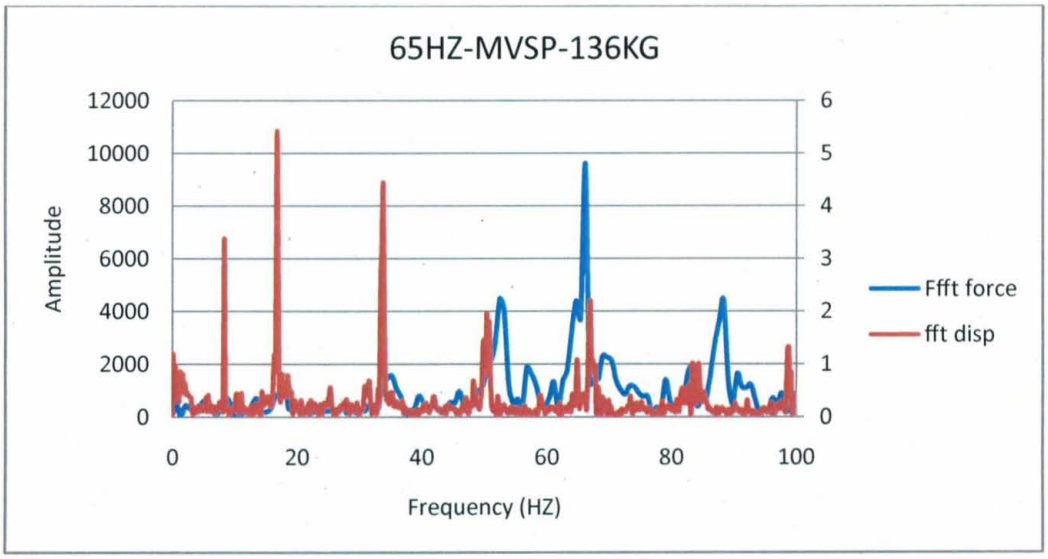
65HZ-MVSP-136KG
Amplitude
12000
10000
8000
6000
4000
2000
0
6
5
4
3
2
1
0
0
20
40
60
80
100
Frequency (HZ)
Ffft force
fft disp

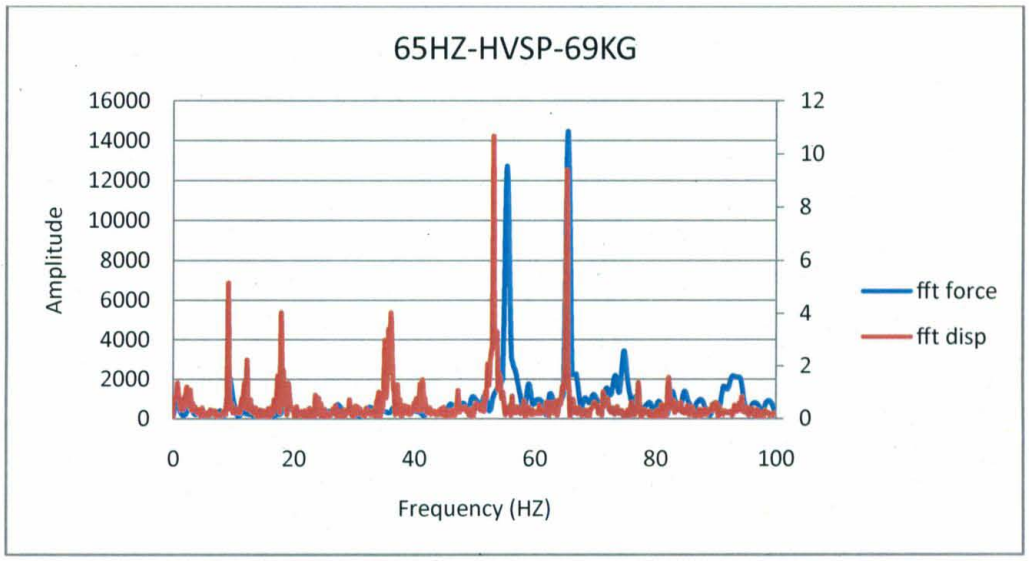
65HZ-HVSP-69KG
Amplitude
16000
14000
12000
10000
8000
6000
4000
2000
0
12
10
8
6
4
2
0
0
20
40
60
80
100
Frequency (HZ)
fft force
fft disp

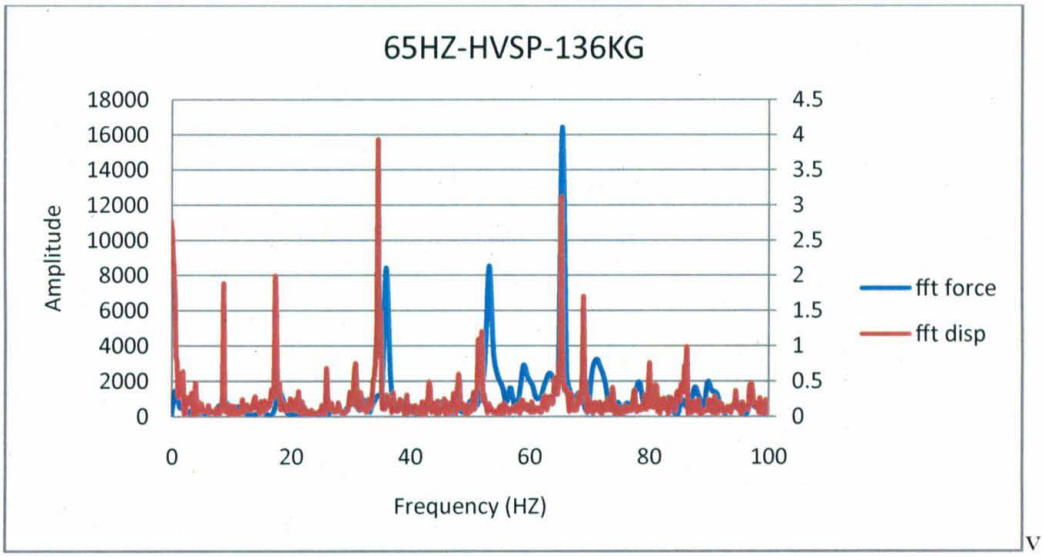
65HZ-HVSP-136KG
Amplitude
18000
16000
14000
12000
10000
8000
6000
4000
2000
0
4.5
4
3.5
3
2.5
2
1.5
1
0.5
0
0
20
40
60
80
100
Frequency (HZ)
fft force
fft disp

V

References

1. Li Heng. "Experimental Investigation of The Rate of Penetration of Vibration Assisted Rotary Drilling - Master's Thesis". Memorial University of Newfoundland, St. John's, NL, Canada. January 2011.

2. R. Simon. "Comparing the Rotary With Potential Drilling Methods". AIME Annual Meeting, New York City, February 16-20, 1958.

3. V.V. Pilipenko et al. "Characteristics of a high-frequency cavitation hydrovibrator for setting up dynamic loads on the rock cutting tool of a drilling assembly". National Mining University Publishers. - pp.66-70.

4. M. Wiercigroch. " Resonance Enhanced Rotary Drilling: Method and Apparatus". College of Physical Sciences, University of Aberdeen, Patent No. WO2007/141550 A1, 2007.

5. J.E Eckel et al. "Vibratory Drilling". U.S, Patent No. 3,016,098. January 1962.

6. Xinghua Tao et al. "Impact Rotary Drilling Technology". World Petroleum Congress. 1997.

7. Li Hengi, S. Butt, K. Munaswamy and F. Arvani. 2010. "Experimental Investigation of bit vibration on rotary drilling penetration rate". 44th U.S. Rock mechanics Symposium and the 5th U.S. – Canada Rock Mechanics Symposium, Salt Lake City, UT 27 -30 June.

8. V.C Kelessidis, P. Dalamarinis. "Monitoring drilling bit parameters allows optimization of drilling rates". International Multidisciplinary Scientific Geo-Conference and Expo, Albena, Bulgaria, June 14-19 2009.

9. W.C Maurer. "Bit-Tooth Penetration Under Simulated Borehole Conditions". SPE Annual Fall Meeting, Denver, Colorado, October 3-6, 1965.

10. R.C Pessier and M.J Fear. "Quantifying Commong Drilling Problems With Mechanical Specific Energy and a Bit-Specific Coefficient of Sliding

Friction". 67th Annual Technical SPE Technical Conference and Exhibition, Washington DC, October 4-7 1992.

11. N. Rafatian et.al. "Experimental Study of MSE of a Single PDC Cutter Under Simulated Presurized Conditions". SPE/IADC Drilling Conference and Exhibition, Amsterdam, Netherland, March 17-19, 2009.

12. F.E Dupriest and W.L Koederitz. "Maximizing Drill Rates with Real-Time Surveillance of Mechanical Specific Energy". SPE/IADC Drilling Conference, Amsterdam, Netherlan, February 23-25 2005.

13. M. Armenta. "Identifying Inefficient Drilling Conditions Using Drilling Specific Energy". SPE Annual Conference and Exhibition, Denver, Colorado, September 21-24 2008.

14. R. Teale. "The Concept of Specific Energy in Rock Drilling". International Journal for Rock Mechanics and Mining Sciences". Volume 2, 57-73, 1965.

15. K. Mohan, F. Adil and R. Samual. "Tracking Drilling Efficiency Using Hydro-Mechanical Specific Energy". SPE/IADC Drilling Conference and Exhibition, Amsterdam, Netherland, March 17-19 2009.

16. M.J Fear. "How to Improve Rate of Penetration in Field Operations". IADC/SPE Drilling Conference, New Orleans, March 12-15 2009.

17. I.T James. The Vibration Analysis Handbook, A practical guide for solving rotating machinery problems. First Edition: VCI. Pg 4 – 23, 2003.

18. B.Z Malgorta and S. Miska. "Mathematical Model of the diamond-bit drilling process and its practical application". SPE Annual Technical Conference and Exhibition, San Antonio, October 5-7, 1982.

19. A.M Paiaman et.al.. "Effect of drilling fluid properties on rate of penetration". NAFTA 60 (3) , Pg 129-134, 2009.

20. F.E Dupriest, J.W. Witt and S.M Remmert. "Maximizing ROP With Real-Time Analysis of Digital Data and MSE". IPTC Conference, Doha, Qatar, November 21-23, 2005.

21. W.A Hurstrulid and C. Fairhurst. "A Theoretical and Experimental Study of the Percussive Drilling of Rock – Theory of Percussive Drilling". Int. J. Rock Mech. Min. Sci. Vol. 8, pp. 311-333. Pergamon Press, Great Britain, 1971.

22. W.A Hurstrulid and C. Fairhurst. "A Theoretical and Experimental Study of the Percussive Drilling of Rock – Force Penetration and Specific Energy Determination". Int. J. Rock Mech. Min. Sci. Vol. 8, pp. 335-356. Pergamon Press, Great Britain, 1971.

23. W.A Hurstrulid and C. Fairhurst. "A Theoretical and Experimental Study of the Percussive Drilling of Rock – Application of the Model to Actual Percussive Drilling". Int. J. Rock Mech. Min. Sci. Vol. 8, pp. 431-449. Pergamon Press, Great Britain, 1971.

24. Luiz Fernando et. al. "Experimental and Numerical Study of a New Resonance Hammer Drilling Model with Drift". Elsevier Ltd, pp 789-801, 2004.

25. Gang Han et. al. "Dynamically Modelling Rock Failure in Percussive Drilling". 40th U.S. Rock mechanics Symposium, Anchorage, Alaska 25 -29 June, 2005.

26. A. Sinor and T.M. Warren. "Drag Bit Wear Model". SPE Drilling Engineering, June 1989.

27. Y.S. Kim and H.L. Hartman. "An ExperimentalStudy of Drag-Bit Drilling Using Dimensional Analysis". Annual AIME Meeting, Chicago, February 14-18 1965.

28. T.M. Warren and W.K. Armogost. "Laboratory Drilling Performance of PDC Bits". SPE Drilling Engineering, June 1988.

29. Bourgoyne, A.T., Millheim, K.K., Chenevert, M.E. and Young, F.S: "Applied Drilling Engineering", Society of Petroleum Engineers, Richardson, TX, 1991, pp 190-240.

30. Dwayne, L., Brock, W., and Pursell, J., "Coiled Tube Drilling – Real Time MWD with Dedicated Power to the BHA", In Proceeding sof the Offshore Technology Conference held in Houston Texas, 6 – 9 May 1996.

31. Detournay, E. and Tan, C.P.: "Dependence of Drilling Specific Energy on Bottom-Hole Pressure in Shales," paper SPE 78221, presented at the SPE/ISRM Rock Mechanics Conference, Irving, TX, 2002.

32. Henri Cholet, " Improved Hydraulics for Rock Bits", Paper SPE 7516 presented at the 1978 SPE Conference held in Houston Texas, October 1-3.

33. Resonant Sonic Drilling, prepared for U.S. DOE, April 1995.

34. Caicedo, Hector, and Calhun, William and Ewy, Russ,: "Unique ROP Predictor Using Bit Specific Coefficient of Sliding Friction and Mechanical

Efficiency as a Function of Confined Compressive Strength Impacts Drilling Performance," paper SPE 92576.

35. Garner, N.E.: "Cutting Action of a Single Diamond Under Simulated Borehole Conditions," Journal of Petroleum Technology, vol. 19, No. 7, pp. 939-942 (July 1967).

36. E. Kuru and A.K. Wojtanowsicz. "A Method for Detecting In-Situ PDC Bit Dull and Lithology Change" IADC/SPE Drilling Conference, Dallas, Texas, Fevruary 28-March 2 1988.

37. M.B Ziaja and S. Miska. "Mathematical Model of the Diamond-Bit Drilling Process and Its Practical Application". Society of Petroleum Engineers of AIME, December 1982.

38. G. Hareland et. al. "A New Drilling Rate Model for Tricone Bits and Its Application to Predict Rock Compressive Strength". 44th U.S. Rock mechanics Symposium and the 5th U.S. - Canada Rock Mechanics Symposium, Salt Lake City, UT 27 -30 June.

39. R.V. Barragan et. al. "Optimization of Multiple Bit Runs". SPE/IADC Drilling Conference, Amsterdam, The Netherlands, March 4-6 1997.

40. G. Hareland et. al. "Drilling Simulation Improves Field Communication and Reduces Drilling Cost in Western Canada". 8th Canadian International Petroleum Conference, Calgary, Alberta, Canada, Jume 12-14 2007.

41. H.I. Biligesu et.al. "A new Approach for the Prediction of Rate of Penetration (ROP) Values". SPE Eastern Regional Meeting, Lexington, KY, October 22-24 1997.

42. H.R. Motahhari et. al. "Method of Optimizing Motor and Bit Performance for Maximum ROP". Journal of Canadian Petroleum Technology, Volume 8, No. 6, June 2009.

43. M. Rastegar et. al. "Optimization of Multiple Bit Runs Based on ROP Models and Cost Equation: A New Methodology Applied for One of the Persian Gulf Carbonate Fields". SPE/IADC Asia Pacific Drilling Technology Conference and Exhibition. Jakarta, Indonesia, August 25-27 2008.

44. B. Rashidi et. al. "Real-Time Bit Wear Optimization Using the Intelligent Drilling Advisory System". SPE Russian Oil and Gas Technical Conference and Exhibition, Moscow, Russia, October 26-28 2010.